THE INVESTIGATION OF SURFACE MODIFICATIONS ON POLYESTER BASED FIBROUS MATRICES FOR CELL EXPANSION IN PACKED BED BIOREACTORS

DOLGULU YATAK BİYOREAKTÖRLERDE HÜCRE ÜRETİMİ İÇİN POLİESTER TEMELLİ FİBRÖZ MATRİSLERDE YÜZEY MODİFİKASYONLARININ ARAŞTIRILMASI

Fayiti FUERKAITI

Supervisor
Dr. Öğr. Üyesi. Işıl GERÇEK BEŞKARDEŞ
Co-Supervisor
Prof. Dr. Menemşe GÜMÜŞDERELİOĞLU

Submitted to
Graduate School of Science and Engineering of Hacettepe University
as a Partial Fulfillment to the Requirements
for the Award of the Degree of Master of Science
in Bioengineering
2020

ABSTRACT

THE INVESTIGATION OF SURFACE MODIFICATIONS ON POLYESTER BASED FIBROUS MATRICES FOR CELL EXPANSION IN PACKED BED BIOREACTORS

Fayiti FUERKAITI

Master of Science, Department of Bioengineering

Supervisor: Asst. Prof. Dr. Işıl Gerçek BEŞKARDEŞ

Co-Supervisor: Prof. Dr. Menemşe GÜMÜŞDERELİOĞLU

This study was financially supported by Hacettepe University Scientific Research Projects Coordination Unit (BAP) with the project entitled "The Investigation of The Effects of Surface Modifications on Fiber Based Polyester Matrices for Mesenchymal Stem Cell Production in Packed Bed Bioreactors" (project no: FYL-2018-17359).

This study aims to investigate the effects of surface modifications on polyester matrices for mesenchymal stem cell (MSC) production in a packed bed bioreactor. Firstly, sulfuric acid and sodium hydroxide treatments were applied on PET with different parameters in order to increase hydrophilicity and all surface-treated groups of PET disks were examined through water contact angle measurements, Attenuated Total Reflectance-Fourier Transform Infrared Spectroscopy (ATR-FTIR), Scanning Electron Microscope (SEM) and Energy Dispersive X-Ray Spectroscopy (EDS) analyses. After characterization studies, 3M H_2SO_4 and 0.05M NaOH treated PET disks were further studied *in vitro* with MC3T3-E1 cells and cell activity was found to be higher in sodium hydroxide treated PET disks than sulfuric acid-treated PET disks.

Secondly, collagen type-1 (30 µg/disk) and vitronectin (0.15 and 0.60 µg/disk) were coated on the PET surfaces via physical and chemical immobilization methods. In the

characterization studies, hydroxyproline analysis and SEM analysis demonstrated that the physical immersive coating technique was more efficient and resulted in evenly distributed collagen type-1 on the PET disk surface. Meanwhile, the results of SEM and ATR-FTIR analyses of collagen type-1 and vitronectin crosslinking on PET disks were similar to that of the control group. Also, the results of static cell culture conducted with rAdMSCs demonstrated no significant differences between collagen type-1 and vitronectin coated PET disks with plain sodium hydroxide treated PET disks. Thus, sodium hydroxide treated PET disks were selected for dynamic cell culture studies.

In the last part of the thesis, rAdMSC expansion was investigated in our custom made packed-bed bioreactor using sodium hydroxide treated PET as packing material. In dynamic studies, two different cell seeding densities were used: 30 x 10^6 cells/ 1 g disks and 10 x 10^6 cells/0.5 g disks. The specific growth rate and doubling time of rAdMSCs with higher seeding density were calculated as 0.06 h^{-1} and 65 h and it was determined that glucose concentration in the culture medium was insufficient. And the specific growth rate and doubling time of rAdMSCs harvested from the bioreactor were calculated as 0.2516 h^{-1} and 42 h, which were comparable to the characteristic values given in the literature. In the differentiation studies of rAdMSCs harvested from the bioreactor, ALP-von Kossa staining was done in the osteogenic differentiation studies, whereas oil red o staining was done for adipogenic differentiation studies. In addition, it was determined that harvested cells had similar SOX2, Nanog and OCT 4 gene expressions in comparison to the control group. However, in the dynamic studies growth rate of cells in the bioreactor exhibited a trend independent of cell seeding density, which should be further investigated in a more comprehensive cell expansion study.

Keywords: Polyethylene terephthalate; Surface Modification; Collagen; Vitronectin; Packed-bed Bioreactor; Mesenchymal Stem Cell Production

ÖZET

DOLGULU YATAK BIYOREAKTÖRLERDE HÜCRE ÜRETİMİ İÇİN POLİESTER TEMELLİ FIBRÖZ MATRISLERDE YÜZEY MODİFİKASYONLARININ ARAŞTIRILMASI

Fayiti FUERKAITI

Yüksek Lisans, Biyomühendislik Anabilim Dalı

Tez Danışmanı: Dr. Öğr. Üyesi Işıl Gerçek BEŞKARDEŞ

İkinci Tez Danışmanı: Prof. Dr. Menemşe GÜMÜŞDERELİOĞLU

Bu çalışma 'Dolgulu Yatak Biyoreaktörlerde Mezenkimal Kök Hücre Üretimi İçin Fiber Temelli Poliester Matrislerde Yüzey Modifikasyonlarının Etkilerinin Araştırılması' başlık tez projesi kapsamında (proje no: FYL-2018-17359) Hacettepe Üniversitesi Bilimsel Araştırma Projeleri Koordinasyon Birimi tarafından desteklenmiştir.

Tez çalışmanın amacı, dolgu yataklı biyoreaktörde mezenkimal kök hücre (MSC) üretimi için poliester fiber matrisler üzerindeki yüzey modifikasyonlarının etkisinin incelenmesidir. Öncelikle PET disklerin hidrofilik özelliğini artırmak amacıyla farklı parametreler kullanılarak sülfürik asit veya sodyum hidroksit muamelesi gerçekleştirildi. Yüzey modifikasyonu işlemi yapılmış olan PET disk gruplarının; su temas açısı ölçümü, zayıflatılmış toplam yansıma- Fourier dönüşümlü kızılötesi spektroskopisi (ATR-FTIR), taramalı elektron mikroskobu (SEM) ve enerji dağılımlı X-ışını spektroskopisi (EDS) analizi gerçekleştirildi. Karakterizasyon çalışmalarından sonra, 3 M H_2SO_4 veya 0.05 M NaOH ile muamele edilmiş PET diskler ile *in vitro* hücre kültürü çalışmaları gerçekleştirildi ve çalışma sonucunda sodyum hidroksit ile muamele edilmiş olan PET disklerdeki MC3T3-E1 hücrelerinin mitokondriyal aktivitesinin daha yüksek olduğu belirlendi.

Tez çalışmasının ikinci aşamasında, kolajen tip-1 (30 µg/disk) ve vitronektin (0.15 ve 0.60 µg/disk), fiziksel veya kimyasal immobilizasyon yöntemleriyle PET disk yüzeyine kaplandı. Hidroksiprolin ve SEM analizi gibi karakterizasyon çalışmalarının sonucunda fiziksel daldırma yöntemiyle kolajen tip-1'in PET disklerin yüzeyine daha verimli ve eşit dağılımlı bir şekilde kaplandığı gözlemlendi. Ayrıca, SEM ve ATR-FTIR analizleri kolajen tip-1 ve vitronektin ile kimyasal yöntem kullanılarak kaplanan PET disklerin kontrol grubuna benzer olduğu görüldü. rAdMSC hücreleri kullanılarak yürütülen statik hücre kültürü çalışmaları sonucunda, sodyum hidroksit ile muamele edilmiş olan kontrol PET disk grubu ile kolajen tip-1 ve vitronektin kaplanmış PET disk grupları arasında istatiksel olarak önemli bir fark olmadığı sonucuna ulaşılmıştır. Bu sebeple, dinamik hücre kültürü çalışmalarında sodyum hidroksit ile muamele edilmiş olan PET disk grubu kullanılmıştır.

Tez çalışmasının son basamağında sodyum hidroksitle muamele edilmiş olan PET diskler ile 2 farklı hücre ekim yoğunluğu kullanılarak (30 x 10^6 hücre/1 g disk and 10 x 10^6 hücre/0.5 g disk) dolgu yataklı biyoreaktörde rAdMSC üretimi araştırıldı. Ekim yoğunluğu yüksek olan deneyde rAdMSC hücrelerinin özgül büyüme hızı ve ikilenme süresi sırasıyla, 0.06 sa^{-1} ve 65 sa olarak hesaplandı ve kültür ortamındaki glikoz miktarının hücre üremesi için yetersiz olduğu belirlendi. Biyoreaktörde üretilen rAdMSC hücrelerinin ise özgül üreme hızı 0.2516 sa^{-1} ve ikilenme süresi ise 42 sa olarak bulundu ve bu değerlerin literatürde verilen değerler ile benzer olduğu bulundu. Biyoreaktörde üretilen rAdMSC hücrelerinin; osteojenik farklılaşma çalışmaları ALP ve Von Kossa boyamaları ile, adipojenik farklılaşma çalışmaları ise Oil red o boyaması ile gerçekleştirildi. Ayrıca dinamik olarak üretilen hücrelerin kontrol grubuna benzer SOX2, Nanog and OCT 4 gen ifadesine sahip olduğu belirlendi. Bununla birlikte, gerçekleştirilen çalışmalarda biyoreaktördeki hücre üreme hızının, hücre ekim yoğunluğundan bağımsız bir eğilim gösterdiği bulunmuştur ve bu konunun daha kapsamlı bir hücre üretim çalışmasında araştırılmasının gerektiği yorumu yapılmıştır.

Anahtar Kelimeler: Polietilen tereftalat; Yüzey Modifikasyonları, Kollajen; Vitronektin; Dolgu yataklı Biyoreaktör; Mezenkimal Kök Hücre Üretimi

ACKNOWLEDGEMENTS

Foremost, I would like to express my sincere gratitude to my Supervisor Dr. Işıl Gerçek BEŞKARDEŞ for continues support during my master study and research. Her knowledge and experience help me overcome difficulties. Her patience, encouragement, motivation and guidance throughout entire research study kept me enthusiastic and enlightened.

I would like to pay my humble regards to my Co-Supervisor: Prof. Dr. Menemşe GÜMÜŞDERELİOĞLU. It has been an honor and privilege working with Cell and Tissue Engineering Research Group, I have learned a lot under her supervision. Her immense knowledge and enlightenment provide me great prospective to my research study, I really thank her from the bottom of my heart.

I wish to show my gratitude for the financial support provided by Hacettepe University Scientific Research Projects Coordination Unit (BAP), project no FYL-2018-17359.

I wish to thank all the people whose assistance was milestone in the completion of this thesis study and special thanks to Özge Ekin Akdere, Öğr. Gör. Dr. Anıl Sera Çakmak and Dr. Öğr. Üyesi Soner Çakmak for their help and support during the experimental study. I would like to thank all my fellow labmates and member of Cell and Tissue Engineering Research Group for their understanding and support and I wish them all the best in their academic career.

Last but not the least, I owe more than thanks to my family which including my parents, my beloved wife Sümeyra Nur Fuerkaiti. Their immense supports and understanding help me overcome difficulties and finish my thesis study. Especially I want to thanks her support and encouragement, I really appreciate her spending time reading this thesis and providing useful suggestion and also correcting my Turkish.

TABLE OF CONTENT

Pages

LIST OF TABLES

LIST OF FIGURES

SYMBOLS AND ABBREVIATIONS

Symbols

H_2SO_4	Sulfuric acid
NaOH	Sodium hydroxide
Na^+	Sodium ion
OH^-	Hydroxyl ion
H^+	Hydrogen ion
H_2O	Water
-COOH	Carboxyl functional group
CO_2	Carbon dioxide
$KMnO_4$	Potassium permanganate
HCl	Hydrochloric acid
Pa	Pascal
℃	Degree Celsius
S/V	Specific surface-to-volume ratio
v/v	Volume per volume
w/v	Weight per volume
EtOH	Ethyl alcochol

Abbreviations

ε_{matrix}	internal porosity
µg	Microgram
µL	Microliter
µm	Micrometer
µM	Micromolar
2D	2-Dimensional
3D	3-Dimensional
AIM	Adipogenesis- inducing cell culture medium
ALP	Alkaline phosphatase
AMM	Adipogenesis-maintenance cell culture medium
ATP	Adenosine triphosphate
ATR-FTIR	Attenuated Total Reflectance -Fourier Transform Infrared Spectroscopy
BMP-2	Bone morphogenic protein
BSA	Bovine serum albumin
Col	Collagen type I
DAPI	4-6-diamidino-2-phenylindole
DMEM	Dulbecco's Modified Eagle Medium
DPBS	Dulbecco's phosphate buffer solution
ECM	Extracellular matrix
EDS	Energy Dispersive X-Ray Spectroscopy
FBS	Fetal bovine serum
FCS	Fetal calf serum
FDA	Food and Drug Administration
g	Gram
GAG	Glycosaminoglycans

GF	Growth factor
GMP	Good manufacturing practice
L	Liter
LV	Left ventricular
MC3T3-E1	Osteoblast precursors
MCs	Microcarriers
hMSCs	Human mesenchymal stem cells
mg	Milligram
min	Minute
mL	Milliliter
MRI	Magnetic resonance imaging
MTT	3-[4, 5-dimethylthiazol-2-yl]- diphenyltetrazolium bromide
α-MEM	Minimum Essential Medium Alpha Modificated
NWPF	Nonwoven polyester fabric
OA	Chronic osteoarthritis
PBR	Packed-bed bioreactor
PBS	Phosphate buffered saline
PD	Population doubling
PET	Poly (ethylene terephthalate)
pH	Potential hydrogen
PL	Platelet lysate
pO_2	Partial pressure of oxygen
RB	Roller bottles
RGD	Arg-Gly-Asp sequence
SCI	Spinal cord injury
SEM	Scanning Electron Microscope
TCPS	Tissue Culture Polystyrene

TGFβ	Transforming growth factor-beta
TGF-β3	Transforming growth factor beta-3
UV	Ultra violet
VN	Vitronectin

1. INTRODUCTION

Human mesenchymal stem cells (hMSCs) isolated from bone marrow, adipose and other tissues have fibroblast-like plastic adherent phenotypes. They have multipotent differentiation capacities at *in vitro* environment. Due to this outstanding ability, hMSCs have become universal cell sources for cell therapy for different diseases, such as acute graft-versus-host diseases (GVHD), steroid-refractory symptom, bone, cartilage and myocardium regeneration, spinal cord injury treatment and etc. Human MSCs-based clinical applications have been conducted for various kind of pathological diseases, some of them have completed phase III trials [1].

Based on disease and trauma types the required dosage of MSCs per patient varies greatly. Furthermore, the labor cost and inefficient nature of the conventional 2D tissue flask culture method limit the clinical application dosages under 10^8 cells per patient [2]. The widely used 2-Dimensional (2D) cell culture systems are unable to sustain many important parameters that are significantly affecting the life cycle of cells, including proliferation, migration, and apoptosis. In order to achieve a better life cycle of cells, different 3-Dimensional (3D) cell culture techniques, such as spheroids, roller bottle bioreactors, microcarrier-based bioreactor systems, packed-bed bioreactor and perfusion bioreactors systems had been developed [3].

In the 3D cell cultures, scaffolds, microcarriers, and packing-materials is an essential aspect in cell expansion and proliferation. Microcarriers as Van Wezel's first description are small particles that anchorage-dependent (AD) cells adhere and proliferate on them in suspension cell culture. On the other hand, packing-materials in perfusion culture provide incredibly high cell density and expansion within a limited size. Packed-bed bioreactors (PBR) are extensively used in mammalian cell expansion and vaccine production [4]. Surface modification techniques used on packing materials dramatically improve their biocompatibility and increase cell attachment and proliferation. The interaction between cell

and packing material is an essential step in evaluating surface modification efficiency and quality. Interactions between packing materials and cells are determined by their physical and chemical properties such as surface porosity, geometry, hydrophilicity, ionic interaction, electric charge, and presence of biological molecules [5-8].

This study aims to increase the expansion efficiency of MSCs by using surface modified nonwoven polyester fabric (NWPF) disks as packing materials in packed-bed bioreactors. Therefore, the material surface modifications were done by treatment with chemical agents or biological molecules, such as collagen type-1 and vitronectin. Then, the efficiency of modification methods were investigated through the static cell culture. Preliminary dynamic cell culture studies were carried out in custom-made small-volume packed-bed bioreactor.

2. GENERAL INFORMATION

The following contents give updated information about the thesis main topics, including the orientation and clinical value of mesenchymal stem cells, introduction and examples of cell culture systems in cell expansion. Cells play an essential role in tissue engineering as the building block. To achieve the sufficient number of cells in therapeutic applications, the advantages and disadvantages of traditional two-dimensional (2D) and advanced three-dimensional (3D) cell expansion methods were compared. The advantage of the packed-bed bioreactor used in cell expansion was discussed alongside with different packing materials. The positive effects of novel surface modification methods on packing material performance were also presented.

2.1 Mesenchymal Stem Cells (MSCs)

Mesenchymal stem cells (MSCs) isolated from bone marrow, adipose, other tissue sources with spindle-shaped plastic-adherent phenotypes, have multipotent differentiation capacity at *in vitro* environment [9]. Frankenstein first reported them as supportive hematopoietic cells of bone marrow. It was also shown that MSCs could differentiate to osteoblasts. They have a high proliferation potential when were seeded at low cell density in cell culture [10].

The standard definition criteria of human MSCs had been proposed by Mesenchymal and Tissue Stem Cell Community of the International Society for Cellular Therapy. First, when maintained in standard culture conditions using tissue culture flasks, MSCs must be plastic-adherent. Second, when measured by flow cytometry, ≥95% of the MSCs population must express CD105, CD73 and CD90. At the same time, these cells must lack expression (≤ 2% positive) of CD45, CD34, CD14 or CD11b, CD79α or CD19, and HLA class II. Lastly, MSCs under standard *in vitro* differentiating conditions must have the ability to differentiate to osteoblasts, adipocytes, and chondrocytes [11].

2.1.1. Sources of Mesenchymal Stem Cells

Human mesenchymal stem cells (hMSCs) are a wide range of plastic adherent fibroblast-like cells, that can be isolated from bone marrow aspirates, skeletal muscle, connective tissue, human trabecular bones, adipose tissue, periosteum, liver and also from umbilical cord blood [12] (Figure 2.1).

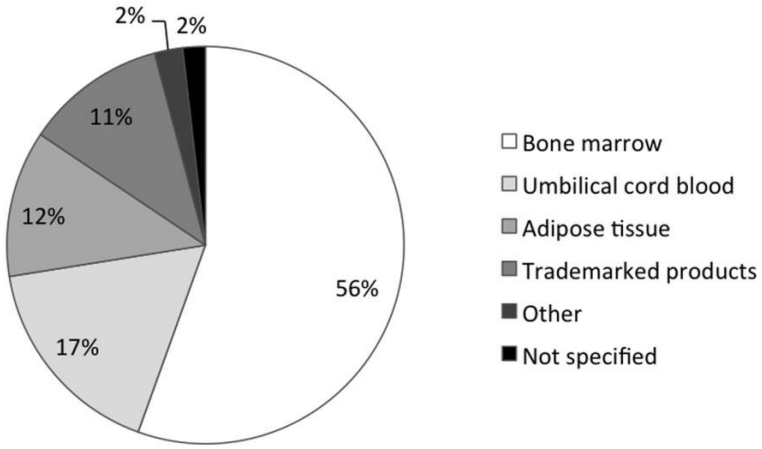

Figure 2. 1. Summary of tissue sources for MSCs currently being used in studies [13].

For example, adipose-derived MSCs can be harvested by the following procedure: The adipose tissue is washed with phosphate buffer saline (PBS) and digested at 37℃ with 0.1% collagenase-A enzyme-containing PBS and bovine serum albumin (BSA) mixed solution for 45 min under shaking. The digested tissue is then washed with α-MEM containing 10% fetal bovine serum (FBS) followed by a 10 min centrifugation at 2500 rpm. Then, the cell pellet is re-suspended in PBS and filtered with 200 μm mesh to remove debris. Then, contaminating erythrocytes are removed with Ficoll density centrifugation which improved the yield of viable cells. The viability of the cells is measured with a trypan blue exclusion assay. Finally, isolated cells are suspended in the mixture (1:1) of cell culture medium and cryoprotective medium and then, stored in liquid nitrogen according to the good manufacturing practice (GMP).

The trilineage differentiation ability (differentiate to adipocytes, osteoblasts and chondrocytes) of MSCs must be determined (Figure 2.2.). For osteogenesis, MSCs should be incubated in fetal calf serum (FCS), β-glycerolphosphate, dexamethasone and ascorbic acid containing medium. MSCs should exhibit osteoblastic morphology with calcium deposition and high alkaline phosphatase (ALP) activity. To observe osteoblastic phenotype, Von Kossa staining is commonly employed to detect calcium phosphate deposits, in which treated cells are fixed with 70% ethanol and treated with 5% (w/v) silver nitrate solution . The mineral salts, black colour is observed with optical microscopy.

For adipogenesis, MSCs form adipocytes with lipid vacuoles under the adipogenesis-inducing cell culture medium (AIM) containing IBMX (0.5 mM), indomethacin (0.2 mM), insulin (0.01 mg/mL), dexamethasone (1 μM) and FBS (10%) in α-MEM. After 3 days, the adipogenesis-inducing cell culture medium is changed to the adipogenesis-maintenance cell culture medium (AMM) which contains insulin (0.01 mg/mL) and FBS (10%) in α-MEM. After 1 day, the medium is switched back to the adipogenesis-inducing cell culture medium and this procedure repeated three times. Then cells are kept in adipogenesis-maintenance cell culture for a week [14]. Lipid vacuoles can be visualized with oil red O and observed by optical microscopy [15].

For chondrogenesis, MSCs are incubated in 3D culture and incubated in high glucose DMEM or in chondrogenic differentiation medium containing insulin (5 g/mL), transferrin and selenosis acid, dexamethasone (0.1 μM), sodium pyruvate (1 mM), ascorbic acid-2-phosphate (0.17 mM), proline (0.35 mM), transforming growth factor-3 with (TGF-β3) (10 ng/L) and BSA (1.25 mg/mL) containing high-glucose DMEM) [16]. To observe the chondrocytes, the samples are fixed with 4% paraformaldehyde, wax embedded and sectioned at 5 μm thickness. Then, sections are stained for glycosaminoglycans (GAG) with 1% alcian blue in HCl (0.1 M) and collagen stained with picrosirius red. The accumulation of collagen type-1 and type-2 in extracellular matrix (ECM) are identified with immunohistochemistry [17].

In another alternative method, MSCs are grown in 3D pellet culture with TGF-β3 containing serum-free medium and differentiate into a matrix specific to cartilage containing GAGs. Differentiation can be detected with a toluidine blue, which is a dye that stains GAGs [18]. Because of this incredible tri-lineage differentiation ability, MSCs are very important cell sources and primary candidates in cell therapy for varies diseases.

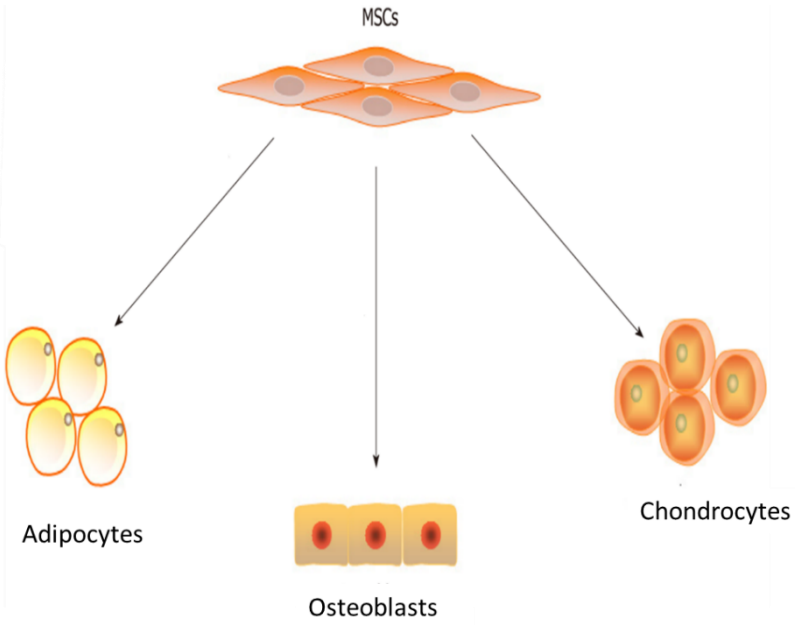

Figure 2. 2. Schematic presentation of the MSCs differentiation diagram.

2.1.2 Growth Conditions

MSCs are plastic adherent cells that grow as a monolayer without any need of additional layers. Recently most favorable protocols for MSCs expansion recommend the use of FCS included medium. FCS concentration range of 10%-20% are favor for cell expansion and the concentration range of 2-10% are favor to induce MSCs differentiation [19]. But there is a large batch to batch uncertainty within the FCS, which may lead to the consequences of significant variation of MSCs growth and differentiation behavior. Thus, it is crucial to test FCS's batch performance regularly to eliminate the batch to batch fluctuation. In addition, the drawbacks of FCS must be kept in mind when performed therapeutic application for clinical uses, because it carries the risk of transmitting viral and prion diseases, and the animal origin

protein may start a xenogeneic immune response. To eliminate these drawbacks, the alternatives have been researched, for example, autologous serum or platelet lysates [20] and chemically defined medium [21]. Recently developed chemically defined medium has been shown to support high MSCs proliferation rates while maintaining multipotency and immunophenotype [22]. This can significantly improve the safety of MSCs in cell therapies, also eliminates the major obstacle to implement the GMP in order to obtain approval from the National and International Regulators for therapeutic applications.

2.1.3 Clinical Applications and Trials

Over the past ten years, MSCs have great enthusiasm as a novel restorative paradigm for different kinds of diseases. Clinical applications of MSCs significantly depend on their four critical biological properties, i) the ability to target the inflammation following tissue damage when injected intravenously; ii) to differentiate into different types of cells; iii) to generate multiple bioactive molecules which enhance the healing of damaged cells; iv) to perform immuno-modulatory functions to inhibit inflammation. Additionally, MSC-based clinical applications have been conducted for various kind of pathological diseases; some of them have completed the clinical trials. The details about MSCs related clinical trials and developments are presented in Figure 2.3.

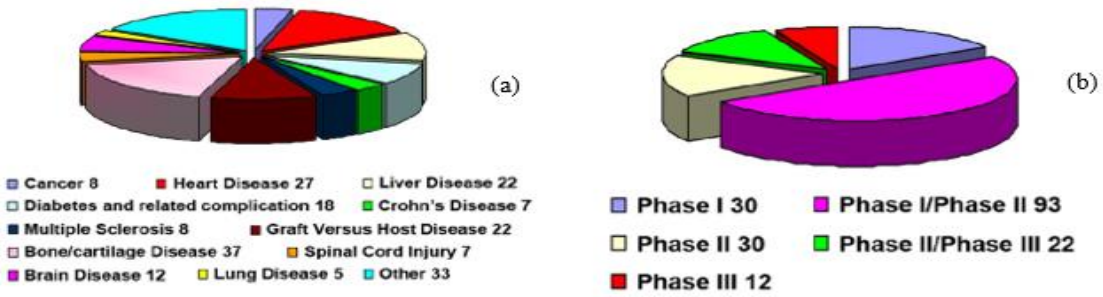

Figure 2. 3. Clinical trials of MSCs are classified by (a) disease types, (b) phases [23].

The dosages of MSCs for clinical applications vary between 10^9 and 10^{10} cells. The estimated cell doses for specific diseases are listed in Table 2.1. To achieve proper cell density, different cell culturing methods have been applied.

Table 2. 1. Estimated MSCs dosages required for different diseases.

Disease	**MSCs dose/patient (1×10^6)**
Cartilage regeneration	15-45
Bone regeneration	40-100
Osteogenesis imperfecta	3000-6000
Crohn's disease	120-1200
Myocardial regeneration	20-200
Graft-versus-host diseases (GVHD)	100-900

Immuno-modulatory therapy: Currently, Prochymal (a product of Osiris Therapeutics), which is obtained by MSCs isolated from from bone marrow of healthy male adults, has been assessed in phase III clinical trials for steroid-refractory GVDH. At the phase II trials, grade II-IV GVHD patients were randomized for 2 Prochymal dosages ($2/8\times10^6$ MSCs/kg) within the corticosteroid infusions. At the end of trials, 94% in overall response rate and very good remission rate of 77% was achieved by Prochymal from 32 participants. After 18 days with MSCs injection, most of the GVHD symptoms had disappeared. Regardless of the dosages, neither ectopic tissue nor administrative harm development occurred, the results showed ability of MSCs for the treatment of acute GVHD [24]. In May 2012, Health Canada approved Prochymal to treat acute-GVHD [25]. Since then there have been other studies with Prochymal applied in clinical trials for other diseases such as Crohn's diseases. In a phase l trial, Crohn's disease activity reduced by cell injection of autologous oriented MSCs on 9 patients with 2 different doses [26]. In a phase II trial, injection of allogeneic MSCs reduced Crohn's disease activity index and endoscopic index of severity value drastically deceased in patients with luminal Crohn's disease refractory to steroid treatment [27].

Bone regeneration: In clinical studies, it is shown that osteogenesis imperfecta, a genetic disorder in the formation of abnormal type l collagen in osteoblasts which leads to osteopenia, multiple fractures, acute bone deformation, and slow bone development, could be treated with allogenic MSCs treatment [28]. Further trials are done with six children treated with purified allogeneic bone marrow MSCs treatment for acute osteogenesis imperfecta. By the first 6 months of MSCs post-infusion, each patient injected with purified allogeneic bone marrow MSCs and 80% of the patient demonstrated engraftment on one or more tissue and accelerated growth velocity of median 70% compared to the control group. Over six-months of MSCs infusions, there was no toxicity appeared and no sign was found for the engraftment of cells expressing the neomycin phosphotransferase gene marker, which implies the possibility of cause immune responds to a foreign protein. Considering all of these clinical results, purified allogeneic bone marrow MSCs gave better therapeutic consequences than standard bone marrow transplantation [29].

Cartilage regeneration: Degeneration of articular cartilage in osteoarthritis is a common health problem. In phase I-II clinical trials *ex vivo* expanded autologous bone marrow MSCs have shown positive results in treating chronic osteoarthritis (OA). Patients (median age 52) with knee OA and grade II or III gonarthrosis and chronic pain were treated with a single dosage of an intra-articular infusion of 4.1×10^7 MSCs, and quantitative T2-mapping and MRI imaging at 0, 6 and 12 months were performed to measure the efficacy of the treatment. Results have shown that after 8 days of infusion there was a decrease in the pain and maintained after 12 months. The physical assessment also presented the improvements in body functioning at month 12. The T2-mapping shown the indication of cartilage healing in all patients at 12 months [30].

Myocardium regeneration: Acute myocardial infarction (AMI) due to its high mortality and morbidity have severely shorted human's life expectancy. Despite exiting treatments like coronary revascularization for ischemic myocardium, there are no effective treatment methods

against necrotic or non-functional myocardium [31]. MSCs improve left ventricular (LV) function and structure through varies effects such as neoangiogenesis, neomyogenesis and reducing fibrosis. The healing effects of autologous MSCs on cardiac structure and function, six patients have received an intramyocardial injection of autologous MSCs into myocardial areas with akinetic/hypokinetic properties. The composite score of MRI at 0, 3, 6 and 18 months was used to estimate scar, perfusion rate and wall thickness in the regions that received MSCs injections. After 18 months the patients received MSCs injections, demonstrating increased LV ejection fraction and decreased scar mass compared to the baseline [32].

Spinal cord injury (SCI) treatment: is an acute neurological damage results in functional lose and paralysis which requires medical maintenance [33] regardless of available treatments, such as surgical repairment, pharmacological intervention and rehabilitated techniques resulted in limited patient [34]. In recent studies, MSCs transplantation demonstrated a better future to SCI therapeutic approach [35]. Different type of cell types have been studied in pre-clinical and post clinical trials; including MSCs, umbilical cord blood and neural stem cells, induced pluripotent stem cells [36-40]. In a phase I trial pilot study, complete SCI patients had been selected, according to the thoracic level and time elapsed from injury divided into sub-acute SCI (less than 6 months) and chronic (more than 6 months). From patient's iliac crest, autologous bone marrow MSCs were isolated and cultured in GMP conditions to reach clinical usage. Quality controlled MSCs were injected back to patients, each patient received two or three injection with a dosage of $1.2x10^6$ MSCs/kg body weight. Despite of, during the observation prior no treatment-related adverse symptoms appeared, there was no significant enhancement of patient's condition reported [41].

2.2 Cell Culture Systems for Cell Expansion

Ex vivo cell expansion is a crucial step to obtain an adequate number of MSCs for therapeutic applications. In the laboratory condition, this is commonly done by growing MSCs in 2D culture systems, for example, expansion in T-flasks, using FBS containing DMEM, and

passaging with trypsin every 4-6 days [3]. 3D cell culture systems such as bioreactors are defined as devices which promote the control of biological or biochemical processes under critical parameters, such as dissolved oxygen, pH, temperature, biochemical input and output, including the level of crucial nutrients and metabolites [42] which capable of rapid and massive production of cells and biomaterials in a relatively short time.

2.2.1 2D Cell Culture Systems

Most of the AD stem cells were cultured on 2D monolayer surfaces. For example, Petri dishes, micro-well plates and tissue culture flasks (Figure 2.4) are commonly used in the laboratory because of convenience, easy use and high cell viability. MSCs are commonly expanded through 2D cell culture to reach sufficient clinically required dosages. MSCs expansion in cell culture is required to overcome the deficiency of MSCs found in the body. *In vitro,* MSCs can be cultivated for 8-15 passages and achieved about 25-40 fold population expansion within 80-120 days [43]. The restricted surface area to volume ratio offered by this classic cell culture approach limits the production of cells. For example, the culture area of T-flasks ranges from 12.5 to 225 cm^2. When a larger surface area more than 225 cm^2 required, results in more than one T-flasks used, take up more incubator space, and each flask needed individually maintaining and passaging. To eliminate this extremely labor-intensive process automated systems have been used, such as the TAP Biosystems SelecT device, which performs the actions of humans with a robotic arm, equipped with its incubator, capable of handling up to 182 T-flasks at the same time [44]. However, these are non-homogeneous systems which had several disadvantages: difficulties in taking cell samples, difficulties in scale-up, and limited potential for controlling and measuring the system, and the impossibility of maintaining homogeneous culture conditions. To eliminate these shortages, in the year of 1967 van Wezel introduced the concept of the microcarrier cell culturing system. In this concept, cells are seeded on the surface of small solid particles suspended in the culture medium at low agitation velocity. Then cells would attach to the surfaces of the microcarriers and grow to the confluence [45]. In other approaches, 3D scaffolds are taken into 2D culture to overcome its limitations. 3D scaffolds demonstrate porous structure which assist cell

expansion, migration and differentiation [46].

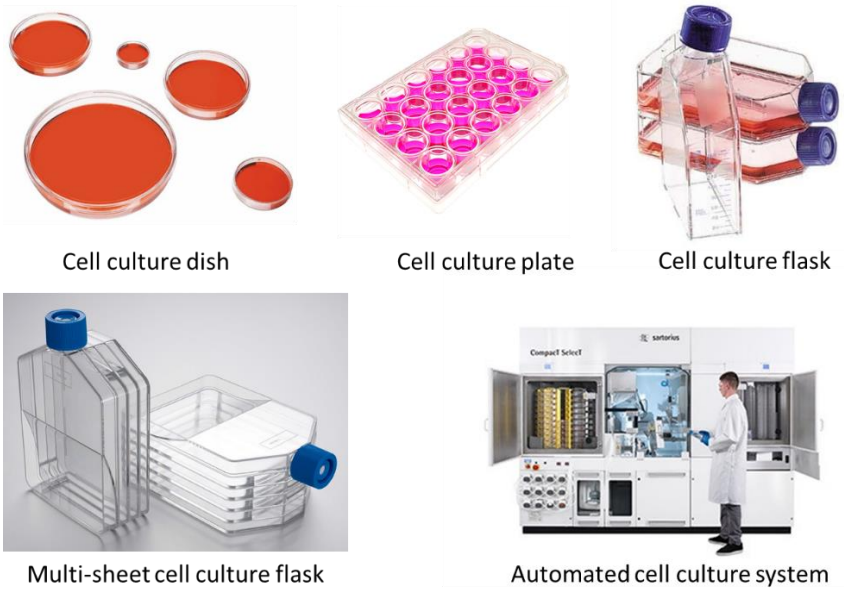

Figure 2.1. Different types of 2D cell culture systems.

2.2.2 3D Cell Culture Systems

The commonly used 2D cell culture systems are noticeably simple and have various crucial parameters demonstrating the cell and tissue physiology [47]. The intercellular communication between cells and interactions with the ECM establishes a 3D communication network that upholds the homeostasis and specificity of the tissue [48]. Organizing principles determined by cellular context had a major effect on the life cycle, including proliferation, migration and apoptosis [49].

3D cell culture systems re-establish physiological cellular interactions and cell-ECM interactions to mimic the real tissue better than 2D cell culture systems. The limited surface area to volume ratio offered by 2D cell culture systems creates a bottleneck in higher cell production. In comparison, 3D cell culture systems had demonstrated a larger free surface for cell expansion in a comparatively small volume [50]. Numbers of 3D systems (Figure 2.5.) have been developed for different types of tissue where the culture environments had played

significant roles. The main intention of these studies is to connect the dots between the application of animal specimen and cellular monolayers [47].

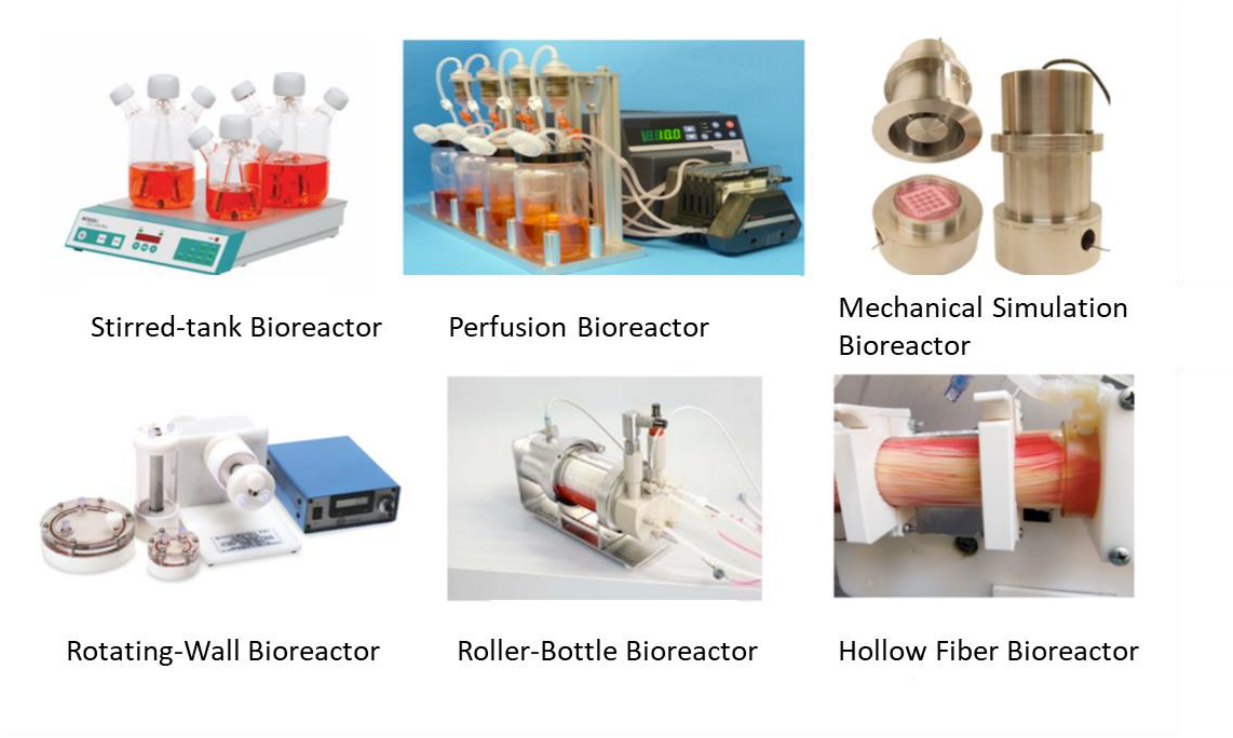

Figure 2.2. Different types of 3D cell culture bioreactors.

3D cell culture systems are critical to producing functional tissues under *in vitro* conditions in tissue engineering applications. In conventional tissue engineering, MSCs can be expanded in bioreactors with two different approaches which are with scaffolds and without scaffolds [51]. In general, isolated cells are seeded on biocompatible and porous tissue scaffolds under suitable culturing conditions, the cells achieved the required quantity for implantation.

The disadvantages in static cell culture studies, necrotic regions are formed inside the scaffolds due to the low-seeding efficiency [52-54] and nonuniform cell distribution within the scaffold interior caused the mass transfer problems [55].

2.2.2.1 Critical Parameters of 3D Cell Culture Systems

For the higher expansion rate of MSCs in cell culture, some critical parameters need to be optimized such as physicochemical variables including pH, temperature and dissolved oxygen concentration, and biochemical input, such as the concentration of essential nutrients and waste products, and growth hormones.

Oxygen tension is one of the essential components of the stem cell microenvironment which appears to affect stem cell expansion, maintenance and differentiation significantly. One study revealed the relationship between oxygen level and MSCs viability in cell culture [56]. Higher oxygen level cause oxygen stress may inhibit cell viability. In order to increase the expansion rate of MSCs, the role of low oxygen level (2%) on MSCs metabolism and kinetics have been studied. The results showed a higher cell expansion appeared at 2% oxygen compared to atmospheric oxygen levels. Also, at the oxygen levels between 2 and 5% the ESC-derived neural stem cells have shown higher cell proliferation without losing any multipotential ability.

Hydrodynamic shear stress: In stirred bioreactor, the kinetic energy generated by the impeller may influence the culture outcome through creating the intense turbulence. Outcomes the conformation of localized shear on the surface of a single cell, cell aggregates and microcarriers, which lead to cell damage [57]. In addition, the optimal value for hydrodynamic shear stress may differ among stem cell subtypes (e.g. $1\text{-}10^{-5}\text{-}1.2\ 10^{-4}$ Pa for human MSCs in 3D continuous perfusion and 0.005-0.015 Pa for human bone marrow MSCs in 3D perfusion bioreactor) need to be optimized individually [58, 59].

Growth factors are the significant players in manipulating stem cell behavior, including cell survival, cell growth and differentiation. For example, TGFβ influences cells originated from chondrogenic linage *in vivo*, enhancing mesenchymal condensation, proliferation, production of ECM and deposition of cartilage-specific molecules, at the meantime inhibiting the differentiation [60]. BMP-2 to BMP-7 are members of the TGFβ superfamily have affects on

bone formation. Mainly BMP-2/4/6 and 7 induce MSCs to form osteoblasts and have a significant impact on MSCs differentiation [61]. BMP-3, another member of the same family, increases MSCs proliferation threefold [62]. Furthermore, the complex multivariate interactions between other process parameters and growth factors complicated the optimization of culture medium. Hence, quantification of these interactions and optimization of the culture parameters are vital.

The concentration of nutrients and metabolites also influences cell expansion, cell differentiation and cell death in the culture. Glucose, as an energy source in cell metabolism, plays a central role for ATP generation. Mammalian cells use glucose through oxidative phosphorylation (1 mole glucose produces 30-38 moles ATP) or anaerobic glycolysis (1 mole glucose produces 2 moles ATP and 2 moles lactate) to generate energy. The inefficient metabolism of glucose leads to the accumulation of lactate [63]. The related study conducted with MSCs has shown that higher cell numbers lead to lower glucose concentrations in the culture medium. The specific glucose consumption rate also correlated with growth rate and shown a linear correlation [64]. It has been shown that while cells grow at high rate, cells consume more glucose compared to a lower rate.

However, the expansion rate is a function of both glucose consumption and efficiency of metabolism. The change of anaerobic glycolysis to oxidative phosphorylation resulted in the yield of lactate from glucose shift over time [63]. In another example, the human ESC metabolic study was evaluated, results in a high concentration of metabolic waste products, especially lactate accumulation, which lead to low pH, which could slow down cell growth and reduce the pluripotent cell number [65].

2.2.2.2 Mode of 3D Cell Culture Systems

Different modes of cell culture systems are used in MSC cultures as well as in bacterial cultures. The most commonly used modes are batch, semi-batch, continuous and perfusion [66]. Cell density, nutrients and metabolites concentrations, and culture system parameters can be demonstrated with mathematical formula with some kinetic equations, such as mass

balances and Monod equation. The modes of cell culture systems are presented below (Figure 2.6.).

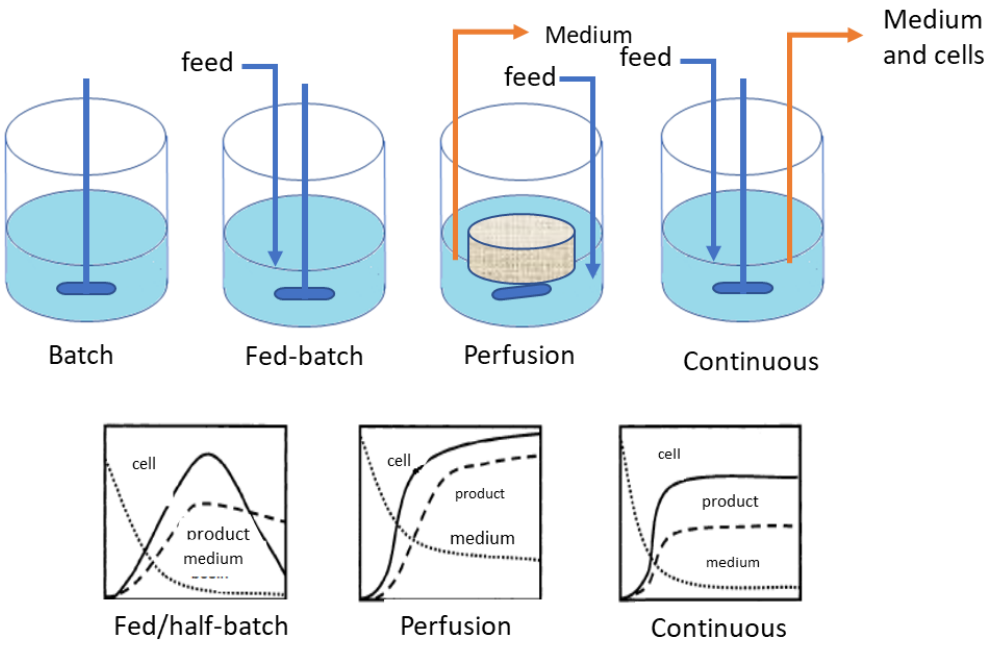

Figure 2.3. Schematic showing different cell culture modes (modified from [66]).

Batch systems include the mode of operation without any nutrient addition after cell inoculation. The working volume of the reactor is constant throughout the culture. On the one hand, as the cells proliferate, the nutrients present in the medium turn into metabolic residues at the end of cell culture. In the batch production process, all nutrients are introduced at the beginning of the culture, while oxygen, which plays a crucial role in intracellular metabolic reactions, is continuously fed from the sparger. In addition, base solutions such as sodium bicarbonate, sodium hydroxide and CO_2 gas are added externally for pH control. Due to its simplicity, the batch culture system is widely used. Generally, the cells use in large-scale studies are cultured in fixed flasks, mixed flasks or small and medium-sized bioreactors. Since the number of cells in the end of cell culture is generally lower than other operating systems, it can be said that the fed-batch system is inefficient. This is mainly due to the fact that nutrients cannot be added above certain limits initially. Because the medium inhibitions are described as a result of changes in osmotic pressure [67]. In addition, during batch production,

the medium of the cells is continuously changing. Again, the most crucial disadvantage of these operating systems is the inhibition effect of metabolites increasing towards the end of culture.

Half batch systems: This production method differs from batch production in that the nutrients consumed by the cell during culture are added to the culture from the outside. In the half-batch production process, the initial working volume is much lower than the final volume. During culture, the final volume is reached by adding medium or concentrated nutrients. The most important feature of the half-batch process is that the number of cells and product concentration is much higher than the batch system. It is possible to keep the culture period on average 7-10 days. In this way, the final cell number has been reported to reach up to 10×10^6 cells/mL [68]. In half-batch cultures, the accumulation of toxic metabolites negatively affects cell proliferation, viability and product formation, thus reducing productivity. Metabolites affecting most of the specified parameters are lactate and ammonia [69]. However, it is possible to reduce the formation of toxic metabolites by providing optimal feeding strategies. The most crucial characteristic of half-batch production is the need for a more complex operation than fed-batch culture, but on the other hand cell and product yields are significantly enhanced. Furthermore, compared to perfusion systems, due to its considerably short culture period makes validation relatively easy. Because of these properties, many biotechnology companies use this production method [70].

Continuous systems: The continuous operating system is based on the introduction of the fresh medium into the reactor at a continuous flow rate, on the one hand, the continuous removal of the homogeneous cell suspension from the reactor at a rate equal to the feed rate, thereby keeping the reactor volume constant. The continuous production process allows a well-defined description of the steady-state between nutrient concentrations in the bioreactor and different rates of biological reactions. Therefore, this operating method is a powerful tool for cell characterization [71]. The most critical limiting parameter in continuous cultures is the gradual decrease in the cell number. This is because the cell uptake rate at the reactor is

equal to or greater than the cell growth rate. The maximum specific growth rates in mammalian cells are between (μ_{max}), 0.02–0.05 h^{-1} (0.50-1 day^{-1}), thus cell uptakes usually not exceed $2x10^6$ cells mL^{-1} in studies.

Perfusion systems: In the perfusion operating system, which similar to the continuous operating system, the cells are immobilized in the reactor. However, the medium is circulated in the system at a specific flow rate. This system is the most complex but also the most efficient operating system. The use of spin filters that hold cells in bioreactors in perfusion cultures is well-known. This operating system has been widely used in laboratory and industrial production [70]. The most significant limitation of the continuous cell culture system, the low productivity caused by cells leaving the bioreactor, is eliminated. Mass equivalents of the nutrient and product are previously applied for continuous cell culture. Thus, the perfusion system can be applied in almost all reactor types. Also, heterogeneous bioreactors often work in perfusion mode. Homogeneous reactors can also be perfused if suitable separation devices such as spin filters are used. Although the maximum number of cells to be reached with the perfusion system in homogeneous reactors is reported as 10^7-10^8 cells/mL, when heterogeneous reactors are used, the cell number can reach much higher values, such as 10^9 cells/mL. Although the product concentrations reported in this production method vary, the most common range is 100-500 mg/L.

2.3 Bioreactors Used for MSCs Cultures

Various models of bioreactor have been applied for the scale production of MSCs, such as multi-sheet cell culture flasks, roller bottles, hollow-fiber bioreactors, stirred bioreactors and fixed-bed bioreactors. Additionally, specific bioreactors had been developed to simulate external forces to accelerate differentiation and maturation of the cells. In conclusion, nowadays many advanced bioreactors can maintain and monitor the culture environment from cell seeding to end of cell culture [72]. However, it is difficult to compare those different bioreactors because specific cell growth requirements may be different according to the bioreactor configuration. Despite the performances and maintenances and specific features of

bioreactors, the practicality of bioreactors must be considered thoroughly. The practical characteristics are listed below:

- User friendly operation
- Achievable cell numbers.
- Single-use parts
- Online sensing.
- Process control and automation.
- The simplicity of harvest.
- Cost and time efficiency.

The selection of bioreactors should be focused on the simplicity of use and attainable high cell nembers. Single-use bioreactors are desirable because there is no need for sterilization. The online sensing of environmental variables favor optimal condirions for cell proliferation. Uniform conditions can be provided by suspension bioreactors. Additionally, suspension bioreactors can save time and decrease operational costs by process control and automation. At the end of the cell culture, surface adherent MSCs are harvested from the substrates like hollow fibers, microcarriers and rigid or porous materials. Thus, ease of harvesting is desirable.

2.3.1 Spheroids

Cellular spheroids are created from hanging drop, concave plate, or rotating culture methods. Additionally, cellular spheroids can be obtained from various cell types, including MSCs [73]. Spheroids, form with the aggregation of cells, are simple 3D models obtained from different cell types. Self-assembly without solid tissue scaffold supports and any external or internal stimulus maturated its final form through self-organization mechanisms. Spheroids are the platforms for 3D cell culture. The advantages of the physical cell to cell connection, mass transport and mechanical properties demonstrate an enhanced model for toxicity study, drug delivery and metabolism analysis compared to traditional 2D cell cultures [74]. In a related study carried out in our lab, combined spheroids and organ-on-chips to establish drug-testing models for the liver [73]. The spheroid production was carried out by the hanging drop

method with hepatocyte and endothelial cells with the 2:1 ratio. After coated with hydrogel to mimic the cell micro-environment, spheroids put in the chips and with the help of a syringe pump, drug testing were carried out, respectively. After 7 days of dynamic culture with the use of a perfusion bioreactor at 5 μL/min flow rate, spheroids and hydrogel gave better cell viability and functionality which favors drug testing.

2.3.2 Roller Bottle Bioreactor

The concept of roller bottles (RB) as a new method for anchorage-dependent cells was first introduced in 1939 [75]. RB is a type of monolayer cell culture system which are cylindrical vessel made of plastic or glass that provide a relatively larger surface area compares to standard T- flasks. Unlike traditional T- flasks and multi-sheet flask, RB can prevent the formation and build-up of gradients which have a negative effect on the cells by allowing the agitation of the culture medium. In the meantime desired agitation speed ensures the thin layer of medium on the cells increasing the gas exchange [76]. Since then, roller bottles have been used in laboratory cell culturing and vaccine production for the biotechnology industry [77] and used to culture hMSCs and other cell types. In a recent study, in CO_2 free atmosphere human hematopoietic cells were cultured in RB with three different culture media, resulted in 17.25 ±3.65 fold of expansion with L-15 Leibovitz's medium which 10 times higher than static control cultures [78]. However, it is tough to manually control a large number of RB in a short time frame.

2.3.3 Microcarrier-Based Stirred Tank Bioreactors

Stirred tank bioreactors are uncomplicated vessels with a centrally located impeller which provides relatively even medium conditions through agitation. The impeller agitation speed is control by, for example, a magnetic stirrer under it or through the motor located on the top. Stirred tank bioreactor has different types of commercially available products, like PAD Rector (Pall Life Sciences), DASGIP Parallel Bioreactor system (Eppendorf) and MiniBio (Applikon Biotechnology). The benefits of stirred tank bioreactors are enabling a large amount of cells cultured in one vessel, eliminates production variability and reduces the costs

related to consumables and labors. At the main time, these bioreactors can operate in different modes. Such as batch, fed-batch and perfusion.

Additionally, these reactors also can be operated with online-monitoring computer-controlled equipment that capable of tight control over the pH, temperature, nutrients and dissolved oxygen concentration. Furthermore, single-use and closed bioreactor systems such as Cultibag STR and Sartorius AG (Germany) are capable of GMP production of cells in class C or D room standards [79]. To sum up, stirred tank bioreactors were commonly used to expand plastic adherent cells such as MSCs on microcarriers. Microcarrier-based stirred tank bioreactors provides a significantly higher surface area upon which cells attach and proliferate under homogenous condition. In a related study, adipose-derived human MSCs were cultivated on 50 L microcarrier-based single-use stirred tank bioreactor under 5% platelet lysate (PL) contained medium and achieved the highest amount of expansion up to date [80].

2.3.3.1 Microcarriers

Microcarriers (MCs) as Van Wezel's first description, are stirred culture systems that anchorage-dependent cells adhered to and growth on small microparticles which brought together the monolayer and suspension cell culture. MCs-supported bioreactors are similar to the traditional mammalian and microbial suspension cell culture, which generates a homogeneity in the culture medium. MCs have some significant advantages over the monolayer culture; increasing the MCs concentration can easily increase the surface to volume ratio. The homogeneity of stirred MCs suspension culture lets controlling and monitoring various types of culture medium parameters possible (e.g., pO_2, pH, concentration of lactose and glucose). Easy access conventional stainless steel and disposable bioreactor, which makes scale-up of MCs culture is much efficient. The use of microporous MCs decreases the damage of cells from stirrer; sparger generated shear force by preventing a direct collision. Cell to cell transfer allows scale-up MCs much safer to the cells due to no use of proteolytic enzymes [81].

Microcarriers are small beads, diameters between 100 and 300 microns. Typically made from various biocompatible materials, such as dextran, collagen and glass, those materials with different surface properties could alter the cell growth and phenotype. They can easily maintain the suspension states in culture media and deliver a high surface per unit volume. For example, micro-porous microcarriers (Cytodex 3 microcarrier) can deliver $30cm^2/cm^3$ in medium with 10g/L of bead loadings, in comparison T-flasks have a relatively small ratio ($3cm^2/cm^3$). Besides, providing higher surface area per unit volume, microcarriers also provide additional advantages of different operation modes like batch, fed-batch and perfusion and process control (pH, temperature, dissolved oxygen), easily sampling and homogenous culture condition via impeller agitation which makes situ harvest accessible [82]. Because of those advantages, a tremendous amount of research is being carried out in this system for both hMSCs [83] and other anchorage-dependent cell types [84]. Also, MCs made of biodegradable materials could be used as tissue scaffolds for *in vivo* transplantation [85].

In conclusion, these outstanding properties of MCs illustrate the benefits from large-scale use of MCs cell culture systems in vaccine production [86] and stem cell expansion [87]. Despite relatively simple scale-up production capability, stirred bioreactors require a large culture volume for the relatively low density of cells. A perfusion culture bioreactor with an appropriate medium perfusion rate can attain cell density between 10^6 and 10^7 cells/mL which is 10-fold higher than a suspension culture bioreactor [88, 89]. However, the performance of perfusion systems were deteriorated by complexity and difficulty in scale-up. In the other hand, packed-bed bioreactor (PBR) can deliver quite high cell density within a small size. PBRs have been extensively used in mammalian cell expansion and vaccine production [90].

2.3.3.2 General Properties of Microcarriers

As seen in Table 2.2, different types of MCs are available (Table 2.2), and these MCs can enhance cell attachment, proliferation and differentiation. Functional groups on the surface of MCs are critical. The functional groups can be positively charged amines or some biological components like gelatin, collagen type-1. Other ECM proteins and peptides can also be used

as coating materials for MCs. The shape and size of MCs may vary, but the sphere is the most widely used one. The reason for that is each MC should have the most prominent surface to volume ratio that can support cell growth for extended time period. This provides cells to go under several doublings. At the end of cell growth, several hundred cells will attach onto each MC surface. Explicitly speaking, diameters of 100-230 μm have reported being the best-preferred size for the spherical MCs [50]. To prevent non-uniform distribution of cells on the spheres, the size distribution of MCs should be low (±25 μm). To maintain the MCs in suspension, with minimum agitation rate, the density of MCs should be above 1 (1.02-1.05 g/mL). Besides, to lower shear acting on the cell and prevent cell detachment, oxygen delivery and agitation method need to be optimized. The structure of MCs should be strong enough to assist cell expansion while enduring physical foces in the culture. Moreover, MCs can be heat tolerant for steam sterilization and light transparent for direct observation of cells.

Table 2. 2. General properties of purchasable microcarriers [50].

Type	Microcarrier	Material	Surface property	Density
Positively charged	Cytodex 1	Dextran	Diethylaminoethyl	0.9-1.32 g/mL
	DE-52	Cellulose		
	DE-53			
	QA-52		Quaternary ammonium	
	P Plus 102-L		Cationic charged	
	FACT 102-L		Cationic charged and Collagen type-1 from porcine	
Collagen coated	Cytodex 3			
		Dextran	Collagen type-1 from pig	
ECM coated	Pro-F102-L	Polystyrene	Recombinant fibronectin	
Non/Negatively charged	P 102-L 2D MicroHex		Uncoated Tissue culture treated	
Macroporous	Cultispher G	Gelatin	Gelatin	
	Cultispher S	Cellulose Polyethylene and silica		
	Cultispher G			
	Cytopore 1		Diethylaminoethyl	
	Cytopore 2			
Aggravated	Cytoline 1		A slight negative charge	

2.3.3.3 Advantages of Microcarriers

The MC cell culture is a combination of suspension and monolayer cell culture systems. The MCs surfaces supports cell growth meanwhile the homogeneity of MCs in the culture medium is similar to the suspension culture system, which commonly applied in mammalian and microbial cell culture. The pros of the MCs cell culture are listed as:

High surface to volume ratio: It can be increased easily by manipulating the MC concentration. For example, 3mg/mL Cytodex in 1 L culture medium could provide a surface area of 13.2x 10^3 cm^2 is equal to 176 T-flasks with 75 cm^2 each. Thus, MC cultivation can reduce the consumption of space and the operation steps, leading to the decrease in the expenses and contamination [50].

Homogeneous culture condition: It is necessary to allow controlling and monitoring the pH, pO_2, and nutrient concentration of the medium. The results are highly reproducible. Simultaneously, samples taken from MCs culture can be directly used for microscopic observation and cell characterization [50].

Easy scale up accessibility: MCs culture can be scaled up with conventional disposable or stainless-steel bioreactors commonly used for the expansion of suspended mammalian cells.

Microporosity: This property of MCs can prevent cells from shear stress generated by the stirrer, impeller or magnetic spinner in the bioreactor [85].

Cell-to-cell transfer: This is a unique ability of MCs culture without using proteolytic enzymes which may damages cells under the cell harvesting process.

Perfusion culture compatibility: Due to MCs culture, the medium can easily be harvested by decantation or filtration, which makes MCs can efficiently operate on perfusion culture [50].

Propagation of cells in 3D culture: MCs can be used as scaffolds to understand the co-culture and cell to cell interaction in culture medium [50].

Biodegradability: A significant advantage of biodegradable MCs makes *in vivo* transplantation of cells possible [85].

2.4 Applications of Packed-Bed Bioreactors in Cell Culture

Microcarrier suspension cultures are simple to deliver a large surface area for adherent cell culture. However, the empty microcarriers do not contribute to the total surface area available to the culture. As an outcome, microcarriers do not reach confluence equally; this requires frequent passaging to overcome unbalance cell distribution [91]. Microcarrier cultures also require agitation to eliminate the formation of nutrient concentration gradients. The shear forces generated from agitation must be carefully set to prevent compromise MSCs differentiation ability during the expansion [81]. Packed-bed bioreactors are providing a continuous and connected surface area and potentially solved the shear forces problem.

Additionally, in perfusion bioreactor cell density is between 10^7 and 10^8 cells/mL which ten times higher than suspension culture. Due to the high cell density, the yield of perfusion bioreactors could be 10-fold greater than the same volume of suspension culture. In other words, perfusion cell culture takes 10-time smaller space than suspension culture [89].

PBR system delivers relatively high yield of production within a small size, which has been applied to produce immobilized mammalian cells in perfusion culture. The application of PBR in bioprocess starts early, the first application was the culturation of foot-and-mouth disease virus (FMDV) on host BHK cells and the glass bead diameter was 3 mm. This PBR was scaled up to a 100 L system with 30 L working volume which achieved 1000-fold of production yield in the 1970s [92]. During the 90s, porous glass spheres (SIRAN®) used as packing materials, and packed-bed volume increased from 0.01 to 5.6 L. It is clear to see that, PBRs have a positive effect on cells viability [93]. Besides, circulation of medium is oxygenated before entering the PBR, improving the oxygen distribution on the cells [94]. The most desired feature of PBR is the continuous and radial circulation growth medium passing though the packed-bed material [95]. Therefore, PBRs had been used for mammalian cell cultivation and proven to achieve the highest cell density in small scales, and the largest volume of PBR is 30 L, as reported [96]. In a related study, a disposable PBR was used for

MSCs culture with comparative analyses. An initial population of 1×10^7 MSCs was inoculated in 25.0 g of Fibra-Cel® disks with 2.5 L of culture medium and incubated at 37℃ and 5% CO_2 condition the 10% of medium exchange performed every day. The end of the cell culture packed-bed bioreactor achieved 9-fold of expansion with the specific doubling time of 2.8 days (67.2 h) in 9 days [97].

2.4.1 Packed-bed Bioreactor Configuration

Packed-bed bioreactors presents multiple advantages such as cell-cell or cell-matrix interaction provide a better mimic of *in vivo* delicate structure and a low-stress environment with a high surface area and high aeration rate is beneficial for cell growth. Additionally, this bioreactor capable of different flow streams such as growth medium down-stream, up-stream or the both, pass through the immobilized cells within the packed bed.

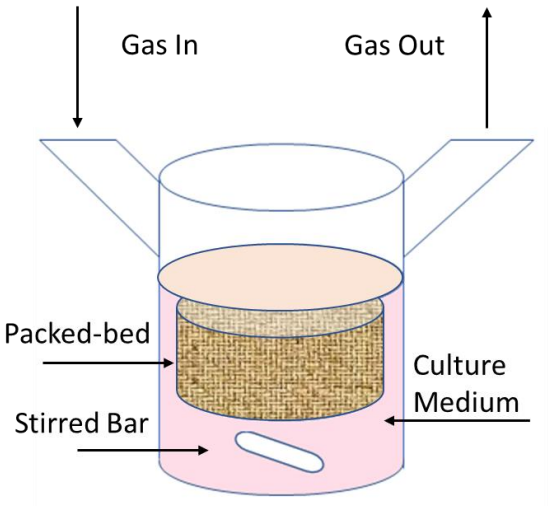

Figure 2.4. Schematic diagram of packed-bed bioreactor.

Generally, PBRs had four major components, i.e., packed-bed which carries the cells on or within carriers (shown in Figure 2.7.), an agitation unit homogenized the culture medium, an air pump and a reservoir used to contain oxygen-rich nutrient medium through the packed-bed [93]. Besides, the flow of the culture medium in the reservoir can be set parallel to the

longitudinal axis of the bed, or medium flow radially (Figure 2.8.) [96]. One of the common approaches in optimizing PBRs is to use a compact system to figure out the optimal packing materials for the particular cell in the study. The optimal packing materials could provide the essential requirement for cell attachment, productivity and proliferation. Then, it is possible to optimize packed-bed height, volume, medium perfusion rate, the linear velocity of the medium, etc. Thus, optimization experiments are generally performed at a laboratory-scale.

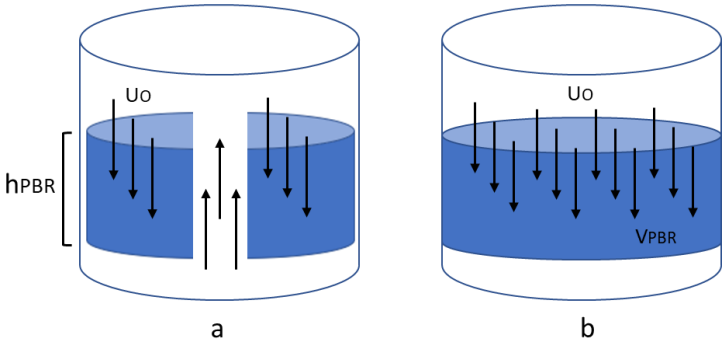

Figure 2.5. The (a) external and (b) internal medium circulation of packed-bed. The parameters are volume (V_{PBR}), height (h_{PBR}), bed (U_0) and linear velocity.

There have been significant numbers of research conducted to develop PBRs, the packing materials, operation parameters and cell densities operated with different cells (Table 2.3.).

Table 2. 3. A brief summary of animal cell culture studies used PBRs [96].

Material	Recirculation type	V_{PBR} (l)	h_{PBR} (cm)	U_{PBR} (mm/s)	$X_{max,PBR}$ (cells/ml)	Run time (days)	Cell type (product)
Glass / Bead	External	0.03–30	3.5 –	0.33	1.4-1.5 × 10^6	4–5	BHK
Fibers	Internal	1.2	10	3.7	6.8 × 10^7	66	CHO (γ-interferon)
Fibra-Cel®	Internal	1.75		–	3 × 10^7	35	CHO (r-hEPO)
		0.5–1.0	14.6	~ 10	1.0–1.2 × 10^8	30	Hybridoma (IgG1)
Cytodex 3	External	0.05–0.35	–	–	–	–	Rat hepatoma (H4IIE)
NWF			–	–	2–5 × 10^7	< 6	Porcine hepatocytes

2.4.2 Packing Materials

In early 1953, solid glass breads were identified as an appropriate material for growing cells as packing material. However, the surface to volume ratio of solid spheres available for cell growth is very low and maximal cell density is 1×10^6 cells/mL. To overcome this issue, in the 1980s, SIRAN® porous glass spheres were introduced that provide a much higher surface to volume ratio compared to solid spheres, and the cell density increased up to ten-times to 1×10^7 cells/mL. However, SIRAN® porous glass sphere is still restricted by its oxygen diffusion limitation caused by comparatively low internal porosity.

At the early stage, PBRs were focused on packing materials. The requirement of carrier materials for PBRs summarized as below:

1. High surface to volume ratio
2. Simple physical configuration and non-toxicity
3. Optimum diffusion rate

4. High chemical and mechanical solidity
5. Support of non-adherent and adherent cells
6. Chemically and biologically stable
7. Economical and reusable
8. Autoclavable
9. Non-animal origin

Non-woven polyester, polypropylene screen, ceramic spheres and glass fibers are the next generation of packing-materials, which delivers much higher internal porosities ranging from 0.80-0.95 [96]. The physical characteristics of the packing materials were summarized in Table 2.4. Among these new materials, Fibra-Cel® raised quite a popularity, which mainly developed for PBR application, requiring a high rate of medium perfusion [98]. Fibra-Cel® is commercially available and manufactured under GMP guidelines. Fibra-Cel® disks are made of non-woven polyester fiber (NWPF) meshes with high porosity and provide an efficient attachment for cells and higher intra-carrier diffusion rates. Also, they provide favorable conditions for achieving to high cell density. Therefore, Fibra-Cel® has been regularly applied for small scale animal cell culture.

In summary, SIRAN® and Fibra-Cel® are the most frequently used packing materials for PBRs. Because of their multi-functional orientation, they can be used to entrap adherent cell and cell aggregates. Furthermore, they have been successfully used in serum-free medium [96].

Table 2. 4. Physical characteristics of cell carriers for PBRs [96].

Type	Material	Size (mm)	ε_{matrix}	S/V (1×10^3 m^{-1})
Glass	Spheres	3	0	2
	Hollow cylinders	9/25	0	0.9
	Fiberglass mat	0.02	0.91	15
Cytodex-3	Collagen cross-linked dextran	0.2	–	34
Fibra-Cel®	Non-woven Polyester fiber	6/0.5	0.90	119
NWPF	Non-woven Polyester fiber	15/0.2	0.90	119
Polyester	Non-woven Polyester fiber	0.55	0.94	119
BioNOC II™	Polyester	5/10	0.94	15

**Size: diameter / length, ε_{matrix}: internal porosity, S/V: surface-to-volume ratio.*

2.4.2.1 Poly (ethylene terephthalate) (PET)

PET is a semi-crystalline, semi-aromatic and thermoplastic polyester, shown in Figure 2.9, which has high transparency, strength, nontoxicity and insolubility in a wide range of solvents. This polymer used in the textile industry and finds applications in packaging, high strength fibers and filtration membrane manufacturing, and the biomedical field. To acquire new application practices such as packing material, PET is required to obtain specific chemical functional groups on its surface [99].

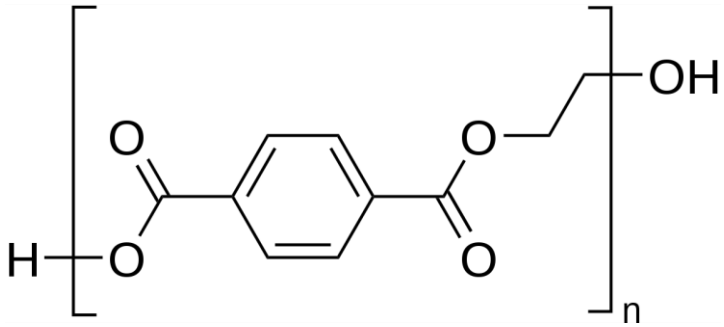

Figure 2.6. Chemical structure of PET.

Surface modification of packing materials has a positive effect on cell expansion and cell proliferation. The development of packing materials for cell expansion creates a perfect surface that can provoke specific cellular responses and maintain cell phenotypes. The improvement in the biocompatibility of packing materials for cell expansion by directed surface modification contributes to packing materials development. Among many packing materials used for cell expansion in packed-bed bioreactors, polyesters such as PET, have been well documented for their excellent biocompatibility, biodegradability and non-toxicity. Therefore, PET has been approved by the US Food and Drug Administration [100]. Despite that, low hydrophilicity and the lack of natural cell-binding sites on the surface of PET have significantly limited its potential in the packed-bed bioreactor as packing material. Therefore, introducing chemical functional groups or bio-molecules to the polyester surface, which improves cell attachment and proliferation, becomes more important [6].

2.4.3 Surface Modification of Packing Materials

In recent years many types of research and advances have been made in polyester surface modification. The advancement of new surface modification techniques to alter polyester surfaces categorized into three groups: morphological, chemical group/charge and biological molecules modifications [101]. For the development of packing materials with suitable properties that improve the biological interactions, surface modification approaches are effective methods. In a packed-bed bioreactor, cell adhesion to packing material is critical because cell adhesion occurs before cell expansion, cell migration and differentiation.The surface modification methods, as shown in Table 2.5., that can be used to manufacture different packing materials.

Table 2. 5. Surface modification methods are used to produce biomaterials in different surface properties [101].

Type of modification	Property of the modified surfaces
Morphological	1. The coating encourages tissue ingrowth. 2. For dental implants: epithelial down growth was inhibited and bone formation was increased on the implant.
Chemical	1. Higher surface energy and cross-linking on polymer surface increase the hardness of the surface and tissue adhesion. Decrease surface permeability. 2. Techniques such as plasma treatment produce negatively charged (acidic and sulfonate) or positively charged (amino). surfaces by adding new functional groups on the surfaces. 3. Successive application of chemical and structural changes to enhance corrosion or wear resistance 4. Immobilization of macromolecules to decrease cell adhesion and protein adsorption.
Biological	1. Immobilization of phosphorylcholine reduces protein adhesion and cell attachment for the blood-contacting surface. 2. Growth factors, fibronectin like proteins or RGD can be immobilized on surfaces to improve cell attachment and cell proliferation.

2.4.3.1 Morphological Modification

Morphological surface modification is a practical and straightforward approach to alter the biological properties of packing materials. Since morphological modification simply changes the outer surface structure of packing materials, but the bulk properties are kept unchanged. In comparison, chemical modification and biological modification which can provide chemical groups and biological molecules added to the surface of packing materials, increase the cell attachments and proliferation. The interaction between cell and packing material is an

essential step in evaluating surface modification efficiency and quality. Interactions between packing materials and cells are determined by its physical and chemical properties such as surface porosity, geometry, hydrophilicity, ionic interaction, electric charge and coatings of biological molecules [5-8]. In a related study, the role of the porosity and non-woven PET fiber diameter on the osteogenic differentiation of MSCs was investigated. Cell experiments indicate that more MSCs attached to the thicker PET fibers than that of the thinner ones and bigger fiber diameter of fabrics with bigger porosity increase MSCs proliferation rate [102]. Thus, surface modification method and cell interaction efficiency need to be optimized through *in vivo* studies.

2.4.3.2 Chemical Modification

Surface properties of packing materials in PBRs are important for achieving high biocompatibility and performance. Thus, surface modifications related to surface chemistry and topography are essential to overcome negative effects and improve *in vivo* responses. Chemical modification of polymers surface could categorize in three different approaches: i) chemical methods, ii) photo-induced grafting modification methods and iii) plasma grafting and plasma treatment. In general, polymers with biodegradability such as poly(lacticacid) (PLA) or poly(glycolicacid) (PGA) could be used for generating surfaces with high a hydrophilicity and roughness for the attachment of cell. This can be achieved through a surface modification with an alkaline solution when a hydrophobic polymer is chosen. In a related study, surface hydrolysis of PET with NaOH solution could improve the attachment efficiency of BMSCs [103]. The hydrolysis process of PET is given in Figure 2.10.

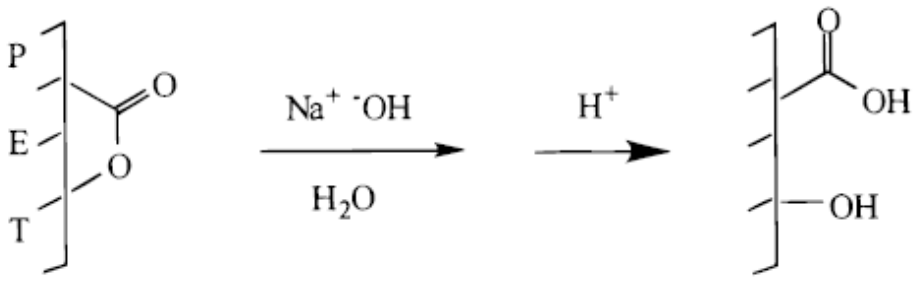

Figure 2.7. The hydrolysis reaction of PET fiber [104].

Different chemical modifications had also been used in a different study to modulate the PET membrane chemical composition and hydrophilicity. Thus, the PET membrane was sterilized and oxidized with 5% (w/v) $KMnO_4$ in 1.2 N H_2SO_4 for 1 h at 60°C. Then, washed with 6N HCl to remove the $KMnO_4$ and rinsed with water to restore pH 7. The radiochemical assay has shown that the treated-PET membrane has significantly more -COOH functional groups than the non-treated-PET, which changes the surface morphology and improves the hydrophilicity of the PET membrane according to the SEM and water contact angle results [105].

2.4.3.2 Biological Modification

Biomacromolecules such as ECM proteins (fibronectin, vitronectin, collagen) and their derivatives are important signals from biological origin for anchorage dependent cells. The initial cell adhesion and cell migration occur through ECM proteins. These proteins have a Arg-Gly-Asp (RGD) sequence (cell-binding domain) that provide specific recognition among the cell surface adhesion receptors [106]. Cell adhesion is the most important issue when polymeric materials with degradation properties are used as packing materials in PBRs [96]. The cell attachment and interactions between the biomaterial and cells will determine the cell`s ability to grow in contact with the material [107]. Different biological modification methods are given in Table 2.6.

Table 2. 6. Biological modification approaches.

Modification	Mechanism	Method
Chemical grafting	The cell adhesion and biocompatibility increased by the immobilization of bioactive peptides, proteins and other molecules	Plasma grafting, chemical and photochemical grafting
Surface coating	The cell affinity enhanced with the immobilization of bioactive molecules such as growth factors	Physical adsorption
Entrapment	The hydrophilicity and blood compatibility increased by the immobilization of water-soluble biomolecules	Entrapment or immerse in a mixture solvent
Electrostatic self-assembly	The cell adhesion or differentiation manipulated by the immobilization of charge, hydrophilic or bioactive molecules	Polycations alternately and depositing polyanions

2.4.3.2.1 Collagen

Collagen, as a member of the ECM proteins family, is the primary building block in the various connective tissues in the body. The name “collagen” is originated from the Greek language meaning “glue” this refers to the early usage of collagen as animal glue isolated from animal skin and tendons. Collagen exists in many different forms; 30 types of collagen have been identified and divided into several groups depending on structure form and all of them contain at least one a triple helix, shown in Figure 2.11. [108]. The collagen helix is a dominant shape in secondary structure, contains a repetitive amino acid sequence of glycine, proline and hydroxyproline [109]. Besides, over 90% of the collagen in the human body is type I collagen.

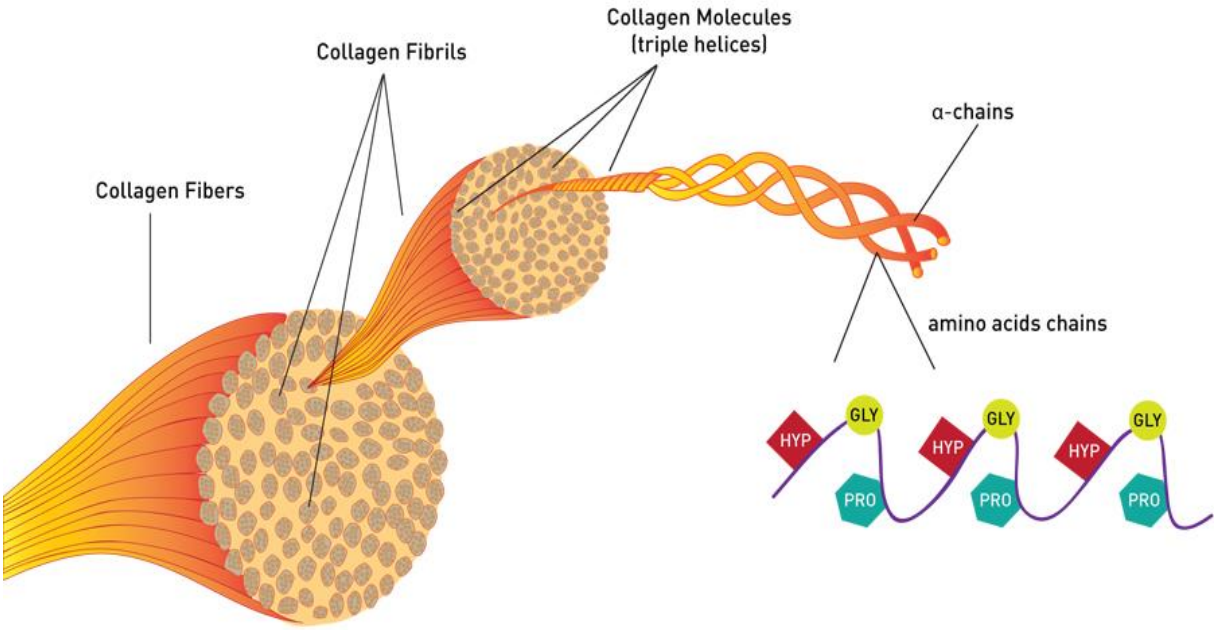

Figure 2.8. Structure of collagen protein.

Collagen has been widely used in laboratory studies to investigate cell behavior and cellular interactions between the biomaterials. In a recent study to increase the performance of PLA membranes for skin tissue, researchers treated the PLA surface by sodium hydroxide followed by collagen type-I coating. Murine and human fibroblast cells were used and cell culture results have shown that the PLA surface was altered by hydrolysis that supported keratinocyte proliferation. This effect was also seen on the collagen-coated PLA surfaces. This work suggested that surface modifications without collagen coating could achieve the same effect [110]. However, collagen-coated biodegradable polymer nanofiber meshes showed positive effects on cell migration, proliferation and adhesion of human endothelial cells in cell culture study [111]. Above all depiction, the collagen coating on the surface of polymers used in cell culture needs further investigation.

2.4.3.2.2 Vitronectin

As a member of the glycoprotein of hemopexin family which was found in ECM, bone and serum, vitronectin (VN) exists in a single chain or clipped form which bond with a disulfide bond. Vitronectin promotes cell adhesion and spreading through binds to integrin alpha-V

beta-3 [112]. The structure of vitronectin is shown in Figure 2.12. represents a 75kDa glycoprotein which consists of 459 amino acid residues. The protein is relatively small, consisting of 3 domains.

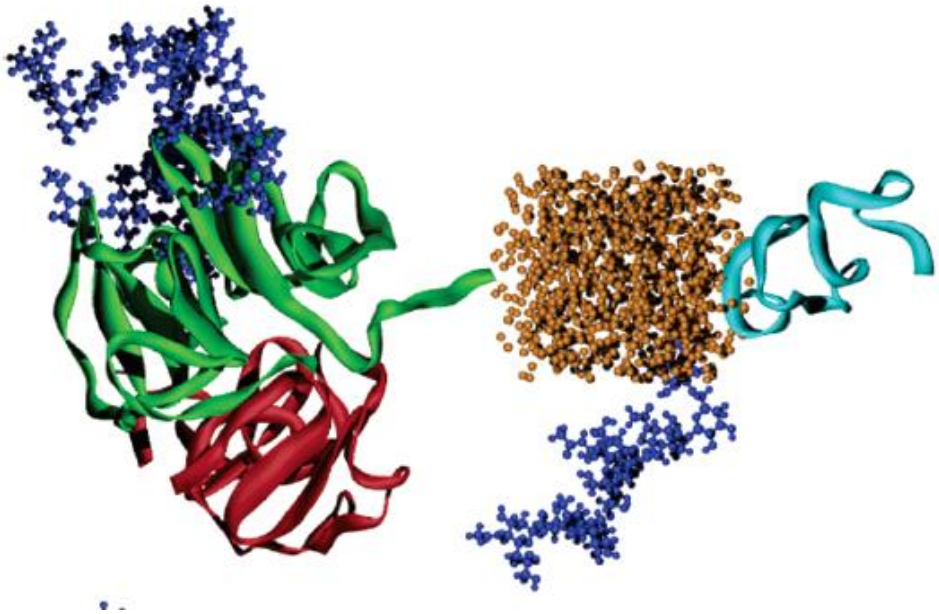

Figure 2.9. Molecular structure of vitronectin [113]. The green: central domain, the red: heparin-binding domain, and the blue: carbohydrates.

Vitronectin, known as an adhesion-mediating protein, has been used in stem cell culture frequently. Vitronectin adsorbed polymer surface was explored for the continuous passage of hESC culture. Cells on the VN-coated TCPS kept their karyotype after the 10^{th} passages and higher cell expansion rate. Also, VN-coated TCPS presented hydrophilicity which water contact angle around 65°. VN-coating on polymer surface gain the same performance of Matrigel which has a highly complex hydrogel composition [8]. The efficiency of VN-coating on 3D culture surfaces was also investigated. The polystyrene microcarrier surface was coated with vitronectin and laminin at two different densities of 450 or 650 ng/cm^2 through absorption. 3D cell culture studies indicate that long term proliferation of hESCs on VN-coated microcarrier with at least 90 % of pluripotent markers expression and maintaining the karyotypic normality. The average yield obtains on the VN-coated microcarrier was 8.5 ± 1.0 [114], demonstrating the full potential of VN-coating and implementation of this technology will benefit the development of packing material in the packed-bed bioreactor.

3. MATERIALS AND METHODS

The thesis study aims to investigate the expansion of rAdMSCs in the packed-bed bioreactor using commercially available product Reemay® non-woven Polyester, Poly (ethylene terephthalate) (PET) mesh, as packing material. In the related literature, it has been shown that hydrophilicity favor to the cell attachments and PET had a high degree of hydrophobicity which inhibits the cell attachment. Thus, surface modification studies were carried out to eliminate the high hydrophobicity of PET disks. The graphical abstract of the present study is shown in Fig. 3.1.

In the first step, the surface hydrophilicity of PET discs (6 mm diameter) was enhanced with sulfuric acid or sodium hydroxide treatment. Then the surface of discs were coated with collagen type 1 through dropping or immersion techniques. Vitronectin was coated by dropping technique. The modified surfaces were characterized with scanning electron microscopy **(**SEM) and energy dispersive x-ray spectroscopy (EDS) analyses. The amount of collagen type 1 coated onto the discs was quantified by hydroxyproline analysis. Static cell culture studies were carried out with rAdMSCs in alpha-MEM medium containing 15% (v/v) FBS and 0.8% (v/v) antibiotic mixture (penicillin, gentamicin and amphotericin B). The effects of different modifications on cell expansion were evaluated by cell counting, MTT tests and fluorescent microscopy. In the dynamic cell culture studies, rAdMSCs were seeded on sodium hydroxide treated PET disks as packing material depending on the results obtained from cell culture studies and production costs. Two different cell seeding densities were studied in order to adjust glucose concentration in the bioreactor throughout the culture. Cell growth was visualized with DAPI and cell activities were determined via MTT tests. Following dynamic cell expansion, differentiation capability of harvested rAdMSCs were also investigated.

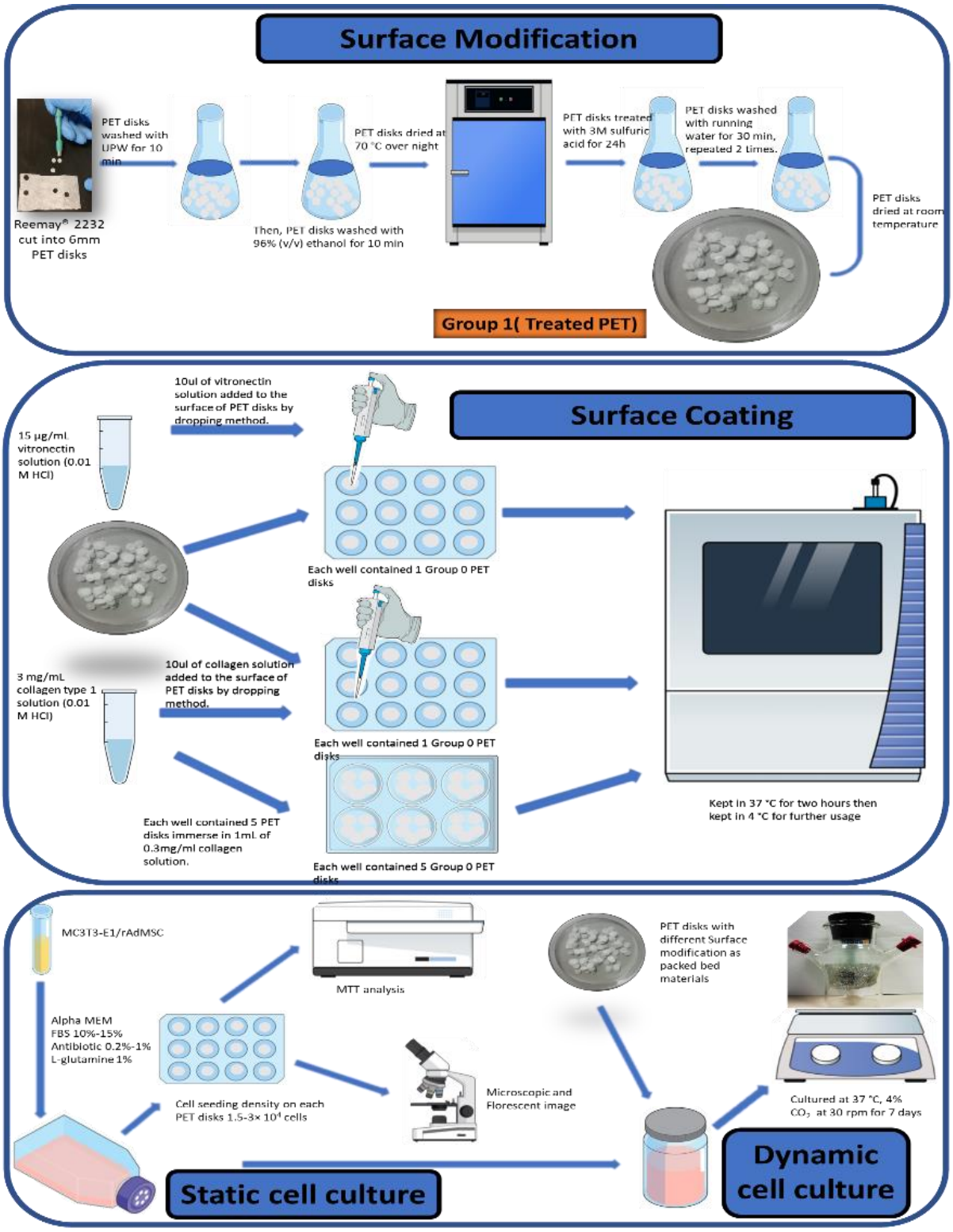

Figure 3. 1. Graphical abstract of the thesis study.

3.1. Materials used in the Experiments

Reemay® non-woven polyester fabric (NWPE, USA) used in this study was supplied by the laboratory. Biopsy punches with a diameter of 6 mm (Kai Medical, Japan) were used to cut the samples in a 6 mm diameter disk shape. For surface modification of PET disks, sodium carbonate (Na_2CO_3) and sodium hydroxide (NaOH) were purchased from Sigma-Aldrich (USA). Absolute ethyl alcohol was bought from Alka med (Turkey). The sulfuric acid (H_2SO_4) used for surface modification was obtained from Merck (Germany).

Collagen type-1 (Human) and Vitronectin (Human) used in PET disks surface coating were obtained from Thermo Fisher (USA) and hydrochloric acid used to dissolve collagen and vitronectin was purchased from Riedel de Haen (Germany). 2-(N-morpholino) ethane sulfonic acid (MES) sodium salt, 1-ethyl-3-dimethylaminopropyl carbodiimide (EDC) and ninhydrin were obtained from Sigma-Aldrich (Germany). N, N- dimethylformamide (DMF) and N hydroxy succinimides (NHS) were purchased from Merck (Germany) and Fluka (Switzerland), respectively. For sterilization of PET disks, ethanol was brought from Sigma-Aldrich (USA). The MC3T3-E1 and rAdMSC cell lines were obtained from the cell bank in our laboratory for previous culture studies. Minimum Essential Medium alpha modification (α-MEM), fetal bovine serum (FBS) used in cell culture studies, Trypsin -EDTA, Dulbecco's phosphate buffer saline (PBS), L-Glutamine, penicillin-streptomycin, gentamycin, and amphotericin B were purchased from Capricorn Scientific (Germany). Dimethyl sulfoxide (DMSO) was purchased from Biowest (USA). To determine the mitochondrial activity of the cells 3- [4,5-dimethylthiazol-2-yl] -diphenyltetrazolium bromide (MTT) and isopropanol were obtained from Sigma-Aldrich (USA). Glutaraldehyde used in fixation of cells for SEM analysis, TritonX-100, and crystal violet used in cell staining were purchased from Sigma-Aldrich (USA). Alexa Fluor 488 Phalloidin conjugated F-actin antibody and 4-6-diamidino-2-phenylindole (DAPI) were obtained from Invitrogen (USA). For the collagen analysis, Hydroxyproline, Chloramine T, and p-dimethylaminobenzaldehyde were purchased from Sigma-Aldrich (USA), perchloric acid and sodium hydroxide were obtained from Merck (Germany).

3.2. Preparation of Non-Woven Polyethylene Terephthalate (PET) Disks

Non-woven polyethylene terephthalate meshes were cut into a disk shape with a diameter of 6 mm biopsy puncher. After that, PET disks were weighted and quantified for further usage.

3.2.1. Surface Modification of PET Disks

Different surface modification methods were applied to PET disks in order to increase their hydrophilicity. Changes in the PET disk surfaces were characterized by water contact angle measurements, scanning electron microscope (SEM), Energy-dispersive X-ray spectroscopy (EDS) and Attenuated total reflectance-Fourier transform infrared (ATR-FTIR) analyses.

3.2.1.1 Sulfuric Acid Treatment

In the sulfuric acid treatment, the degradation of PET surface occurs due to the presence of sulfuric acid. In the related literature it has shown that the different concentrations of H_2SO_4 and different reaction temperatures resulted in different level of hydrolysis [115]. The hydrolysis of PET takes place according to reaction given below (Eqn 3.1.). Details of procedures that were applied were presented in Table 3.1.

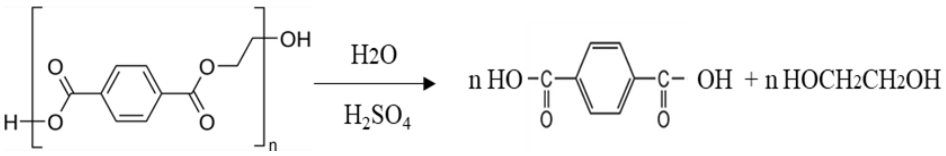

Equation 3. 1 Hydrolysis reaction between sulfuric acid and PET.

Table 3. 1. Sulfuric acid treatments applied to the PET disks.

Group name	Method	Reference
Group 0-PET-blank	• PET disks were first washed 10 min with ultra-pure water, then, treated with 96% (v/v) ethanol for 10 min. • PET disks were dried at 70 °C for 1 h.	-
Group 1-Na_2CO_3-0.3M-H_2SO_4-C(+)	• PET disks were washed with 1% (w/w) Na_2CO_3 solution at 80 °C for 1 h. • Then, they were treated with 0.3M sulfuric acid solution for 15 min and cured at 110 °C for 6 min. • In the final stage, the disks were washed 2 times with ultra-pure water and dried at room temperature.	[7]
Group 2-Na_2CO_3-3M-H_2SO_4-C(+)	• PET disks were washed with 1% (w/w) Na_2CO_3 solution at 80 °C for 1 h. • Then, they were treated with 3M sulfuric acid solution for 15 min and cured at 110 °C for 6 min. • In the final stage, the disks were washed 2 times with ultra-pure water and dried at room temperature.	[7]*
Group 3-EtOH-3M-H_2SO_4	• PET disks were washed with ultra-pure water for 10 min, followed by 10 min with 96% (v/v) ethanol. • They were dried at 70 °C for 1 night. • Then, PET disks were treated with the 3M sulfuric acid solution for 24 h. • In the final step, the treated disks were washed 2 times with flowing ultra-pure water for 30 min and dried at room temperature.	[4]

* Procedure give in related reference procedure was modified.

Abbreviation: C (+): curing was applied.

3.2.1.2 Sodium Hydroxide Treatment

Alkaline hydrolysis in sodium hydroxide (NaOH) solutions at moderate temperatures (70–95 °C) shown to be very effective at depolymerizing of PET [116]. PET disks were boiled in 0.05 M NaOH solution for 1 h to expose carboxyl group and washed 3 times with water. The hydrolysis of PET takes place according to reaction given below (Eqn. 3.2.):

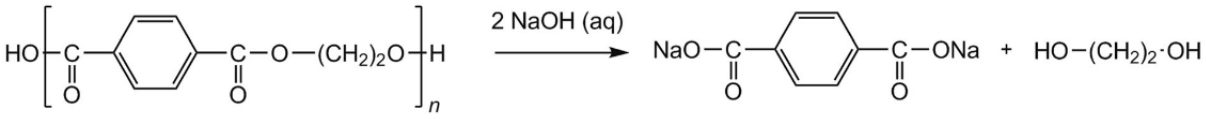

Equation 3. 2 Hydrolysis reaction between sodium hydroxide and PET.

Details of procedures that were applied were presented in Table 3.2.

Table 3. 2. Sodium hydroxide treatments applied to the PET disks.

Group name	Method	Reference
Group 0-PET-blank	• PET disks were first washed 10 min with ultra-pure water, then, treated with 96% (v/v) ethanol for 10 min. • PET disks were dried at 70 °C for 1 h.	-
Group 4-EtOH-0.05 M-NaOH	• PET disks were washed with ultra-pure water for 10 min, followed by 10 min with 96% (v/v) ethanol. • Then, PET disks were dried at 70 °C for 1 night. • PET disks were boiled in NaOH aqueous solution for 1 h to expose carboxyl groups. • In the final step, the treated disks were washed 2 times with flowing ultra-pure water for 30 min and dried at room temperature.	[103]

3.2.2. Water Contact Angle Measurements

The water contact angles of non-treated PET disks and 4 different surface-treated PET disks were measured with sessile drop method. Each group had three parallel measurements and each disk washed with ultra-pure water and dried at room temperature before testing. Disks were separately placed in the platform of Krüss DSA 100 (Germany) and 10 μL of deionized water was dropped on the surface of the disks at room temperature. The water contact angle on the PET disk was measured by Krüss DSA 100 software.

3.2.3. SEM and EDS Analysis

Surface morphology, the fiber structures of surface treated PET disks were visualized by SEM and elemental composition of surfaces were determined via EDS analyses. Samples from 4 groups of surface-treated PET disks were washed with ultra-pure water and dried at room temperature. Then, covered with gold-palladium and analyzed by SEM (TESCAN GAIA3 Triglav ™, USA). During SEM analysis, surface chemical composition was analyzed pointwise with Oxford Xmax 150 Energy Dispersion X-ray Spectrometer (EDS) integrated into the SEM device.

3.2.4. Mechanical Strength Analysis

Texture analyzer (TA. XT plus 100, Stable Microsystem, UK) was used to determine the structural integrity of modified PET disks after surface modifications. PET mesh was cut into 10 cm × 1 cm shape and each of them was treated with different surface modification methods mentioned above. The PET mesh was placed in a texture analyzer, 1 kg of weight was put on the drag with a speed of 1 cm/min. The results were monitored through texture analyzer software and the mechanical integrity of each group was determined.

3.2.5. Cell Culture Studies

To study the cell adhesion and cell expansion on the surface treated PET disks, the MC3T3-E1 cell line was seeded on the surface of modified PET disks. Accordingly, surface treated PET disks were sterilized with 70% ethanol then, exposed to UV for 20 min, and

placed in 48-well cell culture plate. The density of 1.0×10^4 cell/disk was seeded on each disk and after 3 h, 500 μL of 10% FBS contained growth medium was added.

Before surface immobilization of ECM proteins (collagen type-1 and vitronectin) on the surface of PET disks, preliminary studies were conducted to determine the best surface modification method, optimum cell seeding density and the cell expansion on the surface treated PET disks.

3.2.5.1 MTT Analysis

Cell viability on the surface treated PET disks was determined with MTT analysis. Firstly, culture medium was drawn out, then 0.06 mL MTT reagent (2.5 mg/mL 3-[4,5-dimethylthizaol-2-yl]-diphenyltetrazolium bromide in PBS) and 0.6 mL serum-free fresh medium were added and placed in a 5% CO_2 incubator for 3 hours at 37 °C. After then, MTT mixed solution was drawn out and formed purple formazan crystals on the disk surface were dissolved with 0.4 mL of isopropanol solution (containing 0.04 HCl). After gentle mixing, optical density of the resulting solution was measured at 570 nm wavelength with reference to 690 nm with a microplate reader (Spectro UV-VIS Double Beam Spectrophotometer, USA).

3.2.5.2 Cell Counting

In order to determine the cell expansion efficiency on surface treated PET disks, cells counted at the 1st, 3rd, 5th, and 7th day of cell culture. Accordingly, the culture medium was withdrawn, and PET disks were washed with PBS (pH 7.4). Then 200 μL of trypsin was added to each well, it covers the PET disk surface evenly and then, incubated for 5 min. After 5 min cell culture medium was added to stop trypsinization and pipetted thoroughly to achieve homogenous cell suspension. Then, trypan blue was added to the resulting cell suspension and the cells, which were not stained with trypan blue, were counted as living cells by hemocytometer (Neubauer chamber) with an optical microscope (Olympus IX71, USA) at 10x magnification.

3.3. Surface Coating of the PET Disks with Collagen Type-1 and Vitronectin

ECM proteins such as collagen type-1 and vitronectin were immobilized on the surface of PET disks throughout two different approaches: physical and chemical immobilization methods. In the physical methods, absorption via dropping and immersion techniques were applied for collagen type-1 whereas only dropping technique was applied for vitronectin. In chemical immobilization, EDC/NHS crosslinking was applied for both ECM proteins.

3.3.1. Absorption of Collagen Type-1 and Vitronectin on PET Disks

Collagen type-1 coating on the PET disks surface was carried out with two different absorption methods including dropping and immersion. Vitronectin coating on the PET disk surface was carried out with dropping method. Each method used to coat collagen type-1 and vitronectin on the PET disks surface with different concentrations and coating efficiency of each approach was evaluated with SEM, ATR-FTIR, immunofluorescent staining and hydroxyproline analysis.

3.3.1.1 Absorption of Collagen Type-1 on the PET Disks Surface

Three different groups (Group 0-Control, Group 1-Na_2CO_3-0.3M-H_2SO_4-C (+) and Group 3-EtOH-3M-H_2SO_4) from the Section 3.2.1.1. were selected depending on surface modifications and the relevant characterization studies. Those groups were coated with collagen type-1 through dropping and immersion methods. Details of the coating methods are presented in Table 3.3.

Table 3. 3. Methods used to coat collagen type 1 onto PET fiber matrices.

Method	Immersion method	Dropping method
Procedure	1. Collagen type-1 solution (in 0.01 M HCL) (pH 2) with a concentration of 300 µg / mL was prepared. 2. PET disks were placed in 48-well non-treated polystyrene plate (5 disks in each-well pattern). 3. 1 mL of collagen solution was added to each well. 4. PET disks were incubated in solution at 4 °C for 10 h. 5. The solution removed from well and samples were kept under 4°C for further usage.	1. Collagen type-1 solution (in 0.01 M HCL) (pH 2) with a concentration of 3000 µg / mL was prepared. 2. PET disks were placed in 96-well non-treated polystyrene plates separately. 3.10 µL of collagen type-1 solution was dropped onto each PET disk. 4. Disks were first incubated at 37 ° C for 2 h. 5. Then kept at 4 °C for further usage.
Reference	[111]	[111]*
Applied groups	• Grup 0-control • OCGrup 1-Na_2CO_3-0.3M-H_2SO_4-C(+) • Grup 3-EtOH-3M-H_2SO_4	
After coating	• Grup 0-i-col • Grup 1-i-col • Grup 3-i-col	• Grup 0-d-col • Grup 1-d-col • Grup 3-d-col

* related reference procedure were modified.

3.3.1.2. Absorption of Vitronectin on the PET Disks Surface

For this purpose, three different groups listed in Table 3.4 were selected. The selected samples were sterilized by autoclaving in PBS (pH: 7.4) for 20 min at 121 °C. Then, immersive vitronectin coating under sterile conditions was carried out in a laminar cabin.

Table 3. 4. Method used to coat vitronectin onto PET fiber matrices.

Method	**Dropping method**
Procedure	1. Vitronectin solution (in 0.01 M HCL) (pH 2) with a concentration of 15 µg / mL was prepared. 2. PET disks were placed in 96-well non-treated polystyrene plates separately. 3. 10 µL of vitronectin solution was dropped onto each PET disk. 4. Disks were first incubated at 37 ° C for 2 h. 5. Then they were kept at 4 °C for further usage.
Reference	[111]
Applied groups	• Grup 0-control • Grup 1-Na_2CO_3-0.3M-H_2SO_4-C(+) • Grup 3-EtOH-3M-H_2SO_4
After coating	• Grup 0-d-vn • Grup 1-d-vn • Grup 3-d-vn

3.3.2. Chemical Immobilization of Collagen Type-1 and Vitronectin on PET Disks

Collagen type-1 and vitronectin were grafted on the PET disks surface via EDC/NHS immobilization method. Surface-modified PET disks (Group 4) were used in this study. 1-Ethyl-3-(3-dimethylaminopropyl) carbodiimide (EDC) accelerates -COOH (carboxyl) group on the PET disk surface to form N-C=O (amide bond) with amino acid side chain of collagen or vitronectin as crosslinking substrate and N-hydroxysuccinimide (NHS) helps to maintain the structure of EDC grafting substrate [117].

Details of the methods are presented in Table 3.5. The alteration in PET surface characters was investigated by SEM, ATR-FTIR, hydroxyproline analysis and immunofluorescent staining. All PET disks used in cell culture were soaked in 75% (v/v) ethanol for 30 min and irradiated by UV for 20 min.

Table 3. 5. Collagen type-1 and vitronectin grafting on PET fiber matrices via EDC/NHS.

Method	**Collagen type-1**	**Vitronectin**
Procedure	1. PET-COOH disks were dipped in MES buffer (pH 5.5) for 2 h. 2. NHS (0.005 M) and EDC (0.1 M) were added into the solution and stirred for 3 h.	
	3. Collagen type-1 solution (in 0.01 M HCL) (pH 2) with a concentration of 3000 µg / mL was added. 4. Mixed for 24 h at room temperature.	3. vitronectin solution (in 0.01 M HCL) (pH 2) with a concentration of 15 µg / mL was added. 4. Mixed for 24 h at room temperature.
Reference	[103]	
Applied group	Group 4-EtOH-0.05 M-NaOH	
After coating	• Group 4-EDC/NHS-col • Group 4-col • Group 4-EDC/NHS	• Group 4-EDC/NHS-vn • Group 4-vn • Group 4-EDC/NHS

3.3.3. Determination of Collagen Type-1 Coating Efficiency

The amount of collagen type-1 coated on the surface of the PET disk after the absorption and chemical grafting approaches was determined. Collagen coating quantity and coating efficiency were measured by hydroxyproline analysis. Hydroxyproline is a non-proteinogenic amino acid which is a major component of the collagen and composed of between 12-14% (w/w) of mammalian collagen. Measurement of hydroxyproline levels can be used as an indicator of collagen content [5,6]. In addition to hydroxyproline analysis, the density and distribution of collagen type-1 coated on PET matrices were determined by SEM and EDS

analyzes. Biodegradation studies in DPBS (pH:7.4) were performed to evaluate the stability of collagen type-1 coating on PET disks.

3.3.3.1. ATR-FTIR Analysis

To analyze the chemical structure of PET disk surface ATR-FTIR analysis was carried out. In order to achieve this, the spectra of PET disk, collagen type-1 coated and vitronectin coated PET disks were analyzed in the range of 3400-600 cm^{-1} by ATR-FTIR spectrometry.

3.3.3.2. SEM Analysis

To analyze surface morphology and the effects of immobilization of collagen type-1, vitronectin on the morphology and pore structure of PET disks, two samples were taken from each group and covered with gold-palladium and then, analyzed by Zeiss (Evo-50, Germany) SEM.

3.3.3.3. Hydroxyproline Analysis

Hydroxyproline determination was performed for the quantitative analysis of collagen type-1 coated on PET disks. For this purpose, collagen type-1 coated PET disks were transferred to 1.5 mL Eppendorf tube and washed in PBS (pH: 7.4) for 10 min and dried in a vacuum oven overnight. 100 µL of 2M NaOH solution was then added to the PET disks and the samples were autoclaved for 15 min at 121 °C. Then, the tube contents were vortexed for 1-2 sec. Then, 50 µL of obtained liquid transferred to a new tube, 450 µL Chloramine T was added to the tube and the sample was kept under room temperature for 15 min. 500 µL of Enrlish solution was then added to each tube and incubated at 65 °C for 20 min. Then 200 µL of the mixed solution was taken from each tube and transferred to 96-well polystyrene plate and the optical density was measured spectrophotometrically at 550 nm with a microplate reader (Asys UVM 340. Austria). To evaluate the results of the analysis, a calibration curve was prepared to correlate the optical density values with the hydroxyproline concentration. For this purpose, hydroxyproline stock solution was prepared at 400 ng / µL concentration and different dilution rate was applied to obtain different concentration gradients (280, 200, 160,

120, 80, 40 and 0 ng / μL). Then, 50 μL of each gradient was transferred to the tube and autoclaved under the same conditions described above and the following steps were performed accordingly. Finally, collagen type-1 solution at different concentrations (60, 30, 15, 7.5, 3.75 and 1.875 μg / mL) were prepared to confirm the hydroxyproline / collagen ratio in the literature. The procedure described above was performed by adding 1 mL of collagen solution to the tubes, and hydroxyproline ratios were calculated based on the absorbance value obtained from the spectrophotometer.

3.4. Cell Culture Studies

In order to study cell behavior with coated PET disks, surface coated PET disks were selected depending on the results of the characterization studies described in Section 3.3. and investigated with an *in-vitro* cell culture study carried out with MC3T3-E1 and rAdMSC cell line in 48-well cell culture plate. MTT tests and DAPI/ Alexa fluor 488® phalloidin staining were carried out to evaluate the suitability of disks for cell expansion.

3.4.1. Cell Seeding

Cell cultivation was performed according to the following description. Osteoblast precursor cells, MC3T3-E1 passage 16, and, rAdMSCs which were isolated from rat adipose tissue, at passage 8, were used in cell culture studies. Both cells were cultured and grown in 175 cm^2 flasks using FBS containing α-MEM growth medium. Accordingly, collagen type-1 or vitronectin coated PET disks were placed in 48 well non-treated plates for cell behavior analysis. 10μL of cell suspension was added to each PET disk at a density of 3×10^6 cells/mL (equivalent to 2.7×10^4 cells/cm^2) in the growth medium. After 3 h of incubation at 37°C with 5% CO_2, 1 mL of growth medium was added, and then cultured for 7 days at 37 °C containing 5% CO_2 incubation chamber (Heraus, Germany). Growth medium changed on the 3rd and 6th days of the cell culture.

3.4.2 MTT Analysis

MTT analysis was performed as described in **S**ection **3.2.5.1.**

3.4.3. Hemocytometer Counting

Cell counting was performed by hemocytometer as described in **S**ection **3.2.5.2.**

3.4.4 DAPI/ Alexa Fluor 488® Phalloidin Staining

The cytoskeleton and nuclei of the cells grown on PET disks were visualized by Alexa Fluor 488® phalloidin / DAPI stain. Cell staining was performed in the following steps. First step is cell fixation. The culture medium was removed, PET disks placed in Eppendorf tube and washed three times with PBS (pH 7.4) and treated with 2.5% (v/v) glutaraldehyde solution for 20 min at 20 °C. In the second step, the cell fixation solution was removed and washed three times with PBS (pH 7.4) and treated with 0.1% (v/v) Triton X-100 (PBS) for 10 min to increase the permeability of cell membrane. At the third step, 1% (v/v) Alexa Fluor 488® phalloidin PBS solution with 1% (v/v) BSA was added, then 0.1% (v/v) DAPI solution was added and kept in dark for 30 min and then, washed with PBS (pH 7.4). Finally, PET disks were observed using fluorescence microscopy (Olympus IX71, USA) at 10x, 20x magnification.

3.4.5 Crystal Violet Staining

For crystal violet staining, the culture medium was removed from the 48-well plate which contained PET disks and washed three times with PBS (pH 7.4). Then, 1.5 mL of 1:1 of methanol/acetone mixture was added to each well and kept at 4 °C for 30 min for cell fixation. After the fixation solution was removed, and 500 μL of 0.5% (w/v) crystal violet solution was added to each well and incubated at 37 °C for 20 min. After the removal of the solution, PET disks were observed and visualized using an inverted microscope (Olympus IX71, USA).

3.5. Dynamic Cell Culture

This part of the thesis study consisted of three parts. In the first part, a custom-made packed-bed bioreactor was designed. However, the operational parameters applied in this thesis were determined in a previous study that was carried out in our research group [118]. In

the second part study the expansion of the rAdMSCs in this bioreactor was carried out with modified PET disks as packing material. The final part focused on cell harvesting in terms of efficiency and the characterization of harvested cells.

3.5.1 The Design of Packed-Bed Bioreactor

In our study, the working volume of the packed-bed bioreactor was determined as 100 mL to increase cost efficiency and to achieve good results. The packed-bed bioreactor was assembled from two main parts, glass body and stainless-steel basket (Figure 3.2). Accordingly, an autoclavable glass bioreactor with 100 mL working volume provided from Sesim Kimya ltd. (Turkey) and used as a packed-bed bioreactor main body. During the design, the working volume of the packed-bed was calculated and the basket was assembled and placed in the middle of the bioreactor chamber. The basket system in the packed-bed bioreactor to be used in cell culture did not show any oxidation during the 15 days of observation in the water. In the dynamic cell culture study, no problems were encountered in the autoclavation process at 121 °C for 30 min resulted that the packed bed basket did not deteriorate at high temperature. Figure 3.2-a and b show the main assembly part of the packed-bed bioreactor. Since the basket diameter is calculated and designed according to the diameter of the bioreactor, it can be fixed to the inner side of the reactor chamber without any attachment.

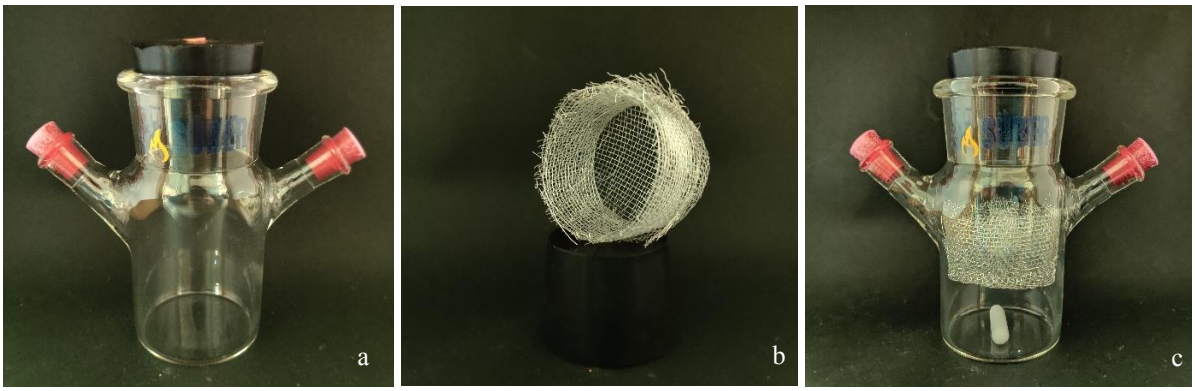

Figure 3. 2. Photographs showing the main parts of packed-bed bioreactor, a) Glass body, b) the basket, c) packed-bed bioreactor with all units.

The packed-bed bioreactor system consists of 3 different parts: i) glass reactor chamber, ii) metallic basket and iii) magnetic agitation unit. There are two sidearms in the glass reactor chamber. The air goes into the bioreactor from side arms with the help of hydrophobic filter and sterile injector needle.

The packed-bed bioreactor building setup was performed under sterile conditions (using surgical gloves in a laminar flow cabinet) and the steps followed are summarized below:

1. Cell seeded packing materials were filled into the basket.
2. The cell culture medium was added to the reactor chamber.
3. The metallic basket was connected to the glass reactor chamber.
4. Disposable hydrophobic filters were installed with the injector needles to the side arms of the reactor.
5. Bioreactor was placed on a magnetic stirrer and put in an incubator supplemented with 5% CO_2 at 37 °C.

3.5.2. Expansion of MC3T3-E1 Cells in Packed-bed Bioreactor

In preliminary cell culture study MC3T3-E1 cells were, expanded in a custom-made bioreactor on commercially available packing material, Fibra-Cel® disks. The purpose of this study was to test the suitability of our bioreactor for cell expansion. Details of working parameters of dynamic cell culture study were taken from a previous study that was carried out in our research group [118].

The packed-bed bioreactor was washed and autoclaved at 121 °C for 30 min. Then, Fibra-Cel® disks were sterilized by autoclaving for 15 min at 121 °C in PBS (pH: 7.4) solution. After sterilization PBS solution was removed and 50 mL of growth medium was added and kept at 37 °C with 5% CO_2 for 24 h. Then, the growth medium was withdrawn and the cells were evenly seeded onto the disks and incubated for 48 h in the incubator. Following this step, cell-seeded packing materials were transferred into the basket and put into the bioreactor chamber. Then, the growth medium was added and agitation was provided by a

magnetic stirrer. For characterization, MTT analysis and DAPI staining was done. In addition, cells were counted by hemocytometer to quantity the cells grown on Fibra-Cel®.

Table 3. 6. Dynamic cell culture operating parameters and conditions [118].

Cell	MC3T3-E1 cells
Packing material	Fibra-Cel®
Amount of packing material	2g (350 pieces of disks)
Cell seeding density	$30x10^6$ cells / bioreactor
Culture Period	7 days
Agitation Speed	50 rpm
Change of growth medium	50% on day 3 and 5

3.5.3 Expansion of rAdMSCs in Packed-bed Bioreactor

In this part of the study, rAdMSCs were seeded on sodium hydroxide treated PET disks and cell expansion in our custom made packed-bed bioreactor was investigated. For this purpose, rAdMSCs (at passage 5) were used and the yield of expansion was calculated at the end of the dynamic cell culture. In addition, differentiation abilities of harvested rAdMSCs were investigated with differentiation studies and SOX2 gene expression was compared to that of control cells with RT-PCR analysis.

3.5.3.1. Characterization of rAdMSCs

In this part of the study, the growth curve of rAdMSCs used in dynamic cell culture was calculated. The 4^{th} passage rAdMSCs were seeded on 48-well TCPS cell culture plate with a seeding density of 8×10^3 cell/cm^2, added 250 µL of standard 15% FBS contained α-MEM growth medium and put in an incubator for 14 days. Cell viability was measured with MTT analysis and cells were counted at the 1^{st}, 3^{rd}, 5^{th}, 7^{th}, 9^{th}, 11^{th} and 14^{th} day of cell culture, cell morphology was visualized with DAPI/ Alexa Fluor 488® phalloidin staining at the 1^{st},

5^{th},10^{th} and last day of cell culture. Also, the doubling time of rAdMSCs was calculated depending on the growth curve.

3.5.3.2 Packed-Bed Bioreactor Culture

In the packed bed bioreactor, sodium hydroxide treated PET disks were used as packing materials and the expansion of rAdMSCs on the packing materials were investigated. Details of working parameters of dynamic cell culture study were presented in Table 3.7. MTT analysis was done to determine cell viability. Cell counting was carried out at the 1^{st},3^{rd}, 5^{th}, 7^{th},9^{th}, 11^{th} and 14^{th} day of cell culture. DAPI/ Alexa Fluor 488® phalloidin staining was done and fluorescence microscopy was used to visualize the 3^{rd}, 7^{th},14^{th}-day samples. The culture medium was monitored with pH measurement and biochemical analyses including glucose, lactate, ammonia analyses, were carried out before and after the medium changes. At the end of the dynamic cell culture, the yield of rAdMSCs expansion was calculated and characterization studies were carried out.

At the beginning of dynamic cell culture, modified PET disks and packed-bed bioreactor were autoclaved at 121 °C. After sterilization, packing material was conditioned with growth medium for 24 h. Following this 10 mL of cell suspension was seeded on the PET disks in a glass chamber and incubated for 48 h. After 48 h, packing materials were transferred into the basket and put into the bioreactor chamber. Then, 100 mL of growth medium was added to the bioreactor through the side arm and agitation was started with the help of magnetic stirrer.

Table 3. 7. Dynamic cell culture operating parameters and conditions.

Cell	rAdMSCs
Packing material	Group 4-EtOH-0.05 M-NaOH
Amount of packing material	1st study: 1g (700 pieces) 2nd study: 0.5 g (350 pieces)
Cell seeding density	1st study: 30 x10^6 cells / bioreactor 2nd study: 10 x10^6 cells / bioreactor
Culture period	1st study: 14 Days 2nd study: 7 Days
Agitation Speed	50 rpm
Change of growth medium	1st study: 50% change on days 3, 5, 7, 9, 11 and 13 2nd study: 50% change in every two days
Ventilation	Through the hydrophobic filters in the side arms of the bioreactor chamber

3.5.3.3 Cell Harvesting

End of packed-bed bioreactor studies, cells were harvested from packing materials with trypsinization. Briefly, the discs were washed with DPBS (pH: 7.4) and trypsin / EDTA mixture was added onto the discs. After incubation at 37°C for 5 min, the trypsin enzyme was inhibited using growth medium and pipetted thoroughly and then, transferred into tubes centrifuged at 4 °C, 1000 rpm for 5 min to obtain the cell pellet. Cells were counted after resuspension with 0.4% (w / v) PBS

3.5.3.4 Glucose, Lactate and Urea Analysis

The changes of nutrients and metabolites concentration in the bioreactor medium during the cell culture were monitored by biochemical analysis. The glucose, lactate and urea concentration were analyzed at Ankara University Ibni Sina Hospital, Biochemistry laboratory using biochemical analyzed device (AU 680 Beckman Coulter, Calif., USA).

3.5.3.5 Cell Differentiation Study

To assure that the harvested rAdMSCs from dynamic cell culture maintain the mesenchymal stem cell characteristics, the adipogenic and osteogenic differentiation studies were done. For this purpose, the harvested cells from dynamic cell culture were cultured for 14 days in the cell culture medium (control group), adipogenic differentiation medium (adipogenic group) and osteogenic differentiation medium (osteogenic group).

Osteogenic Differentiation

For osteogenic differentiation study, 5 % β-glycerol phosphate, 0.5 % ascorbic acid and 0.05 % dexamethasone were added to culture medium. The differentiation was monitored by morphological changes and mineral formation which were observed by an inverted microscope. Mineral production, which is a marker of osteogenic differentiation, was determined by von Kossa staining. ALP enzyme activity was also visualized by ALP staining.

ALP/ Von Kossa Staining

Cell culture medium removed from samples and washed with cold PBS 3 times than 10% neutral formalin was added and incubated for 15 min. tampon was remove and sample washed with distillated water and incubated for 15 min. Then, fresh substrate was added to the sample and incubated at room temperature for 45 min. After that, sample was washed 4 times with distillated water then 2.5 % silver nitrate solution was added and incubated for 30 min. Silver nitrate solution was removed from sample and washed with distillate water several times and observed with optical microscope.

Adipogenic Differentiation

For adipogenic differentiation study, 0.25 % dexamethasone, 5% IBMX, 0.5 % insulin and 0.05% indomethacin were added to culture medium. The differentiation was monitored by oil drop formation, a marker of adipogenic differentiation. Thus, cells were stained with Oil Red O and observed by an inverted microscope

Oil Red Staining

Culture medium was removed from sample and washed with PBS 3 times then 10 % formalin solution was added and incubated for 30 min. Then, formalin solution was removed and sample was washed with PBS 1 time then 60 % isopropanol was added to the sample and incubated for 5 min. Then the medium was removed and oil red working solution was added and incubated for 5 min. The medium was removed from sample and washed with distillated water and observed with optical microscope.

3.5.3.6 Gene Expression Study

RNA isolation

Qiagen RNeasy Mini Kit was used for RNA isolation and instructions were described in details. When isolation procedure started 500 µL of TRIzol solution was added on each sample and it was waited for about 15 minutes at room temperature and then the samples were vortexed for 10 s. In the next step, 100 µL chloroform was added to each sample and mixing was done by shaking the samples up-and-down for 20 times then the samples were incubated for 3 min at room temperature. Subsequently, the samples were centrifuged at 13,000 rpm for 10 min at 4 °C. Then the upper aqueous phase was transferred to a new Eppendorf tube. After equal amount of 70% (v / v) ethanol added to the liquid phase, it was mixed and the solution was transferred to RNeasy spin columns and centrifuged at 13,000 rpm for 1 minute at 25 °C. The liquid under the Eppendorf tube was poured and 700 µL of RW1 buffer was added onto the column and centrifuged at 13,000 rpm for 30 seconds at 25 ° C. Then 500 µL of RPE buffer was added to the samples and centrifuged at 13,000 rpm for 30 s at room temperature. The liquid at the bottom of the Eppendorf tube was removed and same procedure was repeated once more. After that, the column was replaced in a new Eppendorf tube and 30 µL of RNase- free sterile water was added to the membrane and centrifuged at 13,000 rpm for 1 minute at 25 °C. Thus, RNA held in the column membrane was collected in the centrifuge tube by washing the membrane with water. RNA concentrations were measured with NanoDrop2000c (Thermo Scientific). The isolated RNA solution was kept at - 80 °C for further usage.

cDNA Synthesis

For cDNA synthesis, cDNA Kit (Applied Biosystem, USA) was used and the reaction carried out at 25 °C for 10 min, 37 °C for 120 min and 85 °C for 5 min incubated in Applied Biosystems SimpliAmp Thermal Cycler (ThermoFisher Scientific, USA) device.

Real Time Polymerase Chain Reaction (RT-PCR) Analysis

RT-PCR analysis was performed on LightCycler® Nano Instrument (Roche, Switzerland) using 5xHot Fire Pol®Eva Green® qPCRMix Plus or 5xHot Fire Pol®Eva Green® qPCR supermix (SolisBioDyne, Estonia) kit. RT-PCR analysis cycles include activation step at 95 °C for 10 min, denaturation step at 95 °C for 15 s, conjugation step at 56 and 60 °C for 30 s, and extension step at 72 °C for 20 s repeated for 45 cycles. *B-Actin was* used as the reference gene (Housekeeping gene). The results of the analysis are given as relative gene expression. All data were calculated according to the $2^{-\Delta\Delta CT}$ method, the results are given in multiples of the control group. The primary sequences of the genes used in RT-PCR analysis within the scope of the thesis are given in Table 3.8.

Table 3. 8. Primary sequences of genes used in RT-PCR analysis.

Genes	Forward Primer	Reverse Primer	T binding
β -Actin	F-AGCAAGCAGGAGTACGATGAG	R-AAAGGGTGTAAAACGCAGCTC	56 ° C
Sox2	F-AACGGCAGCTACAGCATGATGC	R-CGAGCTGGTCATGGAGTTGTAC	60 ° C
Nanog	F-CCGTGTTGGCTGCATTTGTC	R-ACCTGGGGGAGGATAGAGTG	57 ° C
OCT 4	F-GTCCCTAGGTGAGTCGTCCT	R-CGAAGTCTGAAGCCAGGTGT	57 ° C

3.6. Statistical Analysis

The data generated from the thesis study were verified statistically using the GraphPad Software Instat program. All the data were conducted in triplicates and data were presented as mean ± standard deviation. Different groups were statistically evaluated by a one-way

ANOVA method with Turkey-Kramer post hoc test and the p-value under 0.05 was accepted as statistically significant.

4. RESULTS AND DISCUSSION

In this part, the results obtained from experimental studies are discussed and explained in detail. At the beginning of the study, to increase cell expansion on commercially available PET fiber matrix packing-material (Reemay 2232) in the packed-bed bioreactor, PET disks were treated with different surface modification methods. In such a manner, the best performance surface-modified PET disks were determined in a packed-bed bioreactor for the expansion of rAdMSCs. The experimental studies are summarized into two parts: "Surface modification and characterization studies of PET" and "Packed-bed bioreactor studies". In the first part, surface hydrophilicity of PET discs were altered via sulfuric acid or NaOH treatments. Following this step, surface of PET disks were coated with ECM proteins (collagen, vitronectin) through physical and chemical coating methods, which added RGD binding sites on the PET surface aiming to promote cell adhesion and cell immigration. In the second part, rAdMSCs expansion in packed-bed bioreactor was carried out under optimum operating conditions which was determined in a previous study. After the cell harvest, the yield of expansion was calculated. The final part is the evaluation of *in vitro* differentiation, specific gene expression and cell phenotype of harvested rAdMSCs to determine the effects of bioreactor culture conditions on cells.

4.1 MC3T3-E1 Expansion in Packed-bed Bioreactor

The preliminary dynamic cell culture studies were performed with a small scale packed-bed bioreactor that was designed in our laboratory. To evaluate the suitability of the bioreactor for cell expansion, a preliminary study was conducted in a previous study. Under defined conditions in the packed-bed reactor, MTT analysis, hemocytometer cell counting and DAPI staining were done. The results of the previous study are given in Fig. 4.1. The mitochondrial activity of MC3T3-E1 cells after 3 h of cell seeding was found to be around 0.34, which increased up to 0.70 on the 5^{th} day and remained stable through the end of cell culture (Fig. 4.1-a). The cell numbers on Fibra-Cel® disks have shown a steady increase during the seven days of dynamic cell culture yielding a 4.2-fold expansion. The fluorescence microscopy

images obtained from DAPI staining of MC3T3-E1 on Fibra-Cel® on the 1st and 7th days of dynamic cell culture are shown in Figure 4.1-b and c respectively. The images demonstrated that MC3T3-E1 had uniformly distributed on Fibra-Cel® on the 1st day and cell density increased significantly on the 7th day proving the versatility of our bioreactor [118].

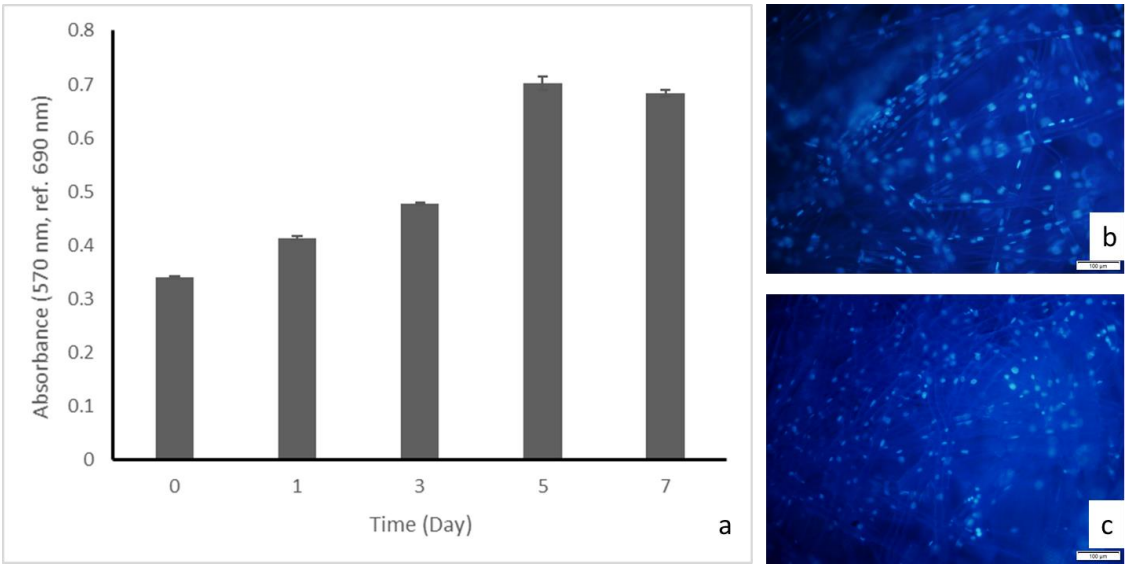

Figure 4. 1. (a) Mitochondrial activity of MC3T3-E1 cells on Fibra-Cel®, (b) DAPI image of MC3T3-E1s on Fibra-Cel® on the 1st day, (c) DAPI image of rAdMSCs on Fibra-Cel® on the 7th day of dynamic cell culture conditions [118].

4.2 Preparation and Characterization of Surface Modified PET Disks

In this part of the study, different surface modification methods were applied on Reemay 2232 nonwoven PET fiber matrix to improve surface hydrophilicity. The details of the applied techniques to prepare Group 0-PET-blank, Group 1-Na_2CO_3-0.3M-H_2SO_4-C(+), Group 2-Na_2CO_3-3M-H_2SO_4-C(+), Group 3-EtOH-3M-H_2SO_4 and Group 4-EtOH-0.05M-NaOH are given in Section 3.2.1. To examine the effects of surface modifications on properties of PET disks, water contact angle measurements, SEM, EDS and ATR-FTIR analyses were done. To analyze the effect of sulfuric acid concentration on surface properties, Group 1 and Group 2 are compared with Group 0. Whereas the comparison of Group 2 and Group 3 were done to evaluate the effect of high temperature curing in sulfuric acid treatment on hydrophilicity. The

properties of Group 4 were determined to analyze the effects of sodium hydroxide surface treatment in comparison to Group 0. Accordingly, modified PET disks with feasible morphology and higher hydrophilicity were chosen to be further used in cell culture studies.

4.2.1 Water Contact Angle Measurement

The water contact angles of the surface-treated PET disks were measured with sessile drop technique and the results are given in Table 4.1. As shown in Table 4.1, Reemay 2232 nonwoven PET fiber matrix as our Group 0-PET-blank has a hydrophobic surface. The samples cured at 110 °C after the sulfuric acid treatment such as Group 1 and Group 2 demonstrated superhydrophilic properties. In addition to that sodium hydroxide treated Group 4 also showed superhydrophilicity. In those groups, the water contact angle was determined as 0° and it was observed that the water drop was absorbed by the material within 1 s while applying the sessile drop method. However, Group 3 which was treated with sulfuric acid at room temperature (no curing) did not demonstrate a significant change in water contact angle when compared to that of Group 0.

Table 4. 1. Water contact angles of surface-treated PET disks.

Group Name	**Water Contact Angle (°)**
Group 0-PET-blank	117.8 ± 7.5
Group 1-Na_2CO_3-0.3M-H_2SO_4-C (+)	0
Group 2-Na_2CO_3-3M-H_2SO_4-C (+)	0
Group 3-EtOH-3M-H_2SO_4	108.8 ± 7.0
Group 4- EtOH-0.05 M-NaOH	0

4.2.2 SEM and EDS Analyses

Among characterization studies, SEM analysis was performed to determine the changes in the surface morphology of PET fiber matrices after sulfuric acid and NaOH treatments, whereas

EDS analysis was carried out to define the elemental composition (pointwise) on the material surface. The results are presented in Figure 4.2 and 4.3. As seen in Figure 4.2 (a), the fibers of the control group have a diameter of approximately 15 μm and their surfaces are smooth. Since there was no sulfuric acid treatment in the control group, only C and O elements were found on the PET surface in EDS analysis. In Figure 4.3 (b) and (c) were belong to Group 1 and Group 2, respectively, the deformation of fibers are seen Figure 4.2 (r) and EDS analysis results of these groups revealed that sulfur element was found at high percentages on the surface. These results indicate that high temperature curing above PET melting point has led to deformation of the fibers which increased surface hydrophilicity. Besides, the deformed areas are thought to encapsulate the sulfur in the fiber surface [115]. In Figure 4.3 (d), as Group 3 in which sulfuric acid treatment performed without curing did not cause any deformation on the fiber surface and no sulfur was observed in the elemental composition of the PET surface. The SEM images and EDS analysis results of Group 4, given in Figure 4.2 (m,n,o) and Figure 4.3. (e) demonstrated that the fiber surface didn't go under any drastic deformation and the elemental composition of the surface didn’t show any trace of sodium. Depending on the morphological observation and chemical composition of PET fiber surfaces, Group 3 and Group 4 presented minimum surficial deformation and less amounts of chemical residue on the surface.

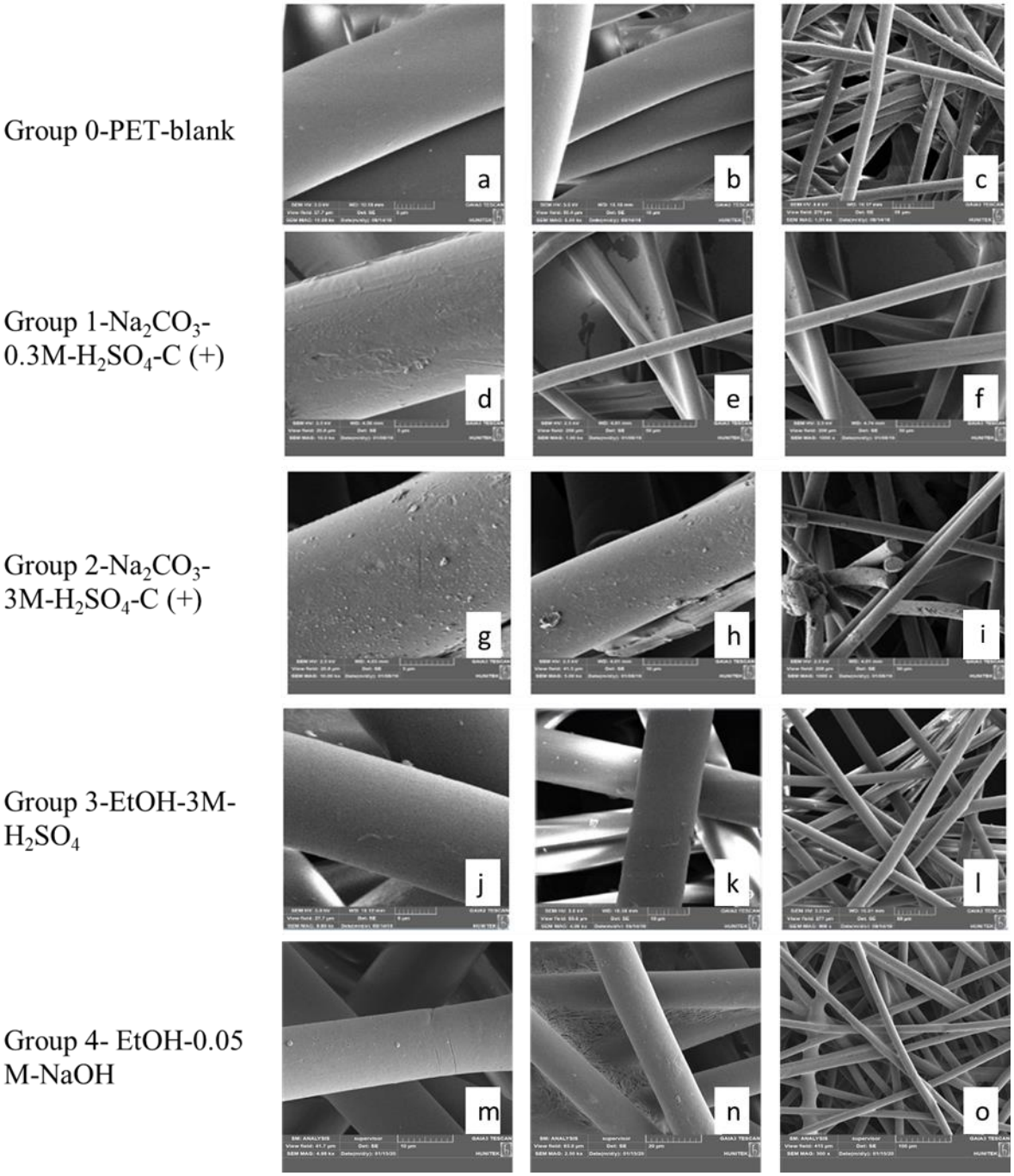

Figure 4. 2. SEM images of PET discs with different surface modifications: Group 0: (a) 5000x, (b) 2500x, (c) 1000x; Group 1: (d) 5000x, (e) 2500x, (f) 1000x; Group 2: (g) 5000x, (h) 2500x, (i) 1000x; Group 3: (j) 5000x, (k) 2500x, (l) 1000x; Group 4: (m) 5000x, (n) 2500x, (o) 1000x

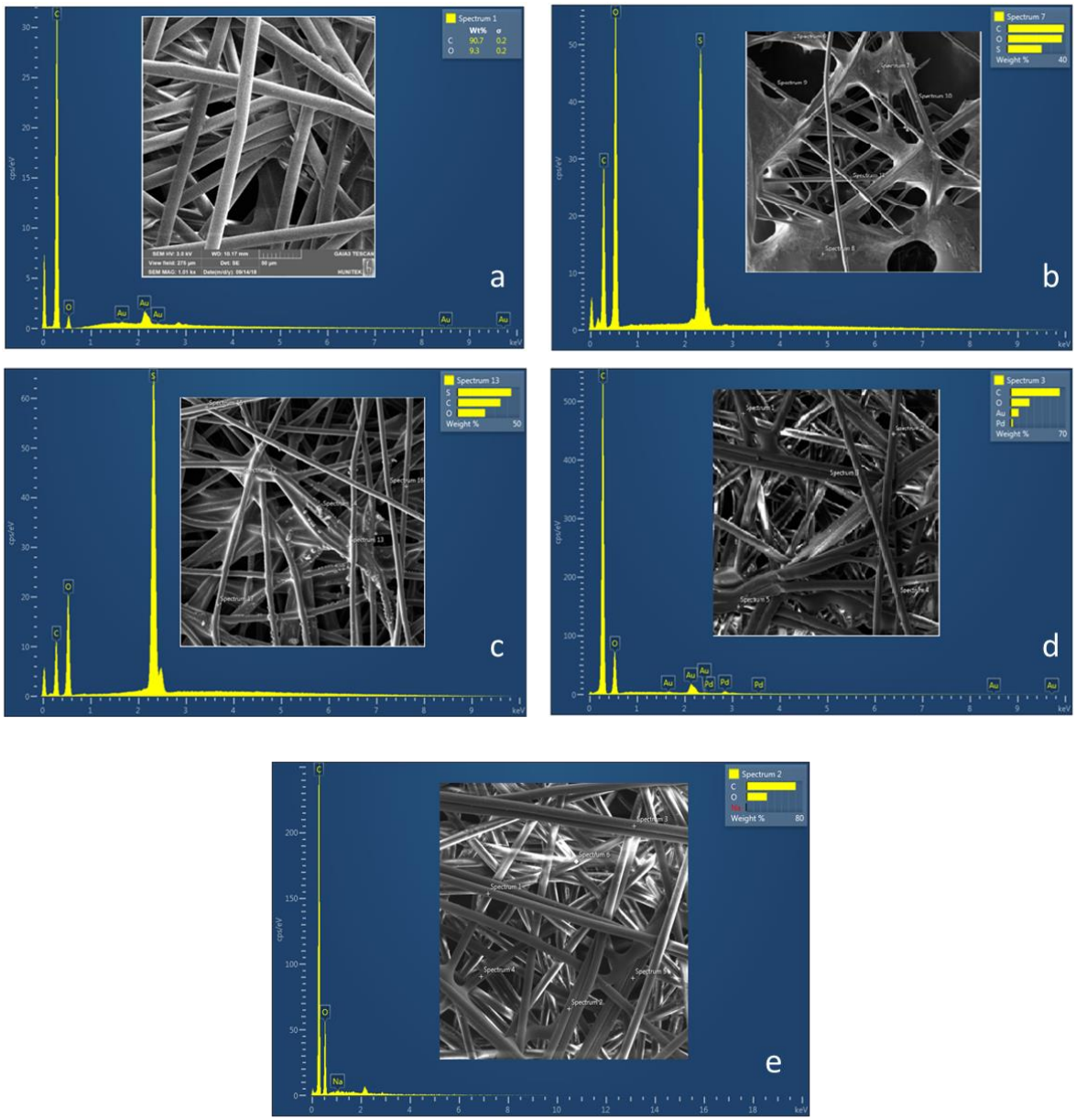

Figure 4. 3. The results of EDS analyses of (a) Group 0, (b) Group 1, (c) Group 2, (d) Group 3 and (e) Group 4 (The magnification of inserted SEM images are 1000x).

4.2.3 ATR-FTIR Analysis

To better understand the surface molecular fingerprint of surface-modified PET disks, ATR-FTIR analysis was made (Figure 4.4). The peak of the carbonyl group (C=O) was observed in 1760 cm^{-1} in all groups which demonstrated that the backbone of PET remained unchanged during the surface modification process. The hydroxyl ion (OH) stretching was

observed only in Group 4 meaning that carboxyl groups were successfully added to the surface of PET. In contrast, sulfuric acid-modified groups and control groups showed similar spectra meaning that the surface molecular composition of PET remained unchanged after sulfuric acid treatment.

ATR-FTIR analysis showed that sodium hydroxide acid treatment achieved carboxyl group addition to the surface of the PET disk which increased the hydrophilicity of Group 3 dramatically. Sulfuric acid treatment in Group 1, Group 2, and Group 3 did not accomplish any functional group changes on the PET surface.

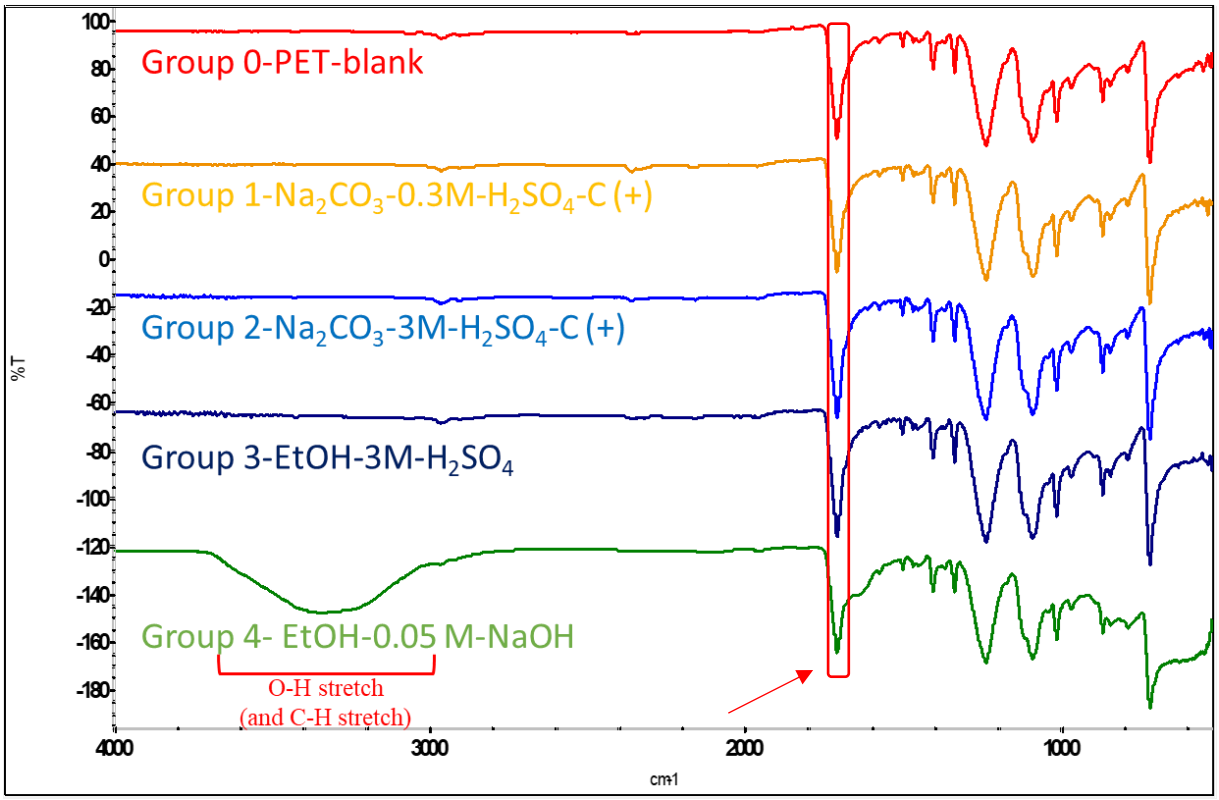

Figure 4. 4. ATR-FTIR analysis of different surface-modified PET disk groups.

4.2.4 *In Vitro* Cell Culture Studies

In order to evaluate the biocompatibility of treated PET surfaces, preliminary cell culture studies with MC3T3-E1 cell line were carried out with Group 0 (as control), Group3 and Group 4, which were selected according to the results of characterization studies. Fibra-Cel® disks were also used to compare the results of the selected groups with a commercially available packing-material. According to the MTT test results in Figure 4.5, mitochondrial activity of MC3T3-E1 cells seeded on all groups increased over the culture period demonstrating that surface modification had no toxic effect on cells. Meanwhile, mitochondrial activity of MC3T3-E1 cells on Group 4 was found to be relatively higher than that of other groups. Especially on the 3rd and 7th days, cell activity on Group 4 overpassed the other three groups ($p<0.001$) for which the absorbance of Group 4 was 1.3 times higher than the second-highest Group 0 and 1.86 times higher than sulfuric acid-treated Group 3 and 2.65 times higher than that of the commercial product Fibra-Cel®. In summary, cell viability of MC3T3-E1 cells on Group 4 was significantly higher than that of the other three groups throughout the study indicating that Group 4 is more favorable for cell proliferation. Besides, sulfuric acid-treated Group3 outperformed the commercial product Fibra-Cel®, which is considered as the second-best for cell proliferation.

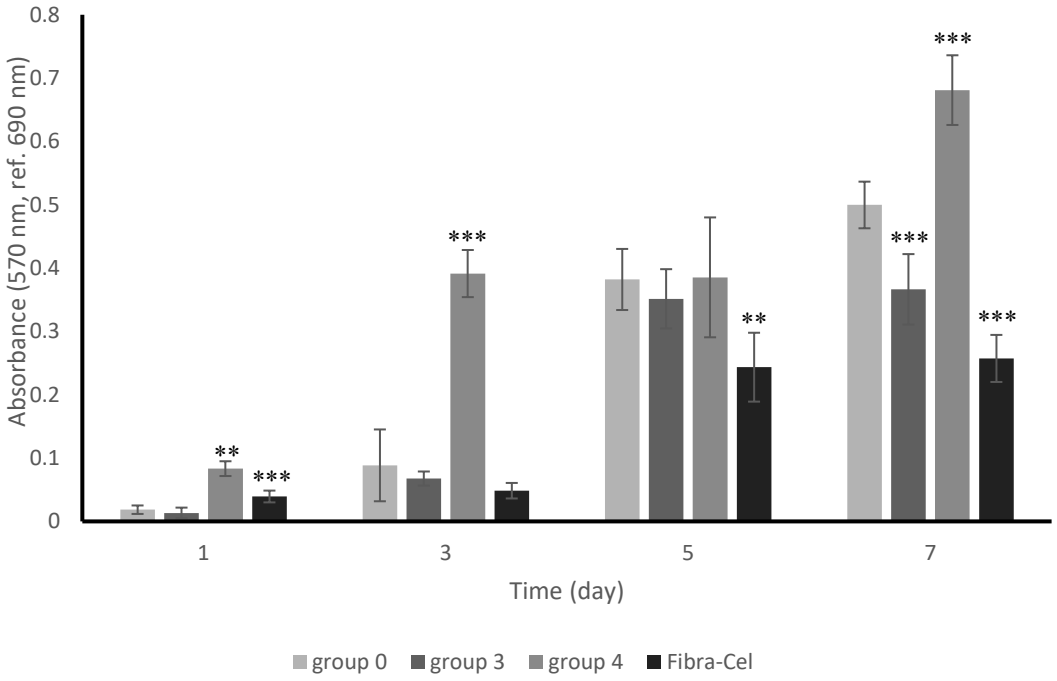

Figure 4. 5. Mitochondrial activity of MC3T3-E1 cells on different surface modified groups in static culture. (Statistical differences when Group 0 are control * $p<0.05$, ** $p<0.01$, *** $p<0.001$).

4.3 Preparation of Collagen Type-1 Coated PET Disks by Physical Methods and Characterization Studies

In this part of the study, collagen type-1 was coated on the surface of Group 0 and Group 3 through immersive and dropping methods. Two groups (Group 0 and Group 3) described in Section 3.2 were selected depending on the results obtained from the relevant characterization studies. The coating density of collagen type-1 was determined with hydroxyproline analysis. SEM and EDS analyses were also performed to characterize collagen coated disks.

4.3.1 Hydroxyproline Analysis

4.3.1.1 Hydroxyproline Calibration Curve

The calibration curve was prepared to determine the relationship between absorbance values and amounts of hydroxyproline. Hydroxyproline analysis performed for quantitative analysis of collagen type-1 amounts coated on PET fiber matrices, As seen in in Figure 4.6, the linear calibration curve between absorption and quantity of hydroxyproline was obtained and the R^2 value is over 0.99. Using the equation in the graph, the amount of hydroxyproline in samples was calculated depending on the absorbance values.

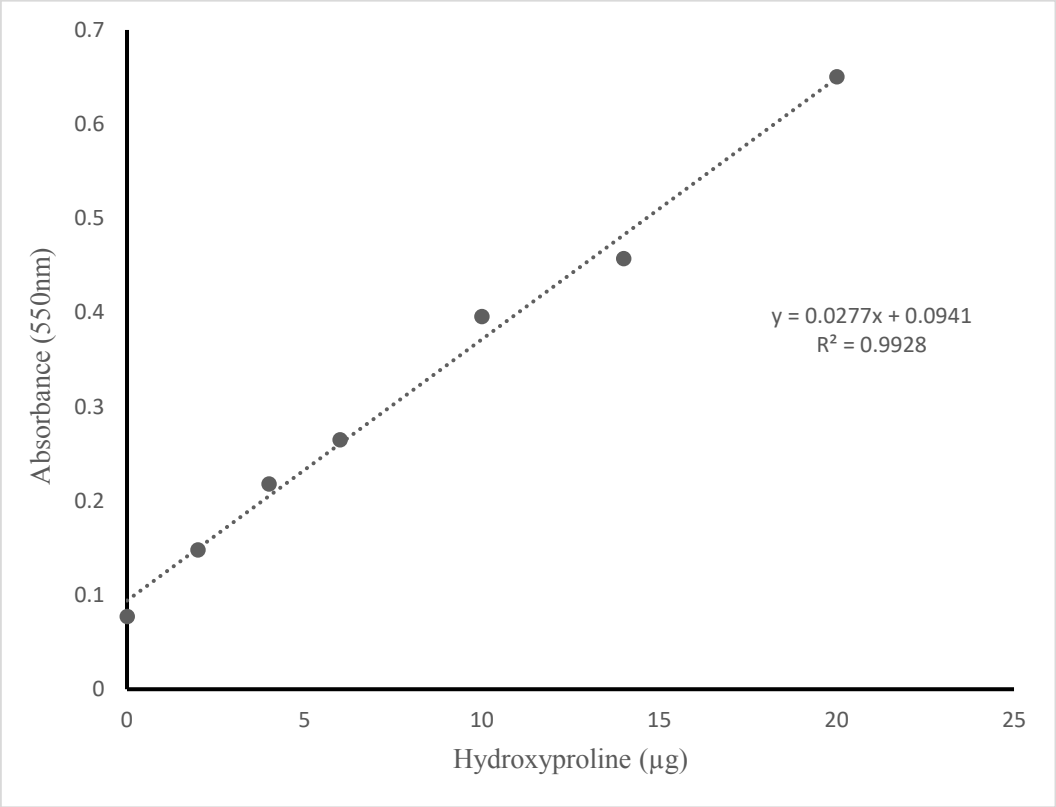

Figure 4. 6. Calibration curve prepared for hydroxyproline determination.

4.3.1.2 Confirmation of Hydroxyproline/Collagen Type-1 Ratio

This analysis was carried out to determine the hydroxyproline/collagen ratio and compare the results with the 12.5% ratio that is given in the literature [119, 120]. As seen in Table 4.2, hydroxyproline/collagen ratio varied between 15.8% and 16.3% in our study. Besides, this study has revealed that the sensitivity of the analysis technique used is not suitable for cases where the amount of collagen is less than 15 µg.

Table 4. 2. Determination of hydroxyproline/collagen type-1 ratio.

Amount of Collagen type-1 (µg)	Optical Density (@ 550 nm)	Amount of Hydroxyproline (µg)	Hydroxyproline/Collagen type-1 ratio (%, w/w)
60	0.121	0.979	16.3
30	0.107	0.474	15.8
15	0.101	0.241	16.1
7.5	0.091	-1.227	-
3.75	0.086	-0.300	-
1.875	0.081	-0.004	-

4.3.1.3 Quantification of Collagen type-1 Coating on PET Disks

The results obtained from the hydroxyproline analysis are presented in Table 4.3. Using the equation given in Figure 4.6., the amount of hydroxyproline in the samples was calculated from the optical density values. At this stage, the amount of hydroxyproline was multiplied by 2, since the concentration of hydroxyproline in the samples was halved by the procedure. For the determination of collagen type-1 amount on the PET disks, the hydroxyproline ratio in collagen was accepted as 16.1% (w / w) and the values obtained are presented in Table 4.3. It was observed that the highest amount of collagen type-1 was found in Group 3-d-col (35.5 µg/disk) followed by Group 0-i-col (25.4 µg/disk). It was found that the dropping method resulted in higher amounts of collagen coating than immersion method.

Table 4. 3. Amounts of collagen type-1 coated on surface modified PET disks with dropping or immersion techniques.

Group	Optical Density (550 nm)	Amount of Hydroxyproline (μg)	Amount of collagen type-1 (μg/disk)
Group 0-i-col	0.207 ± 0.047	4.1 ± 1.697	25.5 ± 10.61
Group 0-d-col	0.165 ± 0.050	2.6 ± 1.765	16.0 ± 11.03
Group 3-i-col	0.125 ± 0.027	1.1 ± 0.990	7.0 ± 6.064
Group 3-d-col	0.251 ± 0.0198	6.1 ± 0.715	38.1 ± 4.575

4.3.2 SEM Analysis

SEM analysis was performed to analyze the presence and distribution of collagen type-1 coating on PET fiber matrices. When Figures 4.7 and 4.8 were examined, it was seen that there was no significant change in Group 0 PET fiber diameters and surface properties after the dropping and immersive coating techniques were applied. In Figures 4.9. and 4.10., it was observed that collagen type-1 was evenly coated on Group 3 PET fiber surfaces with immersive coating method. Especially when immersive technique is applied, it has been determined that Group 3 PET fiber diameters were increased and surface roughness was found to be relatively higher than that of Group 0. In Figure 4.10, it was observed that collagen type-1 formed sheet like structures between PET fibers when dropping method was applied and did not evenly distributed on PET fiber surface. In conclusion, the results of hydroxyproline and SEM analysis of Group 3-i-col and Group 3-d-col demonstrated that immersive coating of collagen type-1 could be more efficient and uniformly distributed on PET fiber surface.

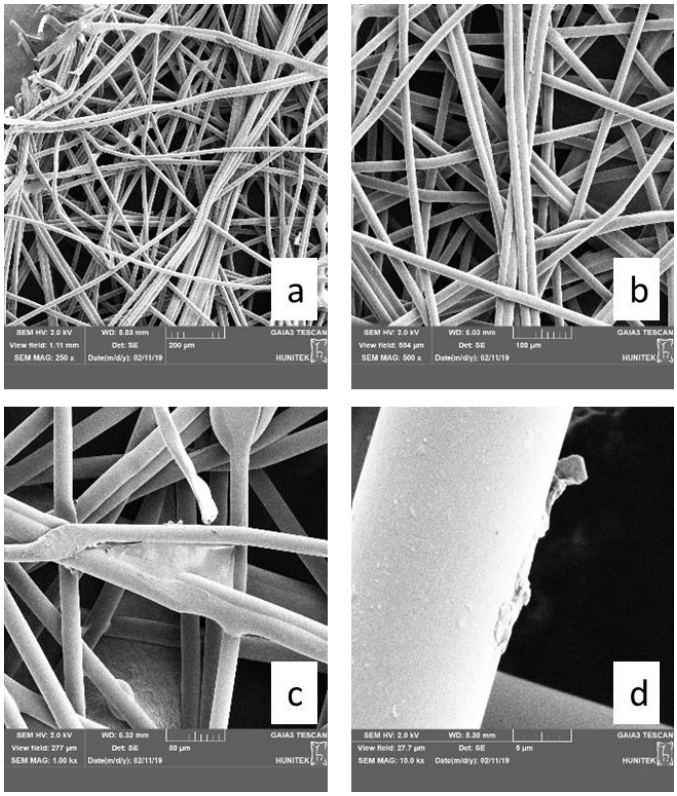

Figure 4. 7.SEM images of Group 0-i-col PET disks: (a) 250x, (b) 500x, (c) 1000x, (d) 10000x.

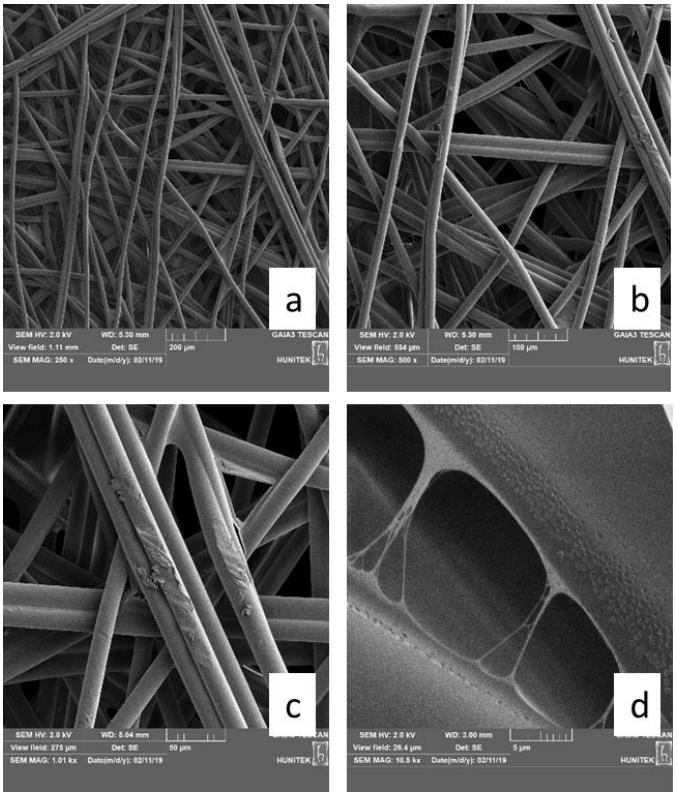

Figure 4. 8. SEM images of Group 0-d-col PET disks: (a) 250x, (b) 500x, (c) 1000x, (d) 10000x.

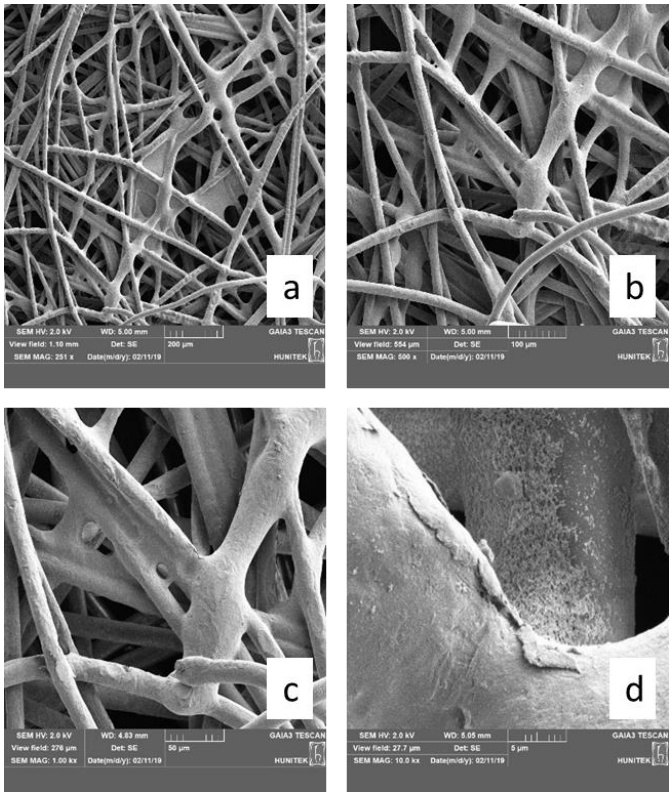

Figure 4. 9. SEM images of Group 3-i-col PET disks: (a) 250x, (b) 500x, (c) 1000x, (d) 10000x.

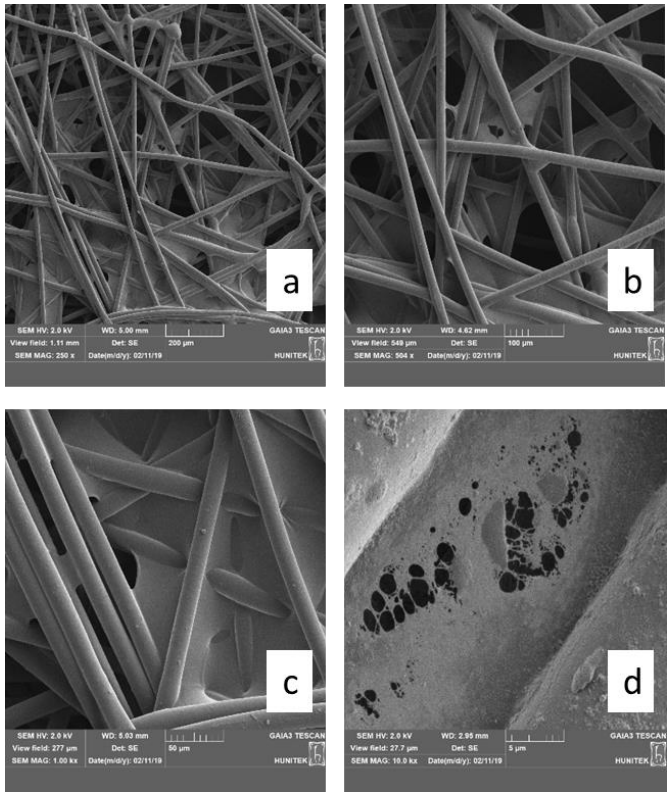

Figure 4. 10. SEM images of Group 3-d-col PET disks: (a) 250x, (b) 500x, (c) 1000x, (d) 10000x.

4.3.3 EDS Analysis

In order to verify the presence of collagen on the surface of the PET disks, the elemental composition of surface was determined by EDS analysis, and the results are presented in Figure 4.11. In Figure 4.11., all groups confirmed the presence of nitrogen in elemental composition which indicates the collagen type-1 was successfully coated on PET fiber matrices. In Figure 4.11. (a) and (b), wt% of nitrogen on the surface of PET fiber in Group 0-i-col is 18.9 which 1.2 times higher than that of Group 0-d-col. Since EDS analysis provide pointwise data regarding to Wt% of nitrogen, which in turn related to collagen content, the results of hydroxyproline and EDS analyses were found to be inconsistent.

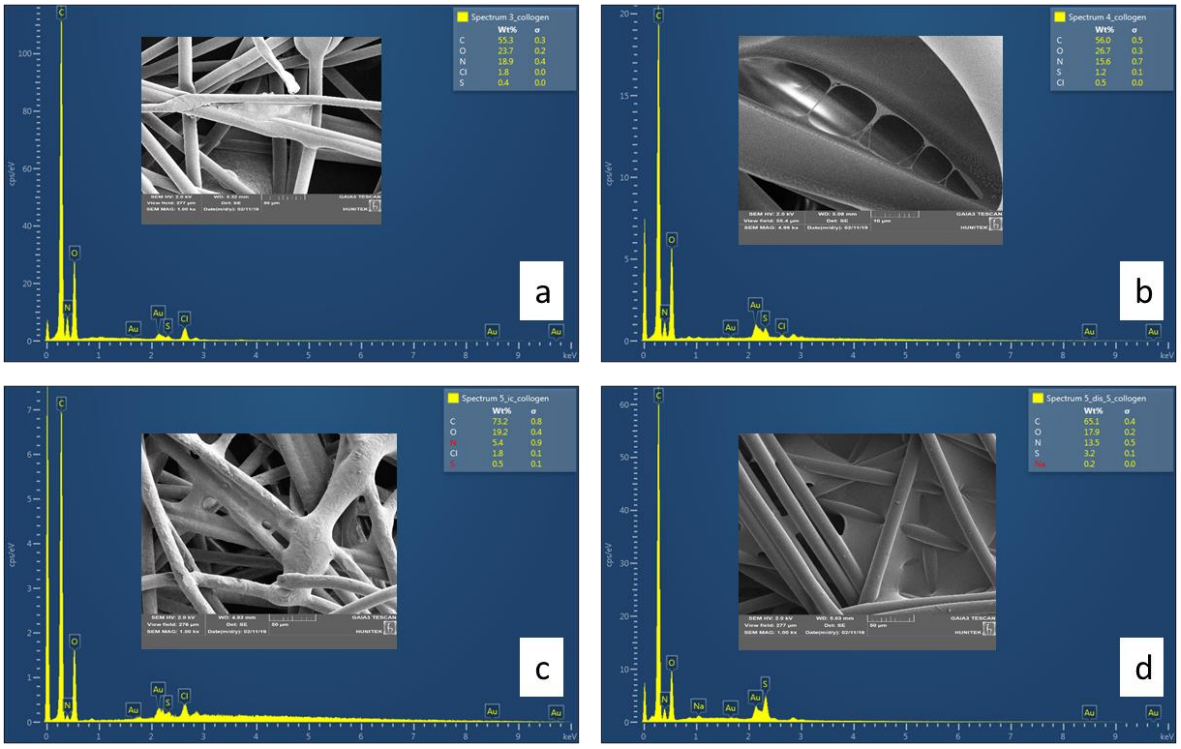

Figure 4. 11. The results of EDS analyses of (a) Group 0-i-col, (b) Group 0-d-col, (c) Group 3-i-col and (d) Group 3-d-col (The magnification of inserted SEM images are 1000x).

4.3.4 Biodegradation Studies

To evaluate the stability of collagen type-1 coating on the surface of the PET disks, biodegradability analysis was carried out with Group 3-i-col samples. Besides, SEM analysis was performed to monitor the presence of collagen coating on PET surface during the biodegradation study. SEM images were taken on the 1st, 3rd, 5th and 7th days of incubation in PBS are presented in Figures 4.12.-15., respectively. In the SEM images of the 1st and 3rd day of incubation, it is seen that the collagen type-1 coating was dense and preserved its integrity (Figures 4.12. and 4.13.). However, it was observed that the coating started to deteriorate on the 5th day (Figure 4.14.). On the 7th day, it was noticed that the integrity of the coating was lost (Figure 4.15.).

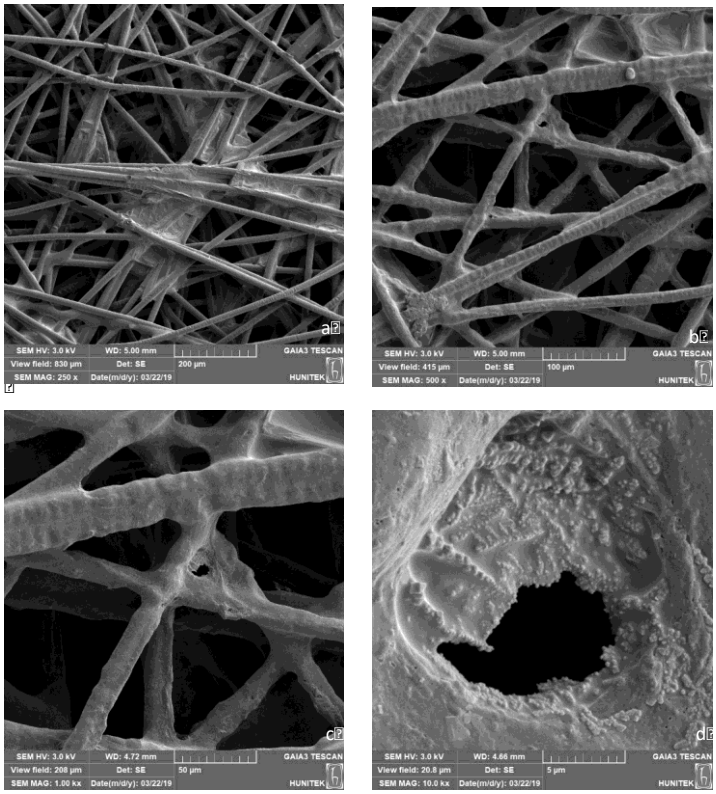

Figure 4. 12. SEM images of collagen type-1 coated Group 3-i-col PET disks on the 1st day of biodegradation study: (a) 250x, (b) 500x, (c) 1000x, (d) 10000x.

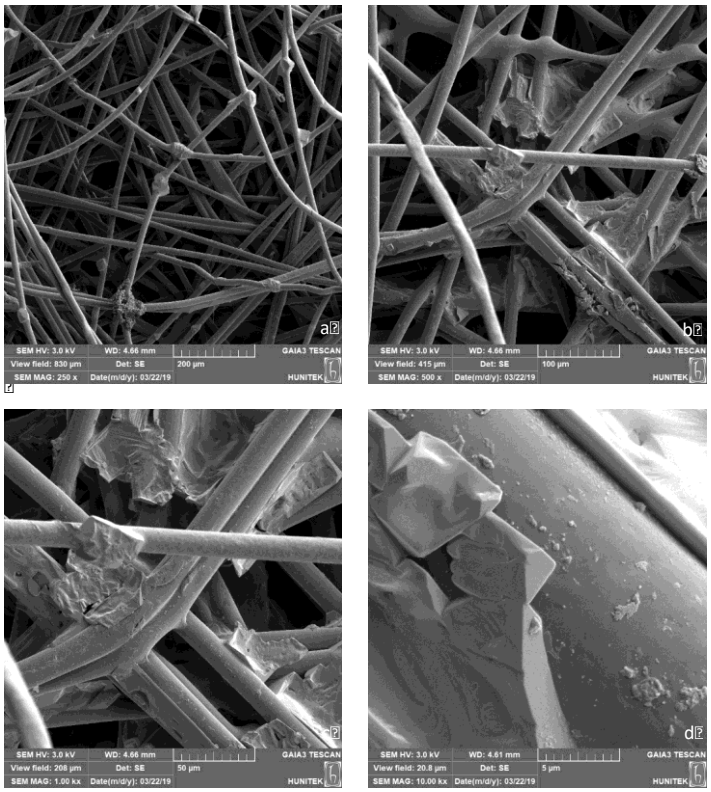

Figure 4. 13. SEM images of collagen type-1 coated Group 3-i-col PET disks on the 3rd day of biodegradation study: (a) 250x, (b) 500x, (c) 1000x, (d) 10000x.

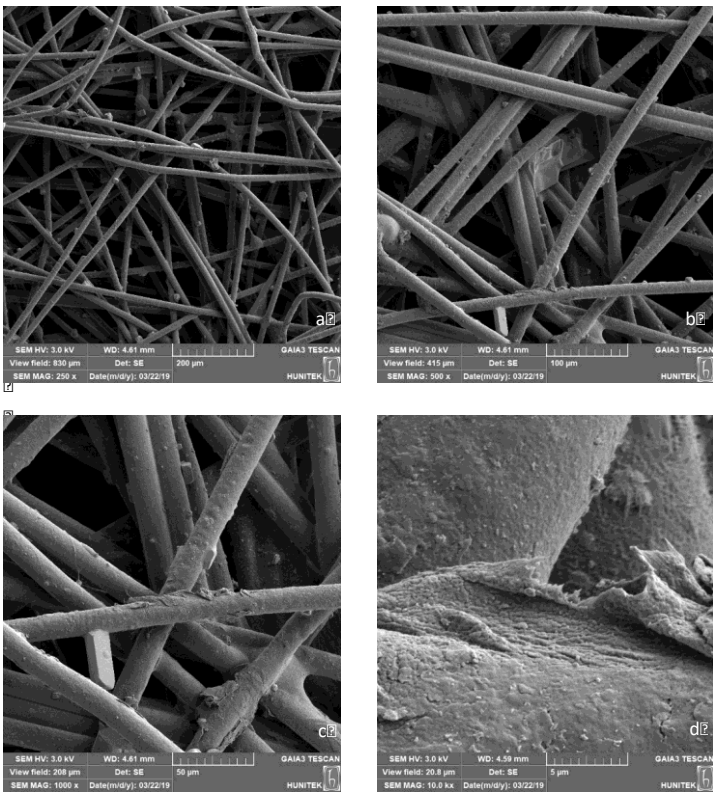

Figure 4. 14. SEM images of collagen type-1 coated Group 3-i-col PET disks on the 5th day of biodegradation study: (a) 250x, (b) 500x, (c) 1000x, (d) 10000x.

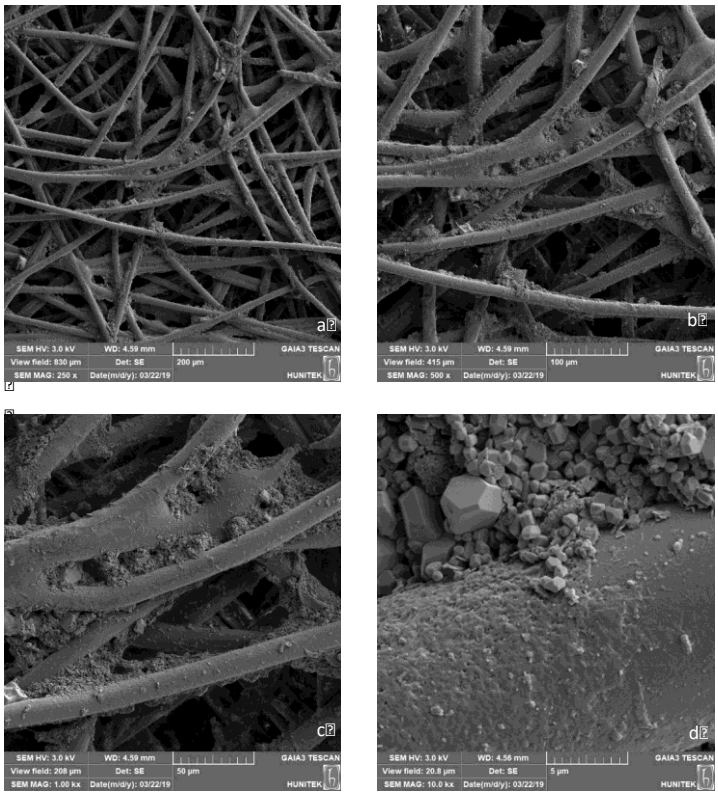

Figure 4. 15. SEM images of collagen type-1 coated Group 3-i-col PET disks on the 7th day of biodegradation study: (a) 250x, (b) 500x, (c) 1000x, (d) 10000x.

4.3.5 *In Vitro* Cell Culture Studies

Evaluating the results obtained from the characterization studies, the preliminary cell culture studies were carried out with Group 0 and Group 3 PET disks with immersive collagen type-1 coating, using MC3T3-E1 cells. In order to determine the mitochondrial activities of cells on PET discs with different surface properties, MTT analysis was performed and the results are presented in Figure 4.16. Mitochondrial activity in all groups increased throughout the culture period. However, it was noteworthy that the absorbance values obtained from different groups during the 7-day culture period were found to be comparable. This may be caused by different reasons such as the lack of a positive effect of collagen type-1 coating on cell growth in PET disks, biodegradability of collagen type-1 coating or insufficient amount of collagen type-1 coating. In addition, the amount of collagen type-1 coated per disk is below 6-10 µg/cm^2,

which is recommended for TCPS surfaces in the collagen coating protocol and this indicates that the amount of collagen coated on PET surface might be insufficient to alter cell behavior.

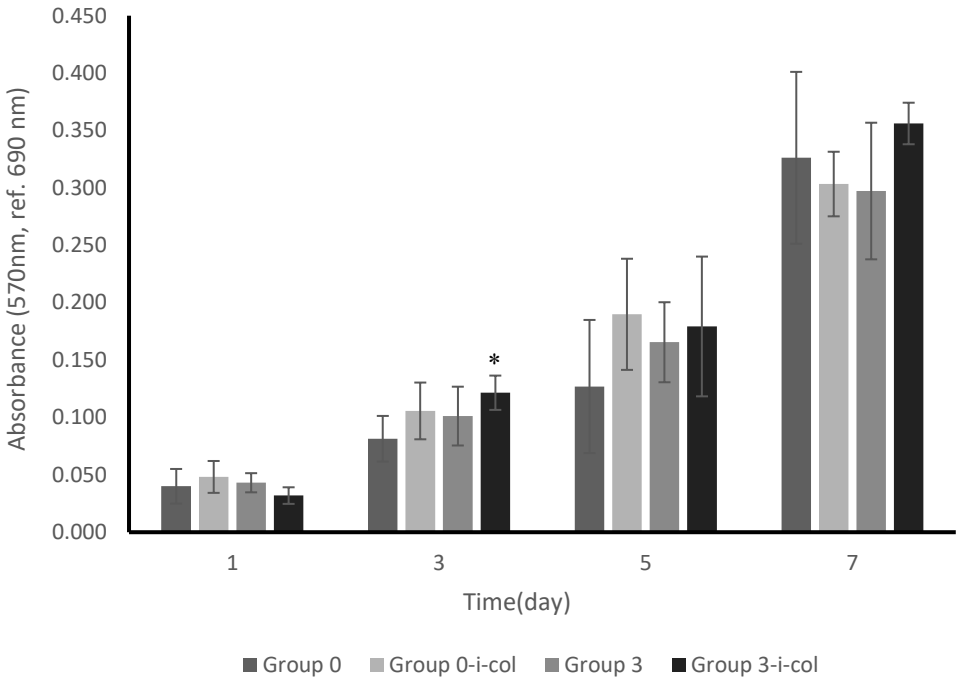

Figure 4. 16. Mitochondrial activity of MC3T3-E1 cells on Group 0 and 3 PET disks with or without immersive collagen type-1 coating under static cell culture conditions (Statistical differences when Group 0 is the control: * $p<0.05$, ** $p<0.01$, *** $p<0.001$).

4.4 Preparation of Vitronectin Coated PET Disks by Dropping Method and Characterization Studies

In this part of the study, Group 3 PET disks were coated with vitronectin through a physical coating method, absorption via dropping. The effect of vitronectin coating was only evaluated with static cell culture studies carried out with rAdMSCs. Two different coating densities, 0.15 µg/disk (Group 3-d-vn) and 0.6 µg/disk (Group 3-d-vn4x), were studied in order to enhance rAdMSCs attachment and viability on PET discs. As seen in Fig. 4.17, mitochondrial activity of rAdMSCs on PET disks with different vitronectin coating densities are comparable to the control group (Group 3), demonstrating presence of vitronectin coating on Group 3 PET

discs did not have positive effects on cell activity. This may be originated from different reasons such as vitronectin coating lack of a positive effect on the cell growth in PET fiber matrices, the biodegradability of the vitronectin coating or the insufficient amount of vitronectin coated

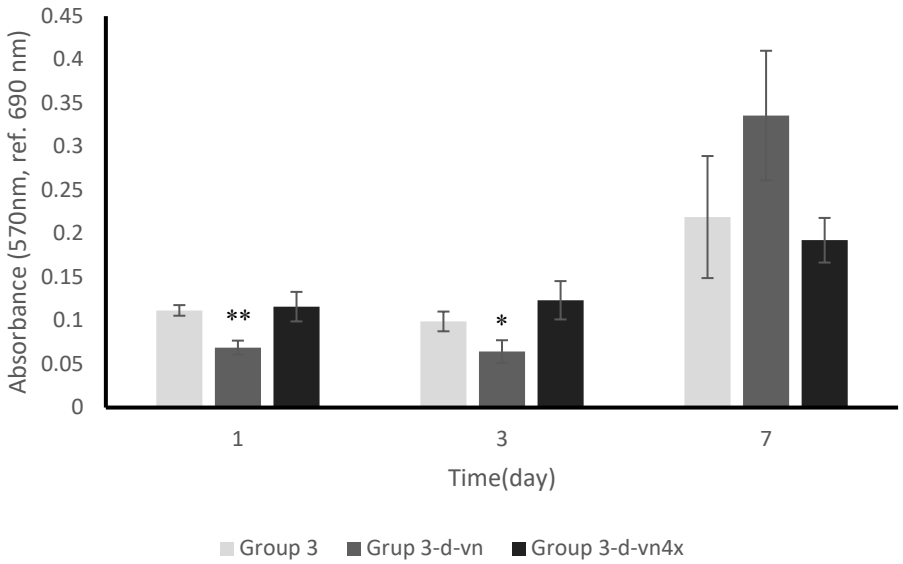

Figure 4. 17. Mitochondrial activity of rAdMSCs on Group 3 PET disks with different vitronectin coating densities (Statistical differences when Group 3 is the control: * $p<0.05$, ** $p<0.01$, *** $p<0.001$).

4.5 Cell Expansion on PET Disks Coated with Vitronectin and Collagen via Physical Methods

Depending on the results of preliminary cell culture studies that were carried out with collagen type-1 and vitronectin coated PET discs, 2 groups were selected to be used in a more comprehensive cell culture study. For this purpose, rAdMSCs (passage 8) were seeded on Group 3, Group 3-d-col and Group 3-d-vn. Cell activity and proliferation was monitored by MTT tests and hemocytometer counting, whereas cell density and distribution were visualized by DAPI and crystal violet staining. MTT analysis results are presented in Figure 4.18. According to the MTT results mitochondrial activity of rAdMSCs increased in all groups

during the cell culture. The absorbance value of Group 3-d-vn at the 1st day was lowest among the other groups. At the 5th day, absorbance of Group 3-d-vn overpass the other groups and reached higher absorbance value at the end of culture period. However, there was no statistical difference observed among Group 3, Group 3-d-col and Group 3-d-vn ($p>0.05$). In addition, according to the cell counting data presented in Table 4.4, the number of cells per disc is below the 3×10^4 which lower than the number of cells recommended for TCPS surfaces in the literature, indicating the cell seeding may be insufficient. When cell numbers at the end of the culture period are compared to the initial cell seeding density on PET surfaces, it is found that cell number increased by 1.3 fold in Group 3, 2.9 fold in Group 3-d-col and 2.1 fold in Group 3-d-vn.

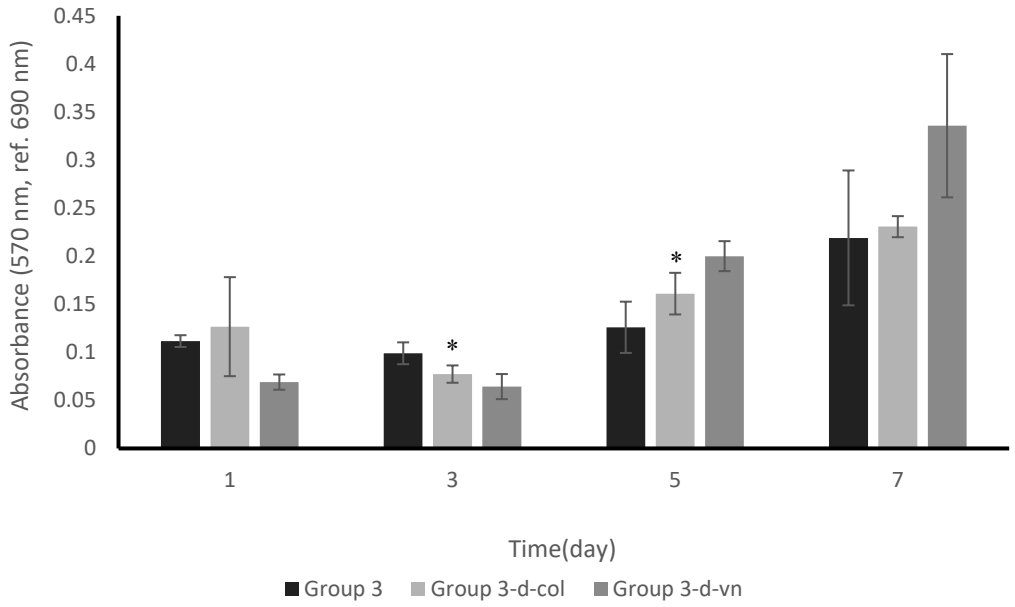

Figure 4. 18. Effects of physical coating of vitronectin and collagen type-1 on mitochondrial activities of rAdMSCs on Group 3 PET fiber matrices.

Table 4. 4. Hemocytometer counting results obtained from the culture of rAdMSC on different PET discs.

	Number of Cells			
Group	**1st Day**	**3rd Day**	**5th Day**	**7th Day**
TCPS	11600 ±958	25800 ±16230	91500 ±11368	91875 ±11023
Group 3	15000 ±820	40000 ±4589	22500 ±4761	19375 ±6206
Group 3-d-col	13125 ±5336	40000 ±4664	15000 ±2017	37500 ±1783
Group 3-d-vn	16667 ±1917	28000 ±5680	24375 ±1899	34167 ±7584

4.5.1 DAPI Staining

The nucleus of rAdMSCs on the 1st and 7th days of cell culture were stained with DAPI and the cells were observed under the fluorescence microscope. DAPI staining images from 1st day of cell culture are given in Figure 4.19. showing that fewer number of cell nuclei spotted on all 3 groups. However, DAPI staining images from 7th day of cell culture in Figure 4.20 presents evenly distributed cell nuclei on all groups. Additionally, DAPI staining of Group 3-d-vn on the 7th day of cell culture, shows higher number of cells on the surface of PET compared to other groups.

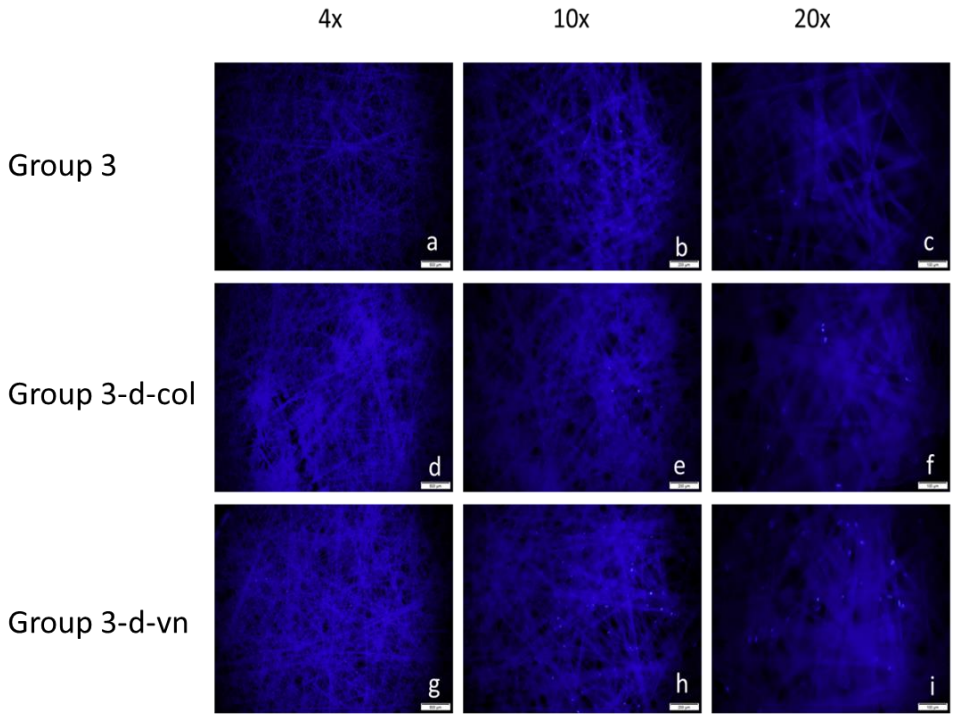

Figure 4. 19. DAPI staining images of the 1st day of culture: Group 3: (a) 4x, (b) 10 x, (c) 20x; Group 3-d-col: (d) 4x, (e) 10 x, (f) 20x; Group 3-d-vn discs: (g) 4x, (h) 10 x, (i) 20x (Scale bar represents x µm).

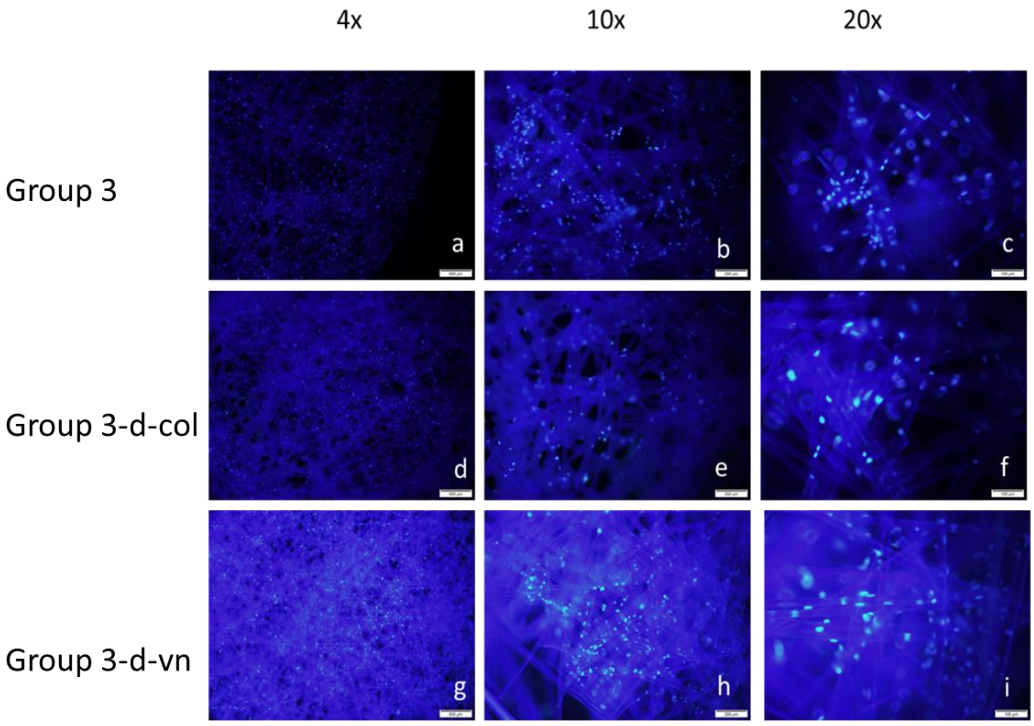

Figure 4. 20. DAPI staining images of the 7th day of culture: Group 3: (a) 4x, (b) 10 x, (c) 20x; Group 3-d-col: (d) 4x, (e) 10 x, (f) 20x; Group 3-d-vn discs: (g) 4x, (h) 10 x, (i) 20x (Scale bar represents x µm).

4.5.2 Crystal Violet Staining

In order to monitor the cell density and distribution on different PET surfaces, samples from all 3 groups on the 1st and 7th days of cell culture were stained with crystal violet and the images are presented in Figure 4.21. and 4.22.

When the crystal violet images given in Figure 4.21-22 were examined, the cell density in all groups from the 1st day of cell culture displayed similar density of cells adhered on the surface of PET fibers. By the 7th day, it is seen that the highest cell density was observed in Group 3-d-vn. Also, it was determined that the cell density was comparable in Group 3 and Group 3-d-col. Overall, the cells in these 3 groups adhere to the surface of PET fibers intensely, spread and exhibit a spindle morphology. In addition, the results obtained from crystal violet staining supports MTT results presented in Figure 4.18.

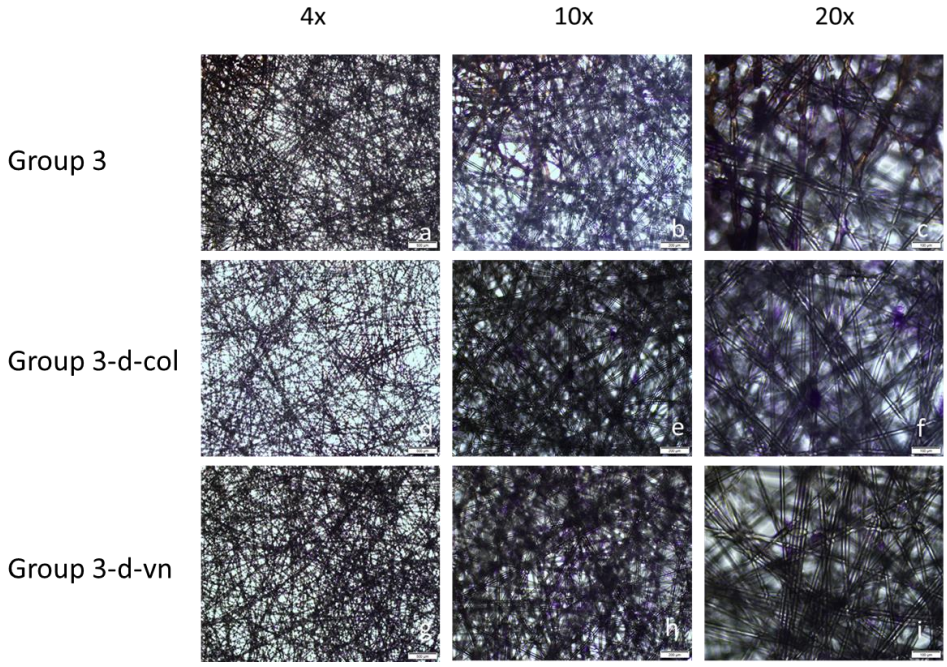

Figure 4. 21. Crystal violet staining images of the 1st day of culture: Group 3: (a) 4x, (b) 10 x, (c) 20x; Group 3-d-col: (d) 4x, (e) 10 x, (f) 20x; Group 3-d-vn discs: (g) 4x, (h) 10 x, (i) 20x (Scale bar represents x μm).

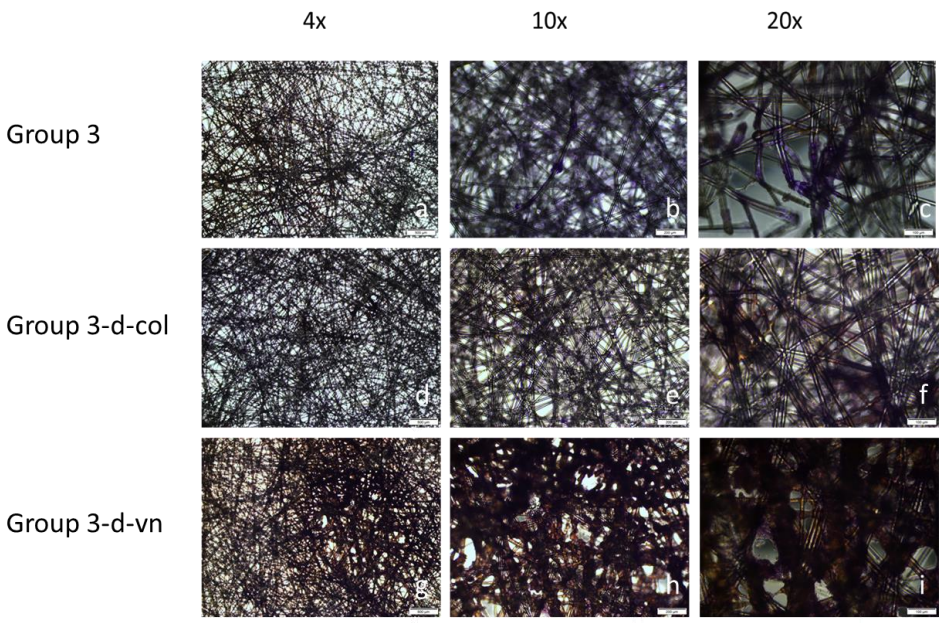

Figure 4. 22. Crystal violet staining images of the 7th day of culture: Group 3: (a) 4x, (b) 10 x, (c) 20x; Group 3-d-col: (d) 4x, (e) 10 x, (f) 20x; Group 3-d-vn discs: (g) 4x, (h) 10 x, (i) 20x (Scale bar represents 50 μm).

4.6 Chemical Immobilization of Collagen Type-1 and Vitronectin on PET Disks and Characterization Studies

According to the literature PET surface needs carboxyl (-COOH) end chains in order to reaction with EDC and NHS and depend on ATR-FTIR analysis Group 4 was selected [121]. In this part of the thesis, collagen type-1 and vitronectin was chemically immobilized on the surface of Group 4 PET disks through EDC/NHS crosslinking method. The amount of collagen type-1 and vitronectin used in EDC/NHS crosslinking is 30 μg and 0.15 μg per disk, respectively. The immobilization efficiency of collagen type-1 was analysed with hydroxyproline, SEM and ATR-FTIR analyses, whereas vitronectin coated samples were characterized by SEM and ATR-FTIR analyses. Cell proliferation of rAdMSCs on collagen and vitronectin coated Group 4 PET disks was investigated through static cell culture studies.

4.6.1 Chemical Immobilization of Collagen type-1 on PET Disks

Collagen type-1 grafting onto PET surface includes three subsequent modification procedures: hydrolysis with NaOH; NHS, EDC grafting; collagen type-1 grafting [121]. In this study, the efficacy of chemical immobilization of collagen type-1 is compared with physical coating with dropping technique (Group 4-col).

4.6.1.1 Hydroxyproline Analysis

The results obtained from the hydroxyproline analysis are presented in Table 4.5. Using the equation given in Figure 4.6, the amount of hydroxyproline in the samples was calculated from the optical density values. It was observed that the highest amount of collagen type-1 crosslinking occurred in Group 4-EDC/NHS-col as 24.1 µg/disk followed by Group 4-col as 17.3 µg/disk. In comparison, EDC/NHS treated Group 4 also demonstrated certain level of optical value which accepted as systematic error of our measurement method. In summary, results of hydroxyproline assay showed that chemical binding method in Group 4-EDC/NHS-col resulted in higher amounts of collagen coating than physical absorption method applied in Group 4-col.

Table 4. 5. Amounts of collagen type-1 coated on surface modified PET disks with different techniques.

Group	Optical Density (550 nm)	Amount of Hydroxyproline (µg)	Amount of collagen type-1 (µg/disk)
Group 4-EDC/NHS-col	0.4 ± 0.28	11.6 ± 6.76	24.1 ± 14.08
Group 4-col	0.3 ±0.15	8.3 ± 2.12	17.3 ± 13.24
Group 4-EDC/NHS	0.2 ±0.00	3.8 ± 0.00	7.9 ± 0.00

4.6.1.2 SEM Analysis

SEM analysis was performed to examine the presence and distribution of collagen type-1 coating on Group 4 PET fibers after the chemical immobilization method. When Fig. 4.23

was examined, it was seen that there was a significant difference between fiber morphology and diameters of Group 4-EDC/NHS, Group 4-col and Group 4-EDC/NHS-col. It was observed that collagen type-1 was evenly coated on Group 4-EDC/NHS-col, PET fiber diameter was increased and surface roughness was increased. Especially, when Group 4-EDC/NHS-col was compared with Group 4-col, it was seen that layer of collagen was formed on the surface of PET fiber when chemical immobilization was applied (Fig. 4.23-d and g). Besides, SEM images of Group 4-EDC/NHS demonstrates that chemical binding method did not altered the surface morphology and diameter of PET fiber (Fig. 4.23-a-c).

In summary, the results of hydroxyproline and SEM analysis of groups demonstrated that chemical binding of collagen via EDC/NHS is more efficient than physical coating. Results also presented that EDC/NHS method had no negative effect on PET fiber surface morphology showing that EDC/NHS chemical binding method is a suitable technique for PET fiber coating.

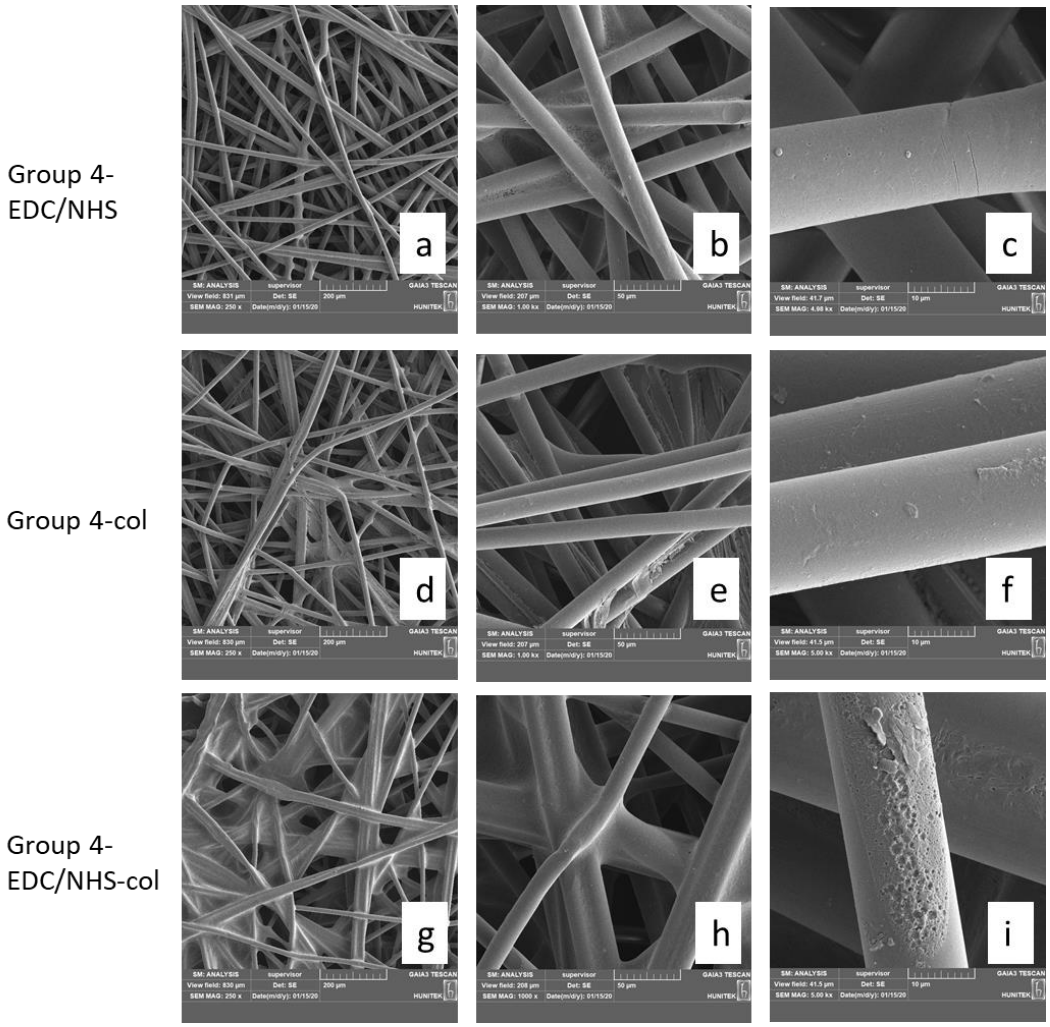

Figure 4. 23. SEM images of PET disks coated with collagen type-1 via physical and chemical methods: Group 4-EDC/NHS: (a) 250x, (b) 1000x, (c) 5000x; Group 4-col: (d) 250x, (e) 1000x, (f) 5000x; Group 4-EDC/NHS-col: (g) 250x, (h) 1000x, (i) 5000x.

4.6.1.3 ATR-FTIR Analysis

To understand the effects of collagen type-1 coating by chemical immobilization on the chemical structure of PET surface, ATR-FTIR analysis was done. The spectra of Group 4-EDC/NHS, Group 4-col and Group 4-EDC/NHS-col are presented in Figure 4.24. All groups exhibited the hydroxyl ion (OH) stretching between 3500 cm^{-1} and 3200 cm^{-1} which was observed for plain Group 4 that was treated with NaOH.. As given in the related literature, collagen type-1 exhibits peaks near 1659 cm^{-1} and 1555 cm^{-1} that are arising from Amide I and Amide II absorption, respectively [122]. In Figure 4.24, these peaks were

observed in the Group 4-col, as shown with black arrows, near 1659 cm^{-1} and 1555 cm^{-1} as an evidence of collagen type-1 presence. However, the peaks were not found in Group 4-EDC/NHS-col and this can be attributed to the low level of collagen amount on the surface of PET fibers. Besides, it appears that ATR-FTIR results of Group 4-EDC/NHS-col were not consistent with the results of hydroxyproline analysis and SEM analysis.

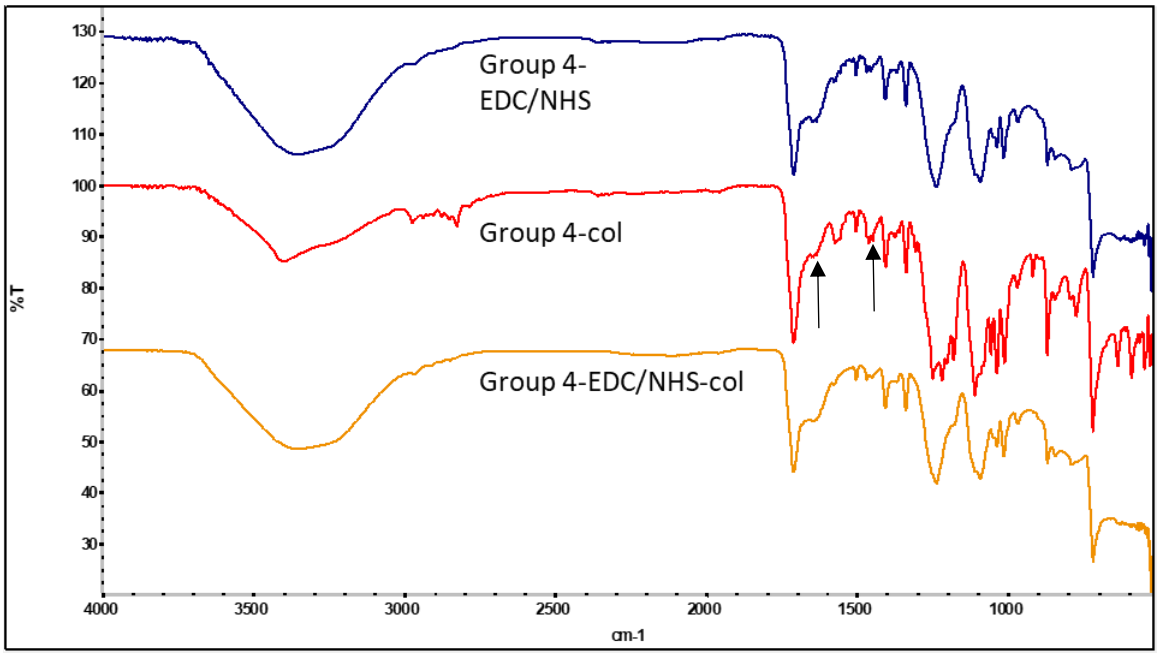

Figure 4. 24. ATR-FTIR spectra of Group 4 PET discs coated with collagen type-1 via chemical and physical methods.

4.6.2 Chemical Immobilization of Vitronectin on PET Disks

4.6.2.1 SEM Analysis

SEM analysis was performed to examine the presence and distribution of vitronectin coating on Group 4 PET fiber after chemical immobilization via EDC/NHS method. When Fig. 4.25 was examined, it was seen that there was a significant difference between fiber morphologies and diameters of Group 4-EDC/NHS, Group 4-vn and Group 4-EDC/NHS-vn. It was observed that vitronectin was evenly coated on Group 4-EDC/NHS-vn, while PET fiber diameter and surface roughness were increased. Especially, when the SEM images of physical

and chemical immobilization methods are compared (Fig. 4.25-d,e,f and Fig. 4.25-g,h,i, respectively) it was seen that layer of vitronectin was formed on the surface of PET fiber when chemical method was applied. In addition, Group 4-EDC/NHS (Fig. 4.25-c) demonstrates that chemical binding method did not alter the surface morphology and diameter of PET fiber.

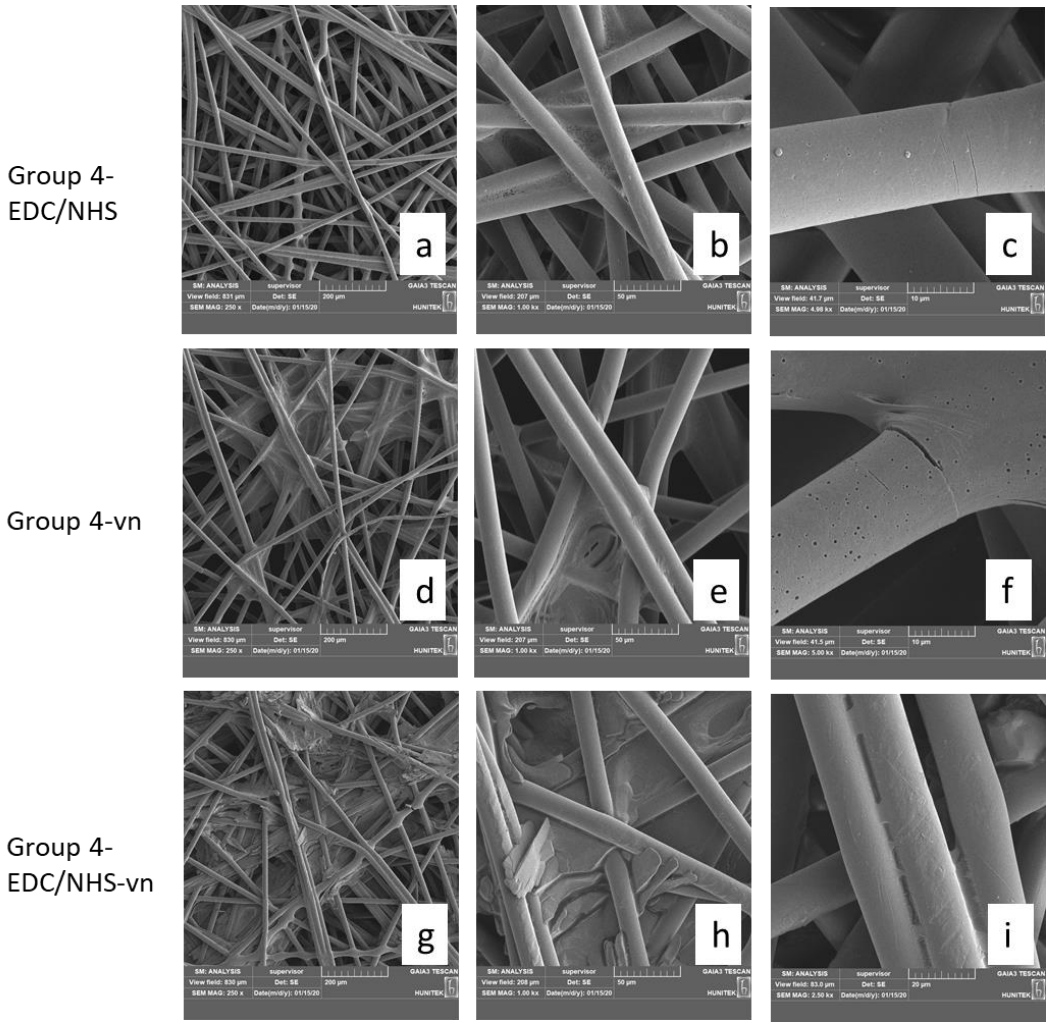

Figure 4. 25. SEM images of PET disks coated with vitronectin via physical and chemical methods: Group 4-EDC/NHS: (a) 250x, (b) 1000x, (c) 5000x; Group 4-vn: (d) 250x, (e) 1000x, (f) 5000x; Group 4-EDC/NHS-vn: (g) 250x, (h) 1000x, (i) 5000x.

4.6.2.2 ATR-FTIR Analysis

To determine the presence of vitronectin on Group 4 Pet discs, ATR-FTIR analysis was carried out. The spectra of all groups are presented in Figure 4.26. It is seen that all groups exhibited the hydroxyl ion (OH) stretching between 3500 cm^{-1} and 3200 cm^{-1} which are previously observed from the spectrum of Group 4**.** In the related literature, it is given that vitronectin exhibits peaks near 1631 cm^{-1}, 2990 cm^{-1} and 3186 cm^{-1} that are specific to such proteins [123]. However, in Figure 4.26. these peaks were not detected in Group 4-vn and Group 4-EDC/NHS-vn. This can be caused by the low level of vitronectin amounts on the surface of PET fibers.

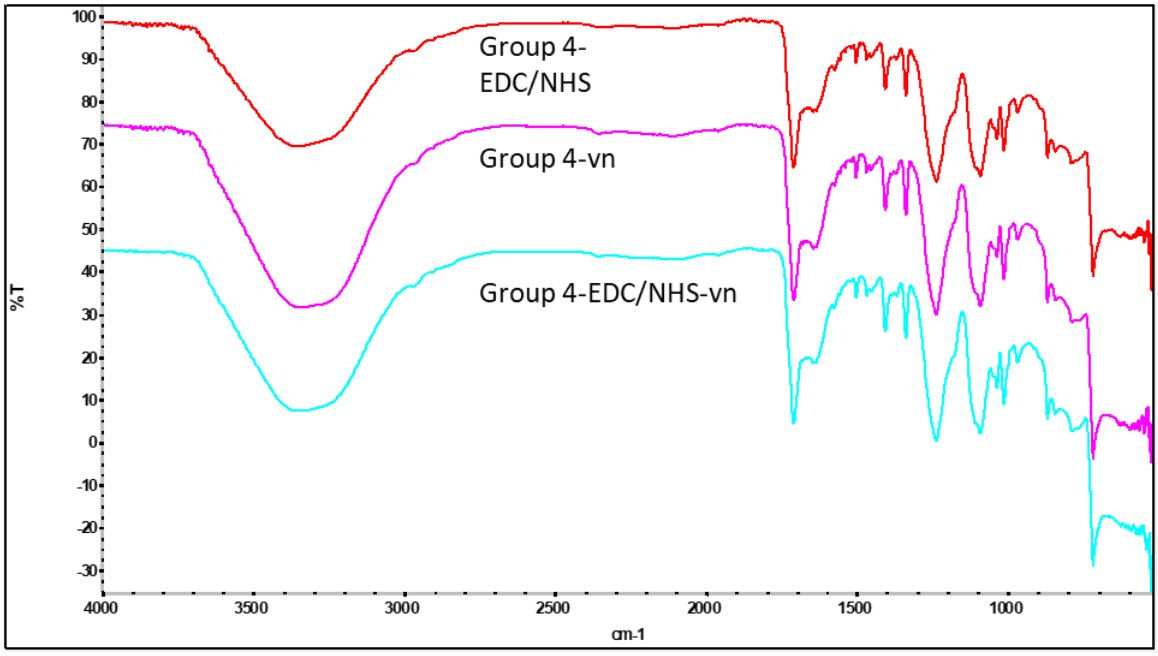

Figure 4. 26. ATR-FTIR spectra of Group 4 PET discs coated with vitronectin via chemical and physical methods.

4.6.3 Cell Expansion on PET Disks coated with Vitronectin and Collagen via Chemical Methods

In this part of the thesis, cell culture studies were carried out with PET disks coated with vitronectin and collagen via EDC/NHS crosslinking. For this purpose, rAdMSCs (passage 8)

were seeded on the groups and cell activity and proliferation were monitored by MTT tests and hemocytometer counting, whereas cell density and distribution were visualized by DAPI and crystal violet staining.

4.6.3.1 MTT Analysis

Mitochondrial activities of cells on collagen type-1 and vitronectin immobilized Group 4 PET disks were determined with MTT analysis. According to the MTT results presented in Figure 4.27, the mitochondrial activities of rAdMSCs on different groups are found to be comparable and had no statistically significant difference.

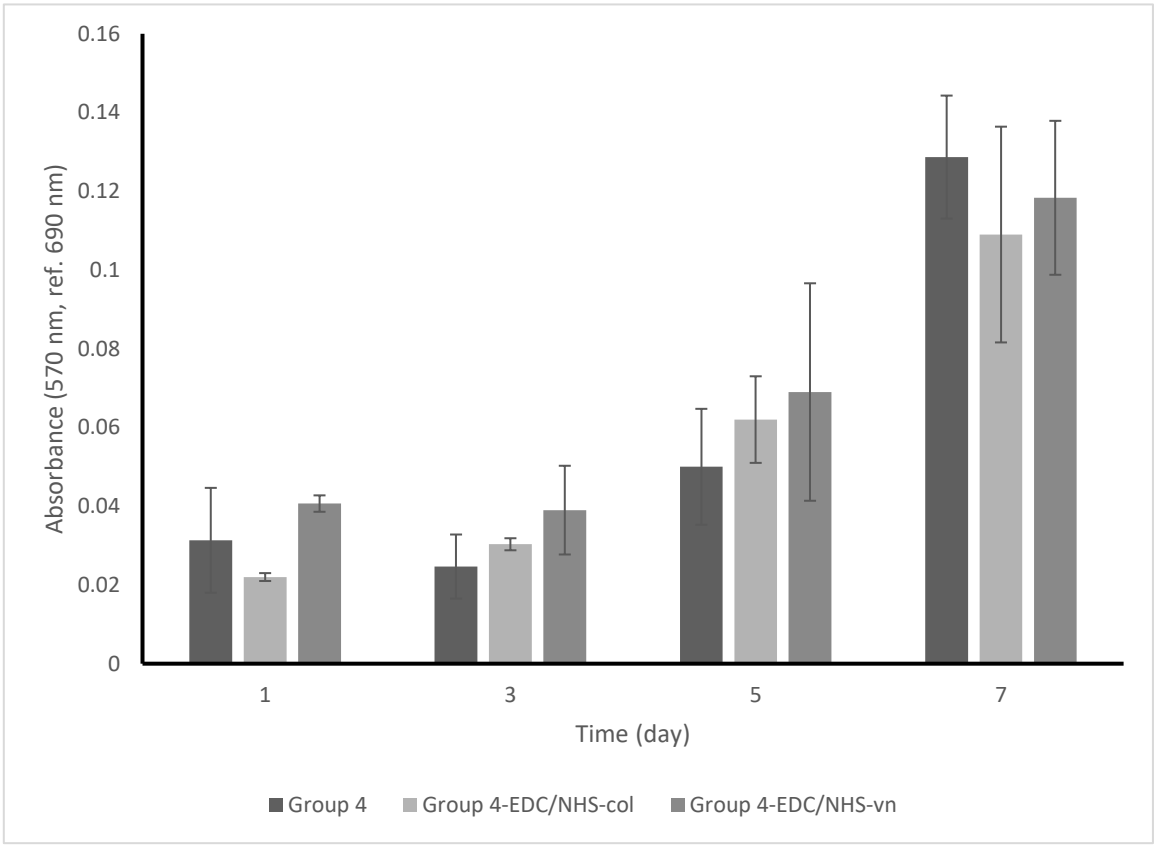

Figure 4. 27. Effects of chemical immobilization of vitronectin and collagen type-1 on mitochondrial activities of rAdMSCs on Group 4 PET fiber matrices.

4.6.3.2 Alexa Fluor 488® phalloidin (F-actin) Staining

F-actin staining images in Figure 4.28 demonstrated the cytoskeleton of rAdMSCs on the Group 4, Group 4-EDC/NHS-vn and Group 4-EDC/HNS-col PET disks. In Figure 4.28. it was observed that of rAdMSC density on PET disks increased in all groups throughout the cell culture. However, it is seen that vitronectin coating on day 1 had significantly higher cell density. In addition to that, after day 3, collagen and vitronectin coated discs had higher number of cells when compared to Group 4 PET disks. Although the results obtained from MTT analysis indicated that there was no significant difference among the groups, F-actin staining demonstrated the positive effects of collagen and vitronectin coating on cell proliferation on PET disk.

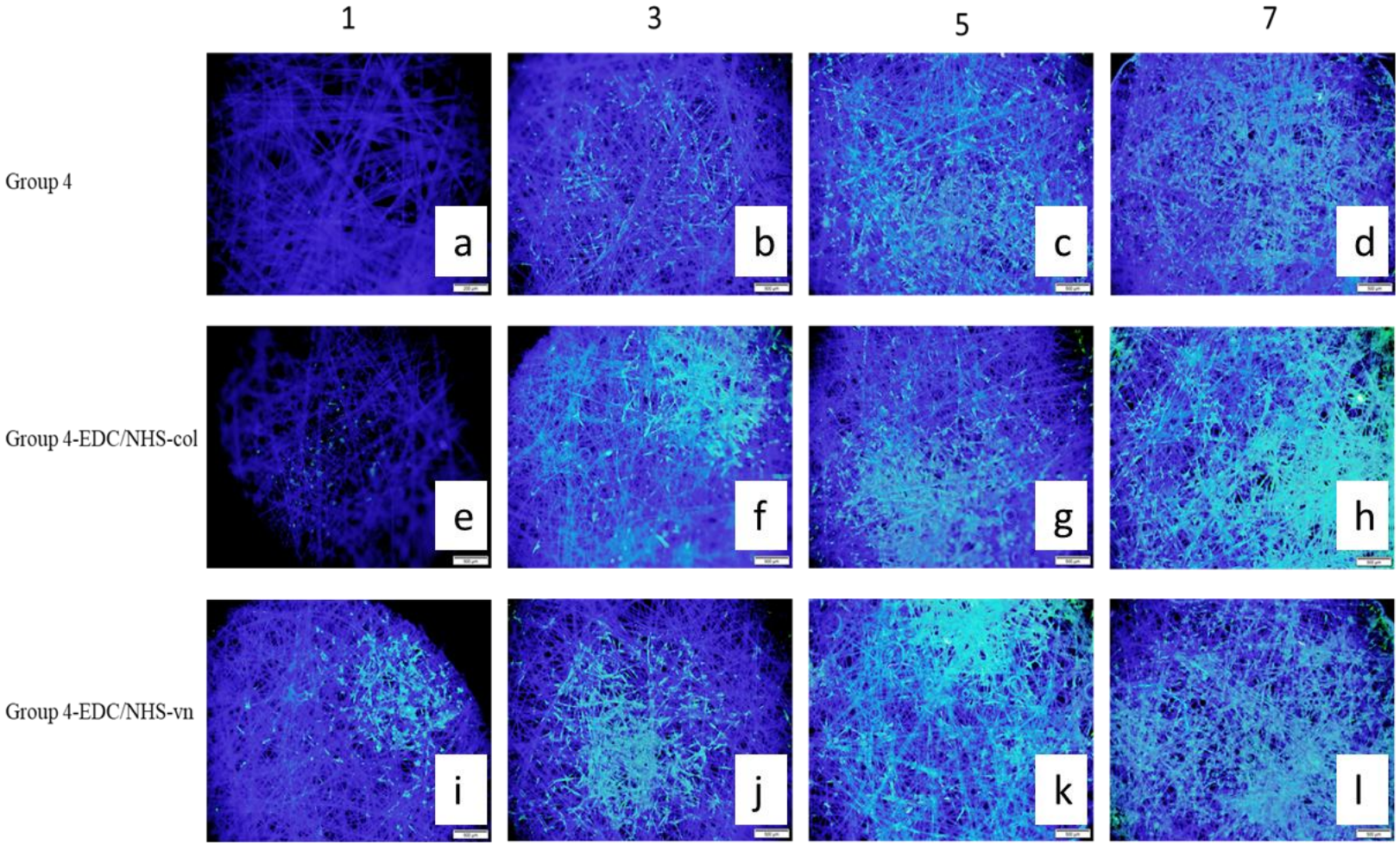

Figure 4. 28. F-actin staining images of rAdMSCs on collagen and vitronectin coated PET disks on different days of culture: Group 4: (a) 1st day, (b) 3rd day, (c) 5th day, (d) 7th day; Group 4-EDC/NHS-col: (e) 1st day, (f) 3rd day, (g) 5th day, (h) 7th day; Group 4-EDC/NHS-vn: (i) 1st day, (j) 3rd day, (k) 5th day, (l) 7th day (Magnification of the images are 4x. Scale bar represents 500 µm).

4.7 Dynamic Cell Culture

The results obtained from preliminary cell culture studies given in Section 4.6.3 were evaluated and Group 4 was selected as the packing material with optimum properties regarding its ability to support rAdMSC proliferation and its low cost. Thus Group 4 PET discs were used in packed bed bioreactor studies.

In this part of the thesis, first the characterization studies of rAdMSCs are presented. Then the results of cell expansion on Group 4 PET discs in packed bed reactor are given. Following this, biochemical analyses of culture medium are presented to characterize dynamic culture conditions in terms of nutrients and metabolic wastes. In addition, characterization studies of cells that were harvested from PET disks after bioreactor culture were also evaluated and the yield of cell expansion was calculated.

4.7.1 Characterization of rAdMSCs

4.7.1.1 DAPI/Alexa Fluor 488® phalloidin (F-actin) staining

To visualize the cytoskeleton and nucleus of rAdMSCs, the DAPI/Alexa Fluor 488® phalloidin (F-actin) staining was performed on 3rd and 7th days of cell culture. In Figure 4.29, rAdMSCs presents spindle-shaped plastic-adherent phenotypes [9], and maintained the phenotype during the 7 day of cell culture.

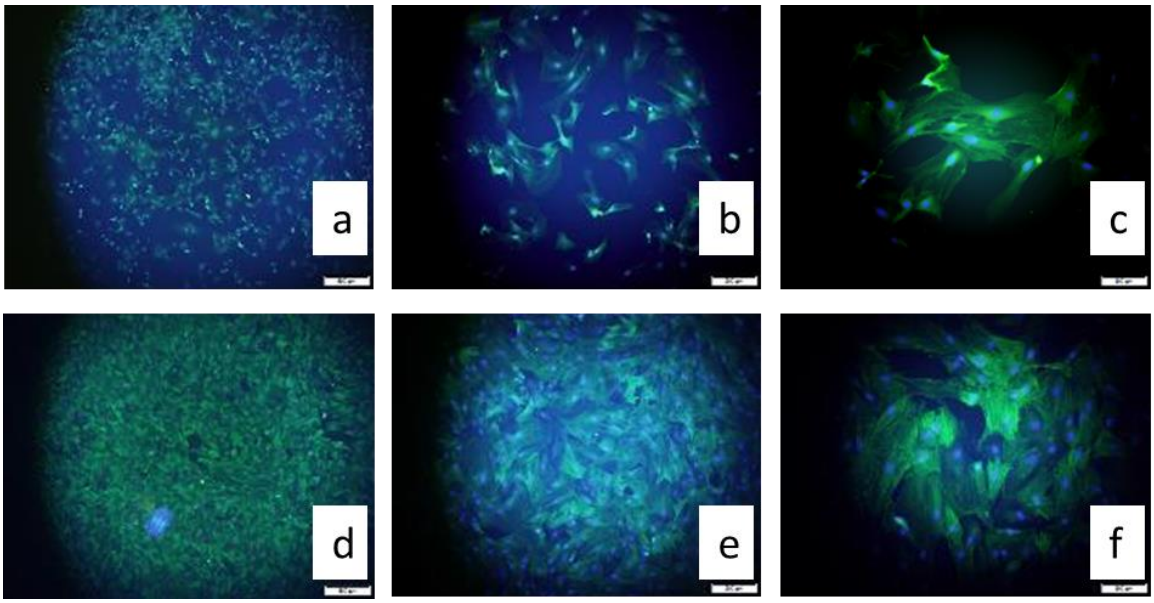

Figure 4. 29. Fluorescence microscopy images of rAdMSCs on different days of monolayer culture: Day 3: (a) 4x, (b) 10x, (c) 20x; Day 7: (d) 4x, (e) 10x, (f) 20x (Scale bar represents 500 μm).

4.7.1.2 Growth Curve of rAdMSCs

Before starting to cell expansion study in the packed-bed bioreactor, the growth curve of rAdMSCs was determined depending on the absorbance data obtained from MTT analysis (Figure 4.30) and cell counting results. In Figure 4.30, lag phase, log phase, stationary phase and death phase of cells are observed. On the 3rd day of cell culture, rAdMSCs enter the log phase. Specific growth rate was calculated by using the Equation 4.1.

$$y=Ae^{Bx} \quad (4.1)$$

Where, y: Absorbance (Optical Density), B: Specific rowth rate and x: Time.

Doubling time (t_d) was calculated according to Equation 4.2:

$$t_d=\ln(2) / B \quad (4.2)$$

After using exponential curve fitting function in Excel, specific growth rate (B) was obtained and the doubling time was calculated. The specific growth rate and the doubling time of rAdMSCs were calculated as 0.3564 h^{-1} and 46 h, respectively.

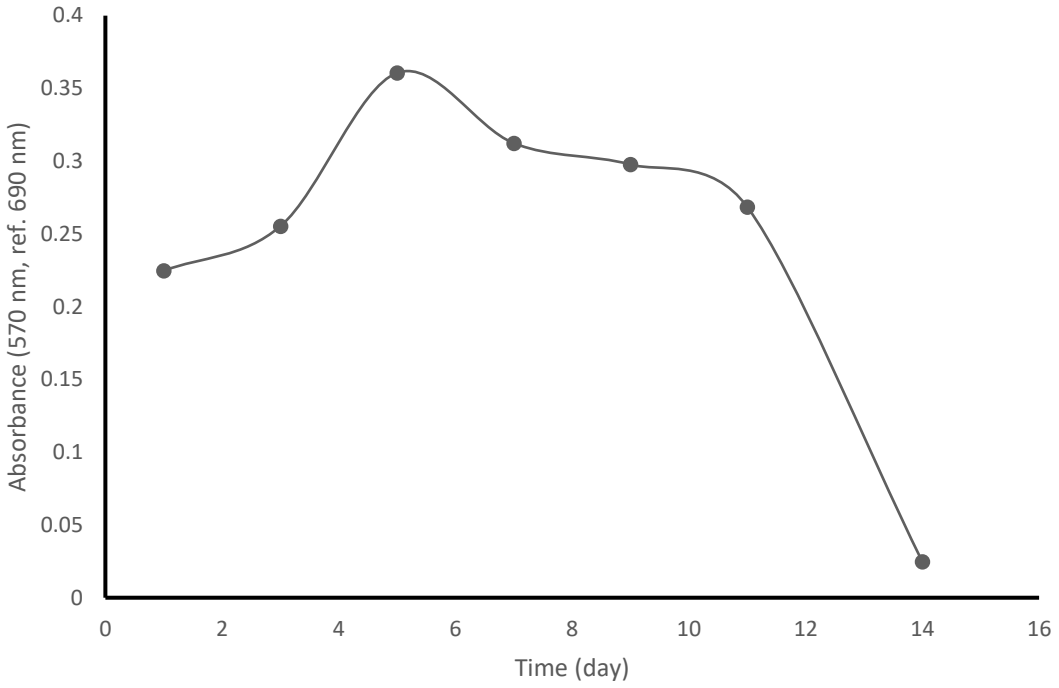

Figure 4. 30. Growth curve of rAdMSCs in monolayer cell culture.

4.7.2 Packed-bed Bioreactor Studies

In this part of study, 30 x 10^6 rAdMSCs (passage 6) were seeded on 1 g of Group 4 PET disks corresponding to a seeding density of 3 × 10^4 cells/disk. After 24 hours of static cell seeding, disks were transferred to our custom-made packed-bed bioreactor, operated under 30 rpm agitation with 100 mL culture medium.

4.7.2.1 MTT Analysis

The mitochondrial activities and hemocytometer counting results obtained from rAdMSCs cultured on Group 4 in our packed-bed bioreactor with seeding density of 30x10^6 cells/ 1g and 1.0x10^7 cells/ 0.5 g disk were given in Figure 4.31, Figure 4.32 and Table 4.6, respectively.

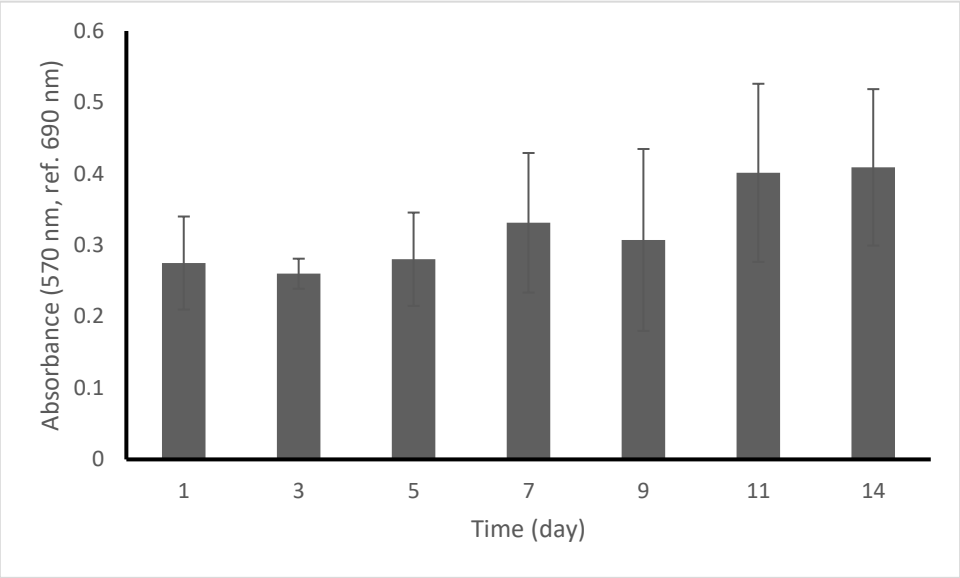

Figure 4. 31. Mitochondrial activities of rAdMSCs cultured on Group 4 in our packed-bed bioreactor with seeding density of $3x10^7$ cells/ 1g disk.

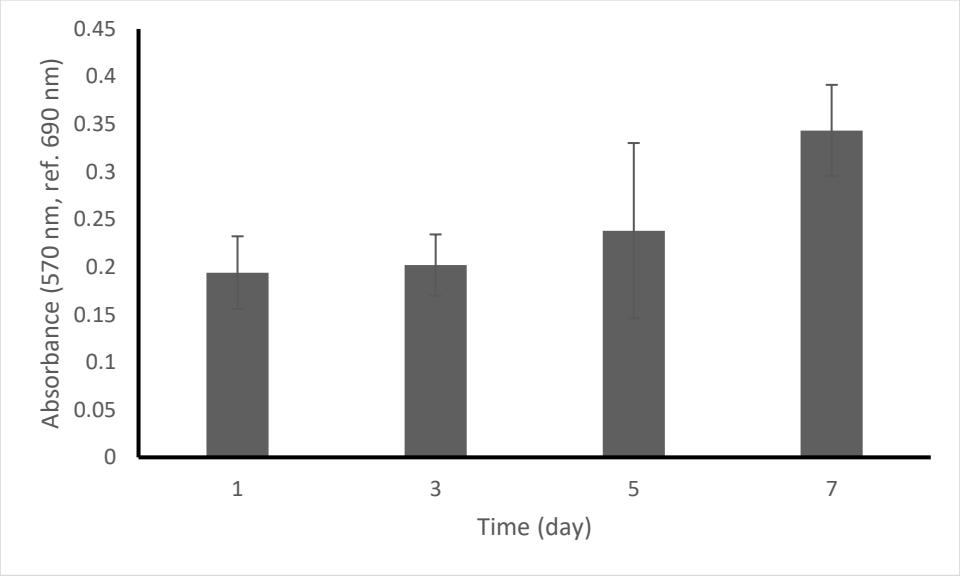

Figure 4. 32. Mitochondrial activities of rAdMSCs cultured on Group 4 in our packed-bed bioreactor with seeding density of $1.0x10^7$ cells/ 0.5 g disk.

Table 4. 6. Hemocytometer counting results of rAdMSC obtained from our packed-bed bioreactor with different amount of packing-material.

	Number of Cells						
Group / Packing-material	**1st Day**	**3rd Day**	**5th Day**	**7th Day**	**9th day**	**11th day**	**14th day**
Group 4 / 1g	16389 ± 1273	19722 ± 4590	16667 ± 833	21667 ± 5833	15833 ± 3819	19722 ± 4276	31389 ± 5422
Group 4 / 0.5 g	15556 ± 899	12500 ± 382	16111 ± 591	16389 ± 127	-	-	-

4.7.2.2 DAPI Staining

In order to visualize cell density and distribution of rAdMSCs on Group 4 PET disks, samples were taken from packed-bed bioreactor at predetermined times throughout the culture. Florescence microscopy images of DAPI staining are presented in Figure 4.33 and Figure 4.34. The cell density on $3x10^7$ cells/ 1g packing material was found to be low at the beginning of culture presented in Figure 4.33. However, as seen in Fig. 4.33-g,h,i, cell density was increased after the 5th of cell culture and evenly distributed on packing material surface. The images indicated that Group 4 PET disks supported cell proliferation and migration. It was observed that number of cells on packing material increased steadily from day 1 to day 9. However, images from day 11 and 14 indicated that proliferation rate of rAdMSCs was decreased.

In Figure 4.34, cell density on $1.0x10^7$ cells/ 0.5 g packing material was observed to be high at the 0th day of culture presented in Figure 3.33. It is also seen in Figure 4.34-d,e,f and Figure 4.34-g,h,I cell density was slightly decreased. It was observed that cell density on packing material started to increase from day 5 to day 7 and evenly distributed on PET fiber surface. The images demonstrated that Group 4 PET disks supported cell expansion and migration.

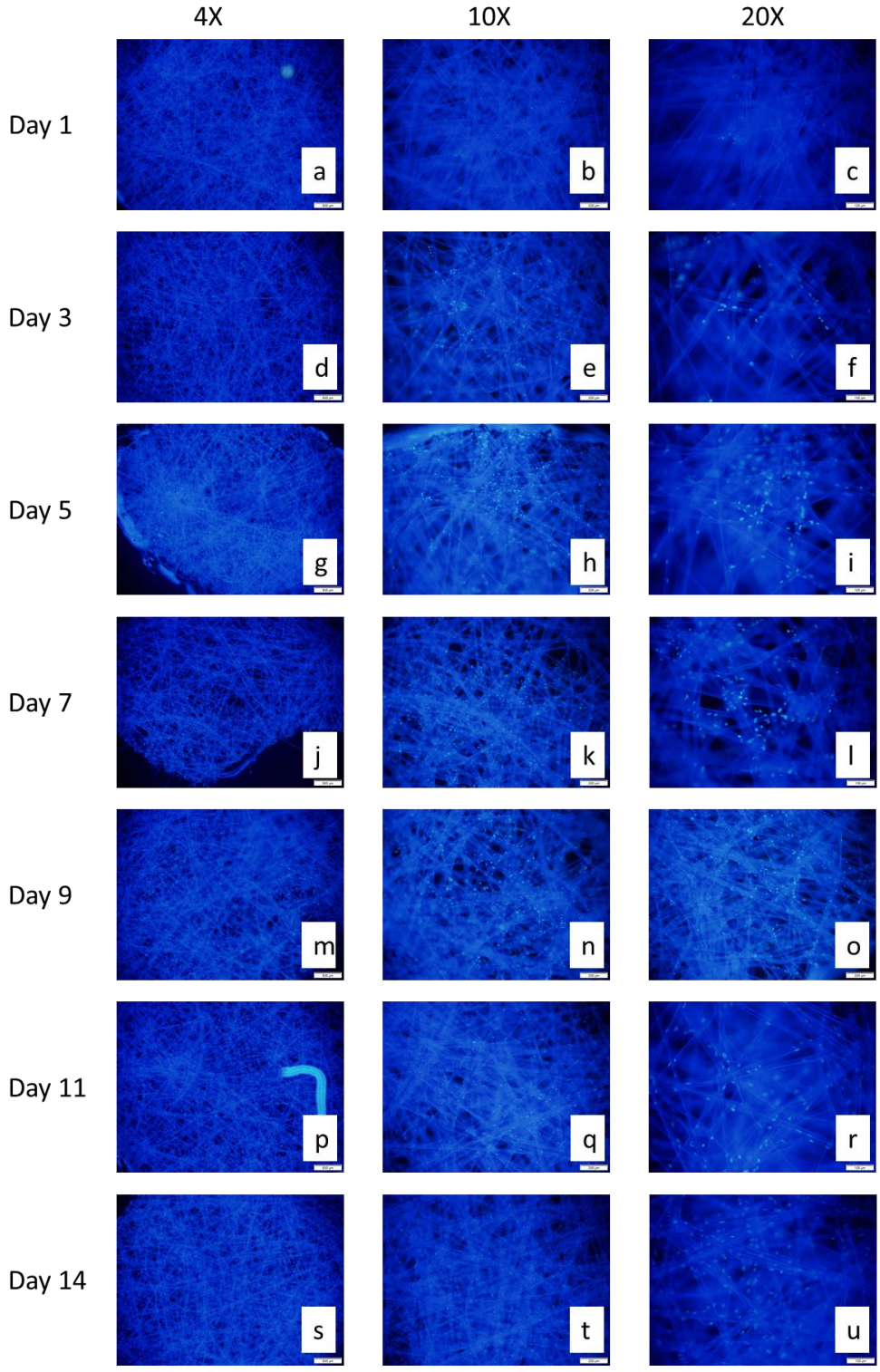

Figure 4. 33. Florescence microscopy images of DAPI staining of rAdMSCs on $3x10^7$ cells/ 1g packing material dynamically cultured in our custom made packed-bed bioreactor: Day 1: (a) 4x, (b) 10 x, (c) 20x; Day 3: (d) 4x, (e) 10 x, (f) 20x; Day 5: (g) 4x, (h) 10 x, (i) 20x; Day 7: (j) 4x, (k) 10 x, (l) 20x; Day 9: (m) 4x, (n) 10 x, (o) 20x; Day 11: (p) 4x, (r) 10 x, (s) 20x; Day 14: (t) 4x, (u) 10 x, (v) 20x (Scale bar represents 100 µm).

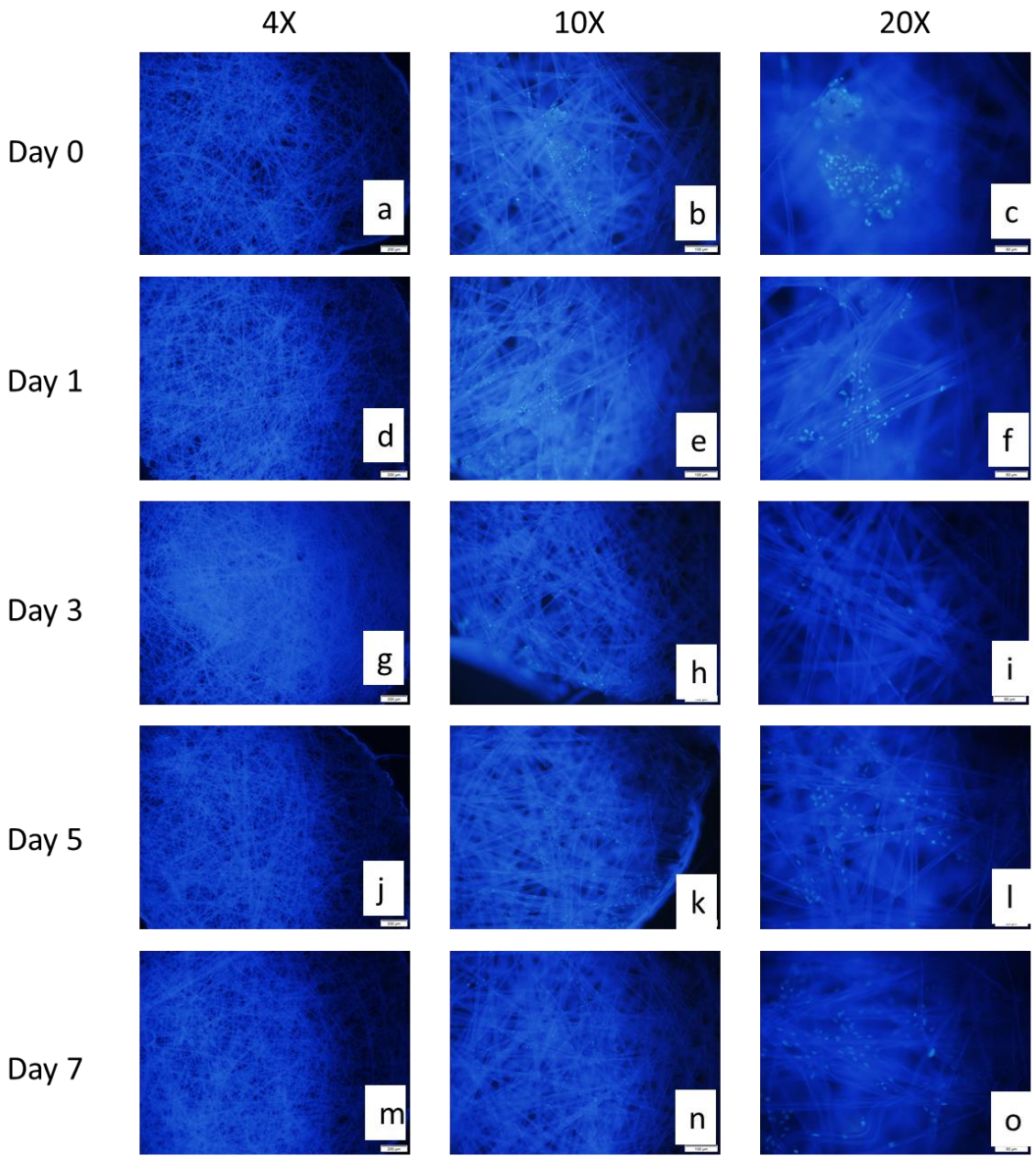

Figure 4. 34. Florescence microscopy images of DAPI staining of rAdMSCs on 1.0x10^7 cells/ 0.5 g packing material dynamically cultured in our custom made packed-bed bioreactor: Day 0: (a) 4x, (b) 10 x, (c) 20x; Day 1: (d) 4x, (e) 10 x, (f) 20x; Day 3: (g) 4x, (h) 10 x, (i) 20x; Day 5: (j) 4x, (k) 10 x, (l) 20x; Day 7: (m) 4x, (n) 10 x, (o) 20x (Scale bar represents 100 µm).

4.7.2.3 Biochemical Analysis of Culture Medium

Figure 4.35 shows the change in glucose, lactate and urea concentrations in packed-bed bioreactor during the 14-day culture. During the first 3 days of cell culture glucose

concentration was decreased to 0 mM and it is determined that cells produced 1.35 mM lactate and 1.5 mM urea. In order to balance the nutrients and metabolic waste concentration, 50% of medium change was performed in every two days from 3rd day of cell culture. However, metabolic analysis demonstrates that 50% of medium exchange was not enough to keep necessary glucose levels for the culture of rAdMSCs in the bioreactor. Glucose consumption rate in bioreactor was found to be much higher than medium exchange rate, which was probably inhibited the cell proliferation. Combining the results obtained from MTT analysis, hemocytometer counting and DAPI staining, it can be concluded that the main limitation of cell expansion in our packed-bed bioreactor is insufficiency of culture medium.

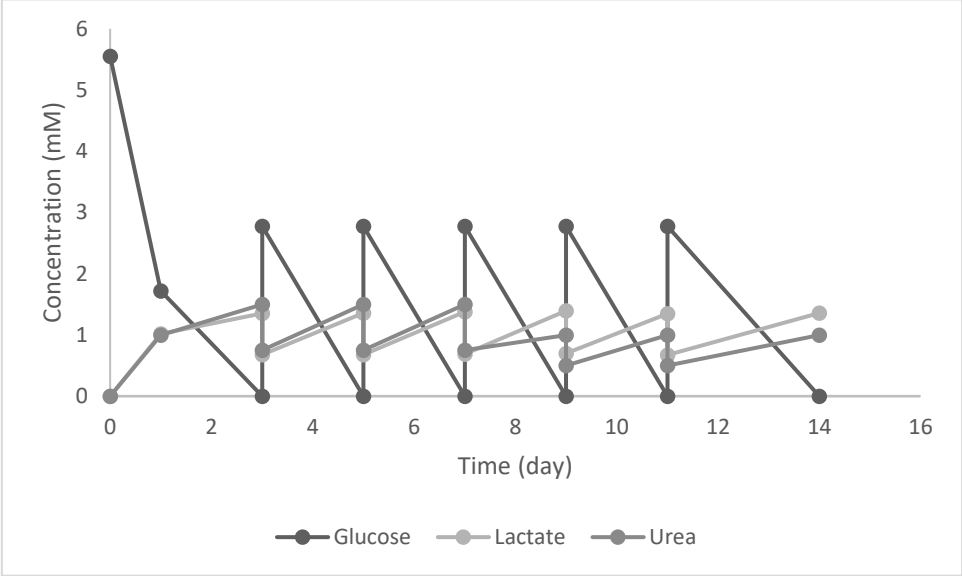

Figure 4. 35. The change of glucose, lactate and urea concentrations changes in packed-bed bioreactor during the 14-day dynamic culture.

4.7.2.4 Cell Harvesting After Dynamic Culture

Rat AdMSCs were harvested from packing material using trypsinization described in Section 3.5.2.2. Packing materials after trypsinization were stained with DAPI in order to examine the cell harvesting efficiency. In Figure 4.36, it was observed that majority of cells were separated from packing material and few cells were remained showing cells could be efficiently harvested via selected procedure. The yield of cells obtained from two separate study

presented in Table 4.7. The yield of cell expansion calculated depend on comparing 1st and 14th day cell number obtain from packing material, the results demonstrated 1.9 fold and 1.2 fold increased achieved from dynamic cell culture, respectively.

Table 4. 7. The number of cells obtained from packing material from the dynamic cell culture.

Group / Packing-material	Initial cell number	Obtained cell number	Yield of expansion
Group 4 / 1g	$1.2 \times 10^7 \pm 1273$	$2.4 \times 10^7 \pm 5422$	1.9
Group 4 / 0.5 g	$5.0 \times 10^6 \pm 8819$	$5.7 \times 10^6 \pm 1272$	1.2

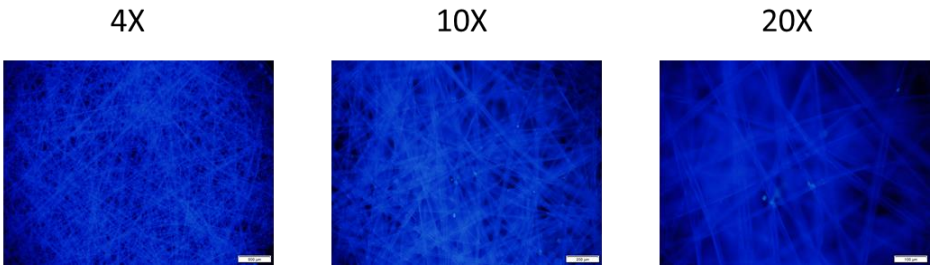

Figure 4. 36. DAPI staining images of packing materials after harvesting of rAdMSCs: (a) 4x, (b) 10x, (c) 20x (Scale bar represents 100 μm).

4.7.3 Characterization of rAdMSCs After Cell Harvesting

To determine the general characteristics of rAdMSCs after cell harvesting from packed-bed bioreactor, cells were inoculated on TCPS and MTT analysis and differentiation studies to osteogenic and adipogenic lineages were carried out in monolayer cultures.

4.7.3.1 Growth Curve of rAdMSCs after Cell Harvesting

By using MTT analysis results, growth curve of rAdMSCs was obtained. After rAdMSCs were harvested from the packed-bed bioreactor, the specific growth rate and doubling time of harvest rAdMSCs was calculated which are 0.2516 h^{-1} and 42 h, respectively. Which is found to be similar to the doubling time of rAdMSCs that were not subjected to bioreactor culture on PET disks (Figure 4.37).

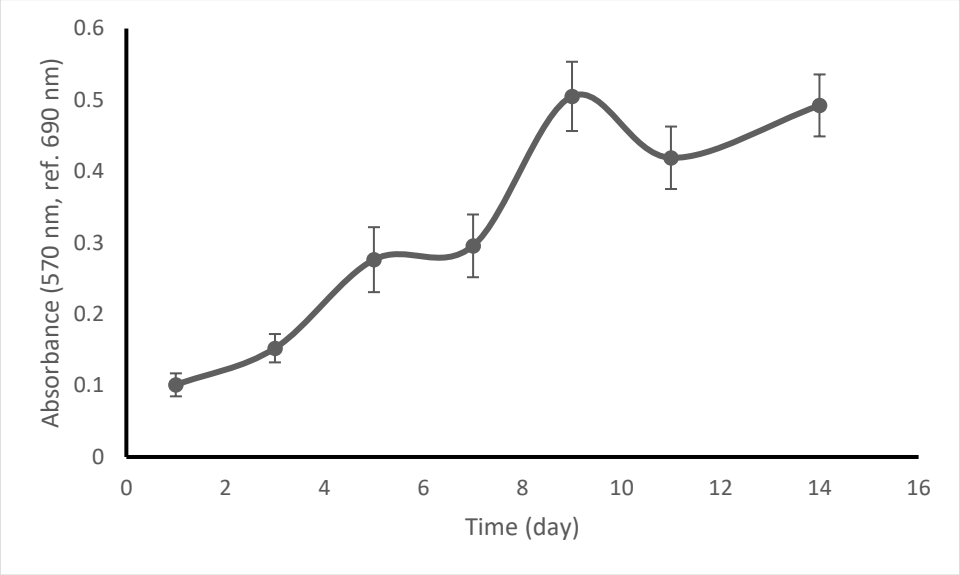

Figure 4. 37. Growth curve of harvested rAdMSCs.

4.7.3.2 Osteogenic Differentiation Studies

Osteogenic differentiation of harvested cells was stimulated by dexamethasone, ascorbic acid and β-glycerol phosphate added to the culture medium. Osteogenic differentiation was monitored by alkaline phosphatase and Von Kossa staining. In the control group, no mineralization of rAdMSCs was observed, but some regions were stained in red as seen in Figure 4.38-a,c, indicating the ALP enzyme activity. In the presence of osteogenic differentiation medium, nodules and black-brown mineralization areas were detected between the cells. The red stained regions in the images, which are the indication of ALP enzyme activity, were only seen on early days of cell culture (Fig. 4.38-b,d).

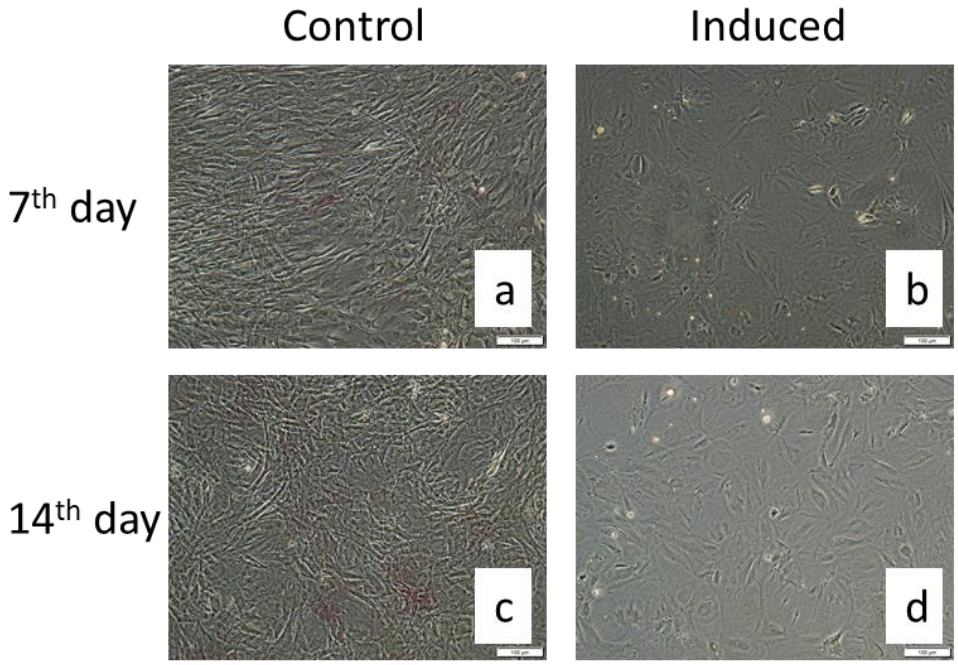

Figure 4. 38. ALP-VC staining of rAdMSCs: Day 7: (a) control group 10x, (b) osteogenic differentiation group,10x; Day 14: (c) control group, 10x , (d) osteogenic differentiation group, 10x.(Scale bar represents x μm).

4.7.3.3 Adipogenic Differentiation Studies

Adipogenic differentiation of harvested cells was induced by IBMX, dexamethasone, insulin and indomethacin added to the culture medium. Inverted microscopy images of control and adipogenic differentiation groups are given in Fig. 4.39. In the staining performed on the 18th day of the culture, no staining was observed in the control group (Fig 4.39-a,b,c), while the cells cultured in adipogenic medium were stained with Oil Red O and red lipid droplets were observed. Lipid-rich vacuoles began to appear in the cells from the second week onwards (Fig 4.39-d,e,f). Later in the culture, lipid vacuoles continued to grow and filled the cells.

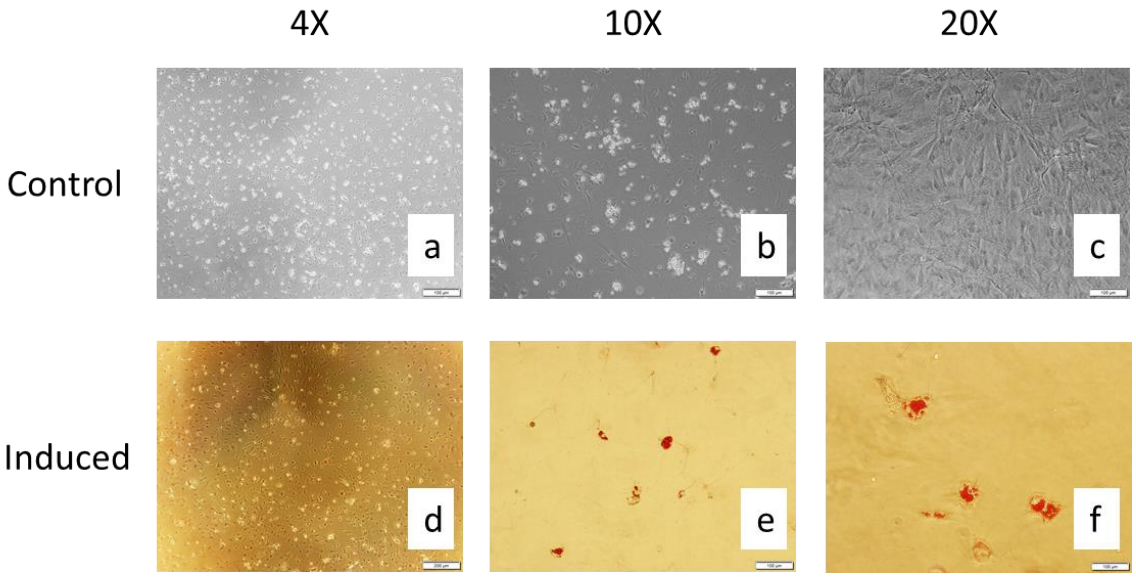

Figure 4. 39. Visualization of oil droplets in rAdMSCs with Oil Red O staining, day 18: Control group (a) 4x, (b) 10x, (c) 20x,; Adipogenic differentiation group: (d) 4x (e) 10x (f) 20x.

4.7.3.4 Gene Expression Studies

SOX2, Nanog and OCT 4 are transcription factors that determine the differentiation of hMSCs, which regulate proliferation by influencing c-MYC. Furthermore, SOX2, Nanog and OCT 4 also had an important role in maintenance of differentiation and growth of adult stem cells [124]. The expression levels of SOX2, Nanog and OCT 4 genes in rAdMSCs (control) and dynamic culture harvested rAdMSCs (dynamic) were presented in Figure 4.40 in order to compare their differentiation ability. In Figure 4.40 expression level of SOX2, Nanog and OCT 4 genes in control and dynamic were found to be similar. Moreover, statistical analysis presented no significate differences between two groups. Therefore, rAdMSCs expansion in our packed-bed bioreactor using Group 4 PET disks as packing materials did not affect the differentiation ability of rAdMSCs.

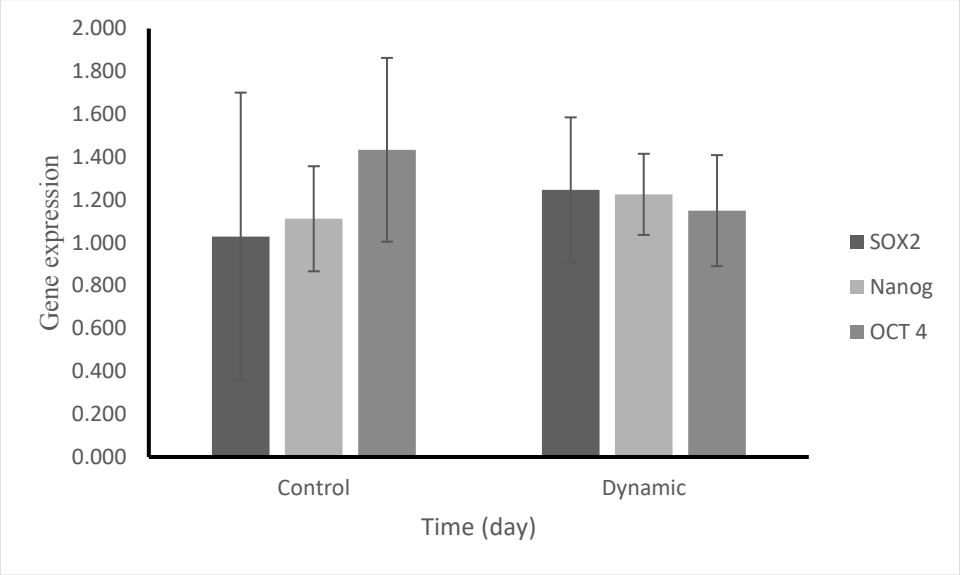

Figure 4. 40. Gene expression of rAdMSCs before and after the dynamic cell culture in our packed-bed bioreactor (Statistical differences when monolayer cell culture is the control: * $p<0.05$, ** $p<0.01$, *** $p<0.001$).

5. CONCLUSION

This study showed the effects of different surface treatments and, collagen type-1 and vitronectin coating onto commercially available PET fiber matrices for the expansion of rAdMSCs in a custom made packed-bed bioreactor. The results obtained from preparation and characterization of surface-modified PET disks and cell culture carried out under static and dynamic conditions are presented below.

- Different surface treatment methods were applied on commercially available PET fiber surfaces to increase surface hydrophilicity. Characterization studies of surface-treated PET disks demonstrated that both sulfuric acid and sodium hydroxide treatments significantly improved the hydrophilicity of the PET fiber surfaces.
- Static cell culture studies carried out with MC3T3-E1 cells on surface-treated PET disks demonstrated that sodium hydroxide treated PET disks had better ability to improve cell activity than sulfuric acid-treated groups.
- For the physical coating of collagen type-1 on PET disks, absorption via dropping and immersion methods were successfully applied. Characterization studies of collagen type-1 coated PET disks displayed that absorption via immersion method could be more efficient and resulted in evenly distributed coating on PET fiber surface when compared with dropping technique.
- For the physical coating of vitronectin on PET disks, absorption via dropping technique was employed. Cell culture studies with rAdMSCs showed that no significant differences on cell activity could be observed when coating densities of 15 μg/disk or 60 μg/disc were applied.
- Static cell culture studies carried out with rAdMSCs showed that there were no significant differences between collagen type-1 and vitronectin coated PET disks when compared to the control group. However, crystal violet staining of collagen type-1 and vitronectin coated PET disk showed higher cell attachment and cell expansion compared to the control group.

- For the chemical immobilization of collagen type-1 and vitronectin on PET disks, EDC/NHS method was successfully applied. Characterization studies of collagen type-1 and vitronectin coated PET disks represented that the chemical immobilization method was more efficient than physical coating method.
- In static cell culture, no significant improvements on the proliferation of rAdMSCs were observed when collagen type-1 or vitronectin were chemically immobilized on PET disks. These results suggested that collagen type-1 and vitronectin coating on PET disk had no positive effects on cell proliferation.
- Depending on the results of cell culture studies, sodium hydroxide treated PET disks were selected to be used in packed bed bioreactor studies.
- For the characterization of rAdMSCs, cell growth curve was plotted by using MTT data. The results demonstrated that cells entered the stationary phase at day 5 and the specific growth rate, and the doubling time of rAdMSCs calculated as 0.3564 h^{-1} and 46 h, respectively.
- For dynamic cell culture, a custom-made packed bed bioreactor, which was designed in our laboratory, was employed. The bioreactor had 100 mL capacity and manually prepared stainless steel basket to accommodate packing materials.
- When Fibra-Cel® was used as packing material in the packed-bed bioreactor, a 4.2-fold expansion of MC3T3-E1 cells was achieved at the end of the cell culture. This showed that our custom-made packed-bed bioreactor was suitable for cell culture usages under defined operating conditions (30 x 10^6 cells/350 disks, 100 mL medium, 50 rpm agitation rate and medium renewal by 50 % in every 2 days).
- In dynamic cell culture studies, packed-bed bioreactor was operated with 2 different cell seeding densities: 30 x 10^6 cells/1g disks and 10 x 10^6 cells/0.5 g disks.
- With 30 x 10^6 cells/1g disks, the specific growth rate and doubling time of rAdMSCs were found to be 0.06 h^{-1} and 65 h. However, the total number of cells harvested from packing material was 2.4 $\times 10^{7,}$ which was below the initial number of cells seeded on PET discs. Biochemical analysis of the culture medium demonstrated that glucose concentration decreased down to 0 mM on the 3rd day of culture.

- In dynamic cell expansion, the total number of cells harvested from PET discs increased by 1.9 folds and 1.2 folds for bioreactor studies with initial cell densities of 30 x 10^6 cells/1g disks and 10 x 10^6 cells/0.5 g disks, respectively.
- The results obtained from biochemical analysis demonstrated that the culture medium run out of glucose at the 3^{rd}, 5^{th},7^{th},9^{th} and 11^{th} days despite culture media renewal in every 2 days. These results suggested that cell proliferation in the bioreactor was limited by insufficient glucose concentration.
- The differentiation study of rAdMSCs that were harvested from the bioreactor demonstrated osteogenic and adipogenic phenotype indicating that the differentiation potential of rAdMSCs was unchanged.
- The results of RT-PCR analysis showed that harvested rAdMSCs had similar SOX2, Nanog and OCT 4 genes expression when compared to that of statically cultured rAdMSCs.
- In the dynamic culture studies, cell expansion could not be enhanced by using different initial cell seeding densities. Thus, it is concluded that optimum operating conditions for higher cell expansion ratios should be further investigated in a more comprehensive cell expansion study.

REFERENCES

[1] N. Kim, S.G. Cho, Clinical applications of mesenchymal stem cells, Korean J Intern Med 28(4) (2013) 387-402.
[2] O. Ringden, M. Uzunel, I. Rasmusson, M. Remberger, B. Sundberg, H. Lonnies, H.U. Marschall, A. Dlugosz, A. Szakos, Z. Hassan, B. Omazic, J. Aschan, L. Barkholt, K. Le Blanc, Mesenchymal stem cells for treatment of therapy-resistant graft-versus-host disease, Transplantation 81(10) (2006) 1390-1397.
[3] Q.A. Rafiq, K. Coopman, C.J. Hewitt, Scale-up of human mesenchymal stem cell culture: current technologies and future challenges, Curr Opin Chem Eng 2(1) (2013) 8-16.
[4] G. ERGIN, Investication of FMD virus production in packed-bed reactors, (2010).
[5] M.D.M. Evans, G.A. McFarland, S. Taylor, G. Johnson, K.M. McLean, The architecture of a collagen coating on a synthetic polymer influences epithelial adhesion, J Biomed Mater Res 56(4) (2001) 461-468.
[6] J.M. Gao, L. Niklason, R. Langer, Surface hydrolysis of poly(glycolic acid) meshes increases the seeding density of vascular smooth muscle cells, J Biomed Mater Res 42(3) (1998) 417-424.
[7] Z. Ma, M. Kotaki, T. Yong, W. He, S. Ramakrishna, Surface engineering of electrospun polyethylene terephthalate (PET) nanofibers towards development of a new material for blood vessel engineering, Biomaterials 26(15) (2005) 2527-36.
[8] J. Li, J. Bardy, L.Y. Yap, A. Chen, V. Nurcombe, S.M. Cool, S.K. Oh, W.R. Birch, Impact of vitronectin concentration and surface properties on the stable propagation of human embryonic stem cells, Biointerphases 5(3) (2010) FA132-42.
[9] A. Keating, Mesenchymal stromal cells, Curr Opin Hematol 13(6) (2006) 419-425.
[10] A.J. Friedenstein, K.V. Petrakova, A.I. Kurolesova, G.P. Frolova, Heterotopic Transplants of Bone Marrow - Analysis of Precursor Cells for Osteogenic and Hematopoietic Tissues, Transplantation 6(2) (1968) 230-+.
[11] M. Dominici, K. Le Blanc, I. Mueller, I. Slaper-Cortenbach, F.C. Marini, D.S. Krause, R.J. Deans, A. Keating, D.J. Prockop, E.M. Horwitz, Minimal criteria for defining multipotent mesenchymal stromal cells. The International Society for Cellular Therapy position statement, Cytotherapy 8(4) (2006) 315-317.
[12] S.K.W. Oh, A.B.H. Choo, 1.25 - Stem Cells, in: M. Moo-Young (Ed.), Comprehensive Biotechnology (Second Edition), Academic Press, Burlington, 2011, pp. 341-365.
[13] R.R. Sharma, K. Pollock, A. Hubel, D. McKenna, Mesenchymal stem or stromal cells: a review of clinical applications and manufacturing practices, Transfusion 54(5) (2014) 1418-1437.

[14] W.H. Yu, Z.G. Chen, J.L. Zhang, L.R. Zhang, H. Ke, L.H. Huang, Y.W. Peng, X.M. Zhang, S.N. Li, B.T. Lahn, A.P. Xiang, Critical role of phosphoinositide 3-kinase cascade in adipogenesis of human mesenchymal stem cells, Mol Cell Biochem 310(1-2) (2008) 11-18.
[15] L.G. Chase, U. Lakshmipathy, L.A. Solchaga, M.S. Rao, M.C. Vemuri, A novel serum-free medium for the expansion of human mesenchymal stem cells, Stem Cell Res Ther 1 (2010).
[16] D. Parsch, J. Fellenberg, T.H. Brummendorf, A.M. Eschlbeck, W. Richter, Telomere length and telomerase activity during expansion and differentiation of human mesenchymal stem cells and chondrocytes, J Mol Med-Jmm 82(1) (2004) 49-55.
[17] S.D. Thorpe, C.T. Buckley, T. Vinardell, F.J. O'Brien, V.A. Campbell, D.J. Kelly, The Response of Bone Marrow-Derived Mesenchymal Stem Cells to Dynamic Compression Following TGF-β3 Induced Chondrogenic Differentiation, Annals of Biomedical Engineering 38(9) (2010) 2896-2909.
[18] B. Zhang, S.H. Yang, Z.B. Sun, Y.K. Zhang, T. Xia, W.H. Xu, S.A. Ye, Human Mesenchymal Stem Cells Induced by Growth Differentiation Factor 5: An Improved Self-Assembly Tissue Engineering Method for Cartilage Repair, Tissue Eng Part C-Me 17(12) (2011) 1189-1199.
[19] A. Shahdadfar, K. Fronsdal, T. Haug, F.P. Reinholt, J.E. Brinchmann, In vitro expansion of human mesenchymal stem cells: Choice of serum is a determinant of cell proliferation, differentiation, gene expression, and transcriptome stability, Stem Cells 23(9) (2005) 1357-1366.
[20] H.J. Prins, H. Rozemuller, S. Vonk-Griffioen, V.G.M. Verweij, W.J.A. Dhert, I.C.M. Slaper-Cortenbach, A.C.M. Martens, Bone-Forming Capacity of Mesenchymal Stromal Cells When Cultured in the Presence of Human Platelet Lysate as Substitute for Fetal Bovine Serum, Tissue Eng Pt A 15(12) (2009) 3741-3751.
[21] A. Meiring, I. Schneider, S. Beasley, E. Woods, Scalable Production of Human Mesenchymal Stem Cells in a Novel Bioreactor Using a Xenogenic Free Culture System, Cytotherapy 18(6) (2016) S7-S7.
[22] B. Lindroos, S. Boucher, L. Chase, H. Kuokkanen, H. Huhtala, R. Haataja, M. Vemuri, R. Suuronen, S. Miettinen, Serum-free, xeno-free culture media maintain the proliferation rate and multipotentiality of adipose stem cells in vitro, Cytotherapy 11(7) (2009) 958-972.
[23] F. Jakob, Clinical applications of mesenchymal stem cells, Bone 44(2) (2009) S206-S206.
[24] P. Kebriaei, L. Isola, E. Bahceci, K. Holland, S. Rowley, J. McGuirk, M. Devetten, J. Jansen, R. Herzig, M. Schuster, R. Monroy, J. Uberti, Adult Human Mesenchymal Stem Cells Added to Corticosteroid Therapy for the Treatment of Acute Graft-versus-Host Disease, Biol Blood Marrow Tr 15(7) (2009) 804-811.

[25] J. Chisholm, C. Ruff, S. Viswanathan, Current state of Health Canada regulation for cellular and gene therapy products: potential cures on the horizon, Cytotherapy 21(7) (2019) 686-698.
[26] M. Duijvestein, A.C.W. Vos, H. Roelofs, M.E. Wildenberg, B.B. Wendrich, H.W. Verspaget, E.M.C. Kooy-Winkelaar, F. Koning, J.J. Zwaginga, H.H. Fidder, A.P. Verhaar, W.E. Fibbe, G.R. van den Brink, D.W. Hommes, Autologous bone marrow-derived mesenchymal stromal cell treatment for refractory luminal Crohn's disease: results of a phase I study, Gut 59(12) (2010) 1662-1669.
[27] G.M. Forbes, M.J. Sturm, R.W. Leong, M.P. Sparrow, D. Segarajasingam, A.G. Cummins, M. Phillips, R.P. Herrmann, A Phase 2 Study of Allogeneic Mesenchymal Stromal Cells for Luminal Crohn's Disease Refractory to Biologic Therapy, Clin Gastroenterol H 12(1) (2014) 64-71.
[28] E.M. Horwitz, D.J. Prockop, L.A. Fitzpatrick, W.W.K. Koo, P.L. Gordon, M. Neel, M. Sussman, P. Orchard, J.C. Marx, R.E. Pyeritz, M.K. Brenner, Transplantability and therapeutic effects of bone marrow-derived mesenchymal cells in children with osteogenesis imperfecta, Nature Medicine 5(3) (1999) 309-313.
[29] E.M. Horwitz, P.L. Gordon, W.K.K. Koo, J.C. Marx, M.D. Neel, R.Y. McNall, L. Muul, T. Hofmann, Isolated allogeneic bone marrow-derived mesenchymal cells engraft and stimulate growth in children with osteogenesis imperfecta: Implications for cell therapy of bone, P Natl Acad Sci USA 99(13) (2002) 8932-8937.
[30] R. Soler, L. Orozco, A. Munar, M. Huguet, R. Lopez, J. Vives, R. Coll, M. Codinach, J. Garcia-Lopez, Final results of a phase I-II trial using ex vivo expanded autologous Mesenchymal Stromal Cells for the treatment of osteoarthritis of the knee confirming safety and suggesting cartilage regeneration, The Knee 23(4) (2016) 647-54.
[31] M. Cai, R. Shen, L. Song, M.J. Lu, J.G. Wang, S.H. Zhao, Y. Tang, X.M. Meng, Z.J. Li, Z.X. He, Bone Marrow Mesenchymal Stem Cells (BM-MSCs) Improve Heart Function in Swine Myocardial Infarction Model through Paracrine Effects (vol 6, 28250, 2016), Sci Rep-Uk 6 (2016).
[32] V. Karantalis, D.L. DiFede, G. Gerstenblith, S. Pham, J. Symes, J.P. Zambrano, J. Fishman, P. Pattany, I. McNiece, J. Conte, S. Schulman, K. Wu, A. Shah, E. Breton, J. Davis-Sproul, R. Schwarz, G. Feigenbaum, M. Mushtaq, V.Y. Suncion, A.C. Lardo, I. Borrello, A. Mendizabal, T.Z. Karas, J. Byrnes, M. Lowery, A.W. Heldman, J.M. Hare, Autologous mesenchymal stem cells produce concordant improvements in regional function, tissue perfusion, and fibrotic burden when administered to patients undergoing coronary artery bypass grafting: The Prospective Randomized Study of Mesenchymal Stem Cell Therapy in Patients Undergoing Cardiac Surgery (PROMETHEUS) trial, Circulation research 114(8) (2014) 1302-10.

[33] A. Rolls, R. Shechter, M. Schwartz, NEURON - GLIA INTERACTIONS - OPINION The bright side of the glial scar in CNS repair, Nat Rev Neurosci 10(3) (2009) 235-U91.
[34] M.B. Bracken, Steroids for acute spinal cord injury, Cochrane Db Syst Rev (1) (2012).
[35] H.C. Park, Y.S. Shim, Y. Ha, S.H. Yoon, S.R. Park, B.H. Choi, H.S. Park, Treatment of complete spinal cord injury patients by autologous bone marrow cell transplantation and administration of granulocyte-macrophage colony stimulating factor, Tissue Eng 11(5-6) (2005) 913-922.
[36] D.D. Pearse, A.R. Sanchez, F.C. Pereira, C.M. Andrade, R. Puzis, Y. Pressman, K. Golden, B.M. Kitay, B. Blits, P.M. Wood, M.B. Bunge, Transplantation of Schwann cells and/or olfactory ensheathing glia into the contused spinal cord: Survival, migration, axon association, and functional recovery, Glia 55(9) (2007) 976-1000.
[37] Y. Ogawa, K. Sawamoto, T. Miyata, S. Miyao, M. Watanabe, M. Nakamura, B.S. Bregman, M. Koike, Y. Uchiyama, Y. Toyama, H. Okano, Transplantation of in vitro-expanded fetal neural progenitor cells results in neurogenesis and functional recovery after spinal cord contusion injury in adult rats, J Neurosci Res 69(6) (2002) 925-933.
[38] S.I. Park, J.Y. Lim, C.H. Jeong, S.M. Kim, J.A. Jun, S.S. Jeun, W.I. Oh, Human Umbilical Cord Blood-Derived Mesenchymal Stem Cell Therapy Promotes Functional Recovery of Contused Rat Spinal Cord through Enhancement of Endogenous Cell Proliferation and Oligogenesis, J Biomed Biotechnol (2012).
[39] A.H. All, P. Gharibani, S. Gupta, F.A. Bazley, N. Pashai, B.K. Chou, S. Shah, L.M. Resar, L.Z. Cheng, J.D. Gearhart, C.L. Kerr, Early Intervention for Spinal Cord Injury with Human Induced Pluripotent Stem Cells Oligodendrocyte Progenitors, Plos One 10(1) (2015).
[40] A.M. Parr, C.H. Tator, A. Keating, Bone marrow-derived mesenchymal stromal cells for the repair of central nervous system injury, Bone Marrow Transpl 40(7) (2007) 609-619.
[41] H.S. Satti, A. Waheed, P. Ahmed, K. Ahmed, Z. Akram, T. Aziz, T.M. Satti, N. Shahbaz, M.A. Khan, S.A. Malik, Autologous mesenchymal stromal cell transplantation for spinal cord injury: A Phase I pilot study, Cytotherapy 18(4) (2016) 518-522.
[42] M. Dağlı Durukan, Mikrodalga-destekli Doku İskelesi Üretimi ve In Vitro Kemik Doku Mühendisliği, (2012).
[43] A. Banfi, A. Muraglia, B. Dozin, M. Mastrogiacomo, R. Cancedda, R. Quarto, Proliferation kinetics and differentiation potential of ex vivo expanded human bone marrow stromal cells: Implications for their use in cell therapy, Exp Hematol 28(6) (2000) 707-715.
[44] R.J. Thomas, A. Chandra, Y. Liu, P.C. Hourd, P.P. Conway, D.J. Williams, Manufacture of a human mesenchymal stem cell population using an automated cell culture platform, Cytotechnology 55(1) (2007) 31-39.
[45] A.L. Van Wezel, Growth of Cell-strains and Primary Cells on Micro-carriers in Homogeneous Culture, Nature 216(5110) (1967) 64-65.

[46] J. Lee, M.J. Cuddihy, N.A. Kotov, Three-dimensional cell culture matrices: State of the art, Tissue Eng Pt B-Rev 14(1) (2008) 61-86.
[47] J.W. Haycock, 3D Cell Culture: A Review of Current Approaches and Techniques, Methods Mol Biol 695 (2011) 1-15.
[48] H.K. Kleinman, D. Philp, M.P. Hoffman, Role of the extracellular matrix in morphogenesis, Curr Opin Biotech 14(5) (2003) 526-532.
[49] M.J. Bissell, D.C. Radisky, A. Rizki, V.M. Weaver, O.W. Petersen, The organizing principle: microenvironmental influences in the normal and malignant breast, Differentiation 70(9-10) (2002) 537-546.
[50] A.K. Chen, S. Reuveny, S.K. Oh, Application of human mesenchymal and pluripotent stem cell microcarrier cultures in cellular therapy: achievements and future direction, Biotechnol Adv 31(7) (2013) 1032-46.
[51] A.I. Hock, J.K. Leach, Concise Review: Optimizing Expansion of Bone Marrow Mesenchymal Stem/Stromal Cells for Clinical Applications (vol 3, pg 643, 2014), Stem Cell Transl Med 4(4) (2015).
[52] C.E. Holy, M.S. Shoichet, J.E. Davies, Engineering three-dimensional bone tissue in vitro using biodegradable scaffolds: Investigating initial cell-seeding density and culture period, J Biomed Mater Res 51(3) (2000) 376-382.
[53] Y. Li, T. Ma, D.A. Kniss, L.C. Lasky, S.T. Yang, Effects of filtration seeding on cell density, spatial distribution, and proliferation in nonwoven fibrous matrices, Biotechnol Progr 17(5) (2001) 935-944.
[54] D.G. Morales-Hernandez, D.C. Genetos, D.M. Working, K.C. Murphy, J.K. Leach, Ceramic identity contributes to mechanical properties and osteoblast behavior on macroporous composite scaffolds, J Funct Biomater 3(2) (2012) 382-397.
[55] J. Rauh, F. Milan, K.P. Gunther, M. Stiehler, Bioreactor Systems for Bone Tissue Engineering, Tissue Eng Pt B-Rev 17(4) (2011) 263-280.
[56] F. Dos Santos, P.Z. Andrade, J.S. Boura, M.M. Abecasis, C.L. Da Silva, J.M.S. Cabral, Ex Vivo Expansion of Human Mesenchymal Stem Cells: A More Effective Cell Proliferation Kinetics and Metabolism Under Hypoxia, J Cell Physiol 223(1) (2010) 27-35.
[57] J.A. King, W.M. Miller, Bioreactor development for stem cell expansion and controlled differentiation, Curr Opin Chem Biol 11(4) (2007) 394-398.
[58] F. Zhao, R. Chella, T. Ma, Effects of shear stress on 3-D human mesenchymal stem cell construct development in a perfusion bioreactor system: Experiments and hydrodynamic modeling, Biotechnology and Bioengineering 96(3) (2007) 584-595.
[59] D.Q. Li, T.T. Tang, J.X. Lu, K.R. Dai, Effects of Flow Shear Stress and Mass Transport on the Construction of a Large-Scale Tissue-Engineered Bone in a Perfusion Bioreactor, Tissue Eng Pt A 15(10) (2009) 2773-2783.

[60] M. Rodrigues, L.G. Griffith, A. Wells, Growth factor regulation of proliferation and survival of multipotential stromal cells, Stem Cell Res Ther 1 (2010).
[61] H.H. Luu, W.-X. Song, X. Luo, D. Manning, J. Luo, Z.-L. Deng, K.A. Sharff, A.G. Montag, R.C. Haydon, T.-C. He, Distinct roles of bone morphogenetic proteins in osteogenic differentiation of mesenchymal stem cells, Journal of Orthopaedic Research 25(5) (2007) 665-677.
[62] A. Stewart, H. Guan, K. Yang, BMP-3 promotes mesenchymal stem cell proliferation through the TGF-β/activin signaling pathway, J Cell Physiol 223(3) (2010) 658-666.
[63] S.S. Ozturk, B.O. Palsson, Growth, Metabolic, and Antibody Production Kinetics of Hybridoma Cell Culture: 2. Effects of Serum Concentration, Dissolved Oxygen Concentration, and Medium pH in a Batch Reactor, Biotechnol Progr 7(6) (1991) 481-494.
[64] D. Schop, F.W. Janssen, E. Borgart, J.D. de Bruijn, R. van Dijkhuizen-Radersma, Expansion of mesenchymal stem cells using a microcarrier-based cultivation system: growth and metabolism, Journal of Tissue Engineering and Regenerative Medicine 2(2-3) (2008) 126-135.
[65] X.L. Chen, A. Chen, T.L. Woo, A.B.H. Choo, S. Reuveny, S.K.W. Oh, Investigations into the Metabolism of Two-Dimensional Colony and Suspended Microcarrier Cultures of Human Embryonic Stem Cells in Serum-Free Media, Stem Cells Dev 19(11) (2010) 1781-1792.
[66] L.R. Castilho, R.A. Medronho, Cell Retention Devices for Suspended-Cell Perfusion Cultures, in: K. Schügerl, A.P. Zeng, J.G. Aunins, A. Bader, W. Bell, H. Biebl, M. Biselli, M.J.T. Carrondo, L.R. Castilho, H.N. Chang, P.E. Cruz, C. Fuchs, S.J. Han, M.R. Han, E. Heinzle, B. Hitzmann, D. Köster, I. Jasmund, N. Jelinek, S. Lang, H. Laatsch, J. Lee, H. Miirkl, L. Maranga, R.A. Medronho, M. Meiners, S. Nath, T. Noll, T. Scheper, S. Schmidt, K. Schüigerl, E. Stäirk, A. Tholey, I. Wagner-Döbler, C. Wandrey, C. Wittmann, S.C. Yim, A.P. Zeng (Eds.), Tools and Applications of Biochemical Engineering Science, Springer Berlin Heidelberg, Berlin, Heidelberg, 2002, pp. 129-169.
[67] A. Wolf, R. Kramer, S. Morbach, Three pathways for trehalose metabolism in Corynebacterium glutamicum ATCC13032 and their significance in response to osmotic stress, Mol Microbiol 49(4) (2003) 1119-1134.
[68] L.Z. Xie, D.I.C. Wang, Integrated approaches to the design of media and feeding strategies for fed-batch cultures of animal cells, Trends in Biotechnology 15(3) (1997) 109-113.
[69] M. Butler, T. Hassell, C. Doyle, S. Gleave, P. Jennings, THE EFFECT OF METABOLIC BY-PRODUCTS ON ANIMAL CELLS IN CULTURE, in: R.E. Spier, J.B. Griffiths, B. Meignier (Eds.), Production of Biologicals from Animal Cells in Culture, Butterworth-Heinemann1991, pp. 226-228.

[70] L. Chu, D.K. Robinson, Industrial choices for protein production by large-scale cell culture, Curr Opin Biotech 12(2) (2001) 180-187.
[71] C. Altamirano, A. Illanes, A. Casablancas, X. Gámez, J.J. Cairó, C. Gòdia, Analysis of CHO Cells Metabolic Redistribution in a Glutamate-Based Defined Medium in Continuous Culture, Biotechnol Progr 17(6) (2001) 1032-1041.
[72] I. Martin, D. Wendt, M. Heberer, The role of bioreactors in tissue engineering, Trends in Biotechnology 22(2) (2004) 80-86.
[73] Ş. Bektaş, Sferoid yüklü ECM--mimetik peptit amfifil hidrojellerle çip-üstü-karaciğer geliştirilmesi, Bioengineering, Hacettepe, 2018.
[74] G. Mehta, A.Y. Hsiao, M. Ingram, G.D. Luker, S. Takayama, Opportunities and challenges for use of tumor spheroids as models to test drug delivery and efficacy, J Control Release 164(2) (2012) 192-204.
[75] G.O. Gey, An Improved Technic for Massive Tissue Culture, The American Journal of Cancer 17(3) (1933) 752-756.
[76] J.M. Melero-Martin, In vitro expansion of chondrocytes, Topics Tissue Eng. 3 (2007) 1-37.
[77] Y.L. Liu, K. Wagner, N. Robinson, D. Sabatino, P. Margaritis, W. Xiao, R.W. Herzog, Optimized production of high-titer recombinant adeno-associated virus in roller bottles, Biotechniques 34(1) (2003) 184-+.
[78] H. Andrade-Zaldivar, M.A. Kalixto-Sanchez, A.P.B. de la Rosa, A. De Leon-Rodriguez, Expansion of Human Hematopoietic Cells from Umbilical Cord Blood Using Roller Bottles in CO2 and CO2-Free Atmosphere, Stem Cells Dev 20(4) (2011) 593-598.
[79] L. Sensebe, M. Gadelorge, S. Fleury-Cappellesso, Production of mesenchymal stromal/stem cells according to good manufacturing practices: a review, Stem Cell Res Ther 4 (2013).
[80] T. Lawson, D.E. Kehoe, A.C. Schnitzler, P.J. Rapiejko, K.A. Der, K. Philbrick, S. Punreddy, S. Rigby, R. Smith, Q. Feng, J.R. Murrell, M.S. Rook, Process development for expansion of human mesenchymal stromal cells in a 50L single-use stirred tank bioreactor, Biochemical Engineering Journal 120 (2017) 49-62.
[81] G. Blüml, Microcarrier Cell Culture Technology, in: R. Pörtner (Ed.), Animal Cell Biotechnology: Methods and Protocols, Humana Press, Totowa, NJ, 2007, pp. 149-178.
[82] S. Jung, K.M. Panchalingam, R.D. Wuerth, L. Rosenberg, L.A. Behie, Large-scale production of human mesenchymal stem cells for clinical applications, Biotechnol Appl Bioc 59(2) (2012) 106-120.
[83] S. Frauenschuh, E. Reichmann, Y. Ibold, P.M. Goetz, M. Sittinger, J. Ringe, A microcarrier-based cultivation system for expansion of primary mesenchymal stem cells, Biotechnol Progr 23(1) (2007) 187-193.

[84] S.J. Lu, T. Kelley, Q. Feng, 3D microcarrier system for efficient differentiation of induced human pluripotent stem cells into hematopoietic cells without feeders and serum (vol 8, pg 413, 2013), Regen Med 8(5) (2013) 672-672.
[85] Y. Martin, M. Eldardiri, D.J. Lawrence-Watt, J.R. Sharpe, Microcarriers and Their Potential in Tissue Regeneration, Tissue Eng Pt B-Rev 17(1) (2011) 71-80.
[86] B. Hundt, C. Best, N. Schlawin, H. Kaßner, Y. Genzel, U. Reichl, Establishment of a mink enteritis vaccine production process in stirred-tank reactor and Wave® Bioreactor microcarrier culture in 1–10L scale, Vaccine 25(20) (2007) 3987-3995.
[87] A.M. Fernandes, M.M. Diogo, C.L. da Silva, D. Henrique, J.M.S. Cabral, Mouse embryonic stem cell expansion in a microcarrier-based stirred culture system, Tissue Eng Pt A 14(5) (2008) 757-758.
[88] S.S. Ozturk, Engineering challenges in high density cell culture systems, Cytotechnology 22(1-3) (1996) 3-16.
[89] D. Voisard, F. Meuwly, P.A. Ruffieux, G. Baer, A. Kadouri, Potential of cell retention techniques for large-scale high-density perfusion culture of suspended mammalian cells, Biotechnology and Bioengineering 82(7) (2003) 751-765.
[90] <Gencay- Yüksek lisans tezi[801].pdf>.
[91] A.K. Chen, Y.K. Chew, H.Y. Tan, S. Reuveny, S.K. Weng Oh, Increasing efficiency of human mesenchymal stromal cell culture by optimization of microcarrier concentration and design of medium feed, Cytotherapy 17(2) (2015) 163-73.
[92] R.E. Spier, J.P. Whiteside, The production of foot-and-mouth disease virus from BHK 21 C 13 cells grown on the surface of DEAE sephadex A50 beads, Biotechnology and Bioengineering 18(5) (1976) 659-667.
[93] W. Liu, D. Hu, C. Gu, Y. Zhou, W.S. Tan, Fabrication and in vitro evaluation of a packed-bed bioreactor based on an optimum two-stage culture strategy, J Biosci Bioeng 127(4) (2019) 506-514.
[94] T.-W. Chiou, S. Murakami, D.I.C. Wang, W.-T. Wu, A fiber-bed bioreactor for anchorage-dependent animal cell cultures: Part I. Bioreactor design and operations, Biotechnology and Bioengineering 37(8) (1991) 755-761.
[95] A. Bohmann, R. Portner, J. Schmieding, V. Kasche, H. Markl, The Membrane Dialysis Bioreactor with Integrated Radial-Flow Fixed-Bed - a New Approach for Continuous Cultivation of Animal-Cells, Cytotechnology 9(1-3) (1992) 51-57.
[96] F. Meuwly, P.A. Ruffieux, A. Kadouri, U. von Stockar, Packed-bed bioreactors for mammalian cell culture: bioprocess and biomedical applications, Biotechnol Adv 25(1) (2007) 45-56.
[97] A.-C. Tsai, Y. Liu, T. Ma, Expansion of human mesenchymal stem cells in fibrous bed bioreactor, Biochemical Engineering Journal 108 (2016) 51-57.

[98] Z. Bohak, A. Kadouri, M.V. Sussman, A.F. Feldman, Novel Anchorage Matrices for Suspension-Culture of Mammalian-Cells, Biopolymers 26 (1987) S205-S213.
[99] L. Bech, T. Meylheuc, B. Lepoittevin, P. Roger, Chemical surface modification of poly(ethylene terephthalate) fibers by aminolysis and grafting of carbohydrates, J Polym Sci Pol Chem 45(11) (2007) 2172-2183.
[100] M.J. Yaszemski, R.G. Payne, W.C. Hayes, R. Langer, A.G. Mikos, Evolution of bone transplantation: Molecular, cellular and tissue strategies to engineer human bone, Biomaterials 17(2) (1996) 175-185.
[101] Y.P. Jiao, F.Z. Cui, Surface modification of polyester biomaterials for tissue engineering, Biomed Mater 2(4) (2007) R24-37.
[102] Y. Takahashi, Y. Tabata, Effect of the fiber diameter and porosity of non-woven PET fabrics on the osteogenic differentiation of mesenchymal stem cells, Journal of Biomaterials Science, Polymer Edition 15(1) (2004) 41-57.
[103] C.C. Ai, J.Y. Cai, J. Zhu, J. Zhou, J. Jiang, S.Y. Chen, Effect of PET graft coated with silk fibroin via EDC/NHS crosslink on graft-bone healing in ACL reconstruction, Rsc Adv 7(81) (2017) 51303-51312.
[104] W. Chen, T.J. McCarthy, Chemical surface modification of poly(ethylene terephthalate), Macromolecules 31(11) (1998) 3648-3655.
[105] S. Jaumotte-Thelen, I. Dozet-Dupont, J. Marchand-Brynaert, Y.J. Schneider, Covalent grafting of fibronectin and asialofetuin at surface of poly(ethylene terephthalate) track-etched membranes improves adhesion but not differentiation of rat hepatocytes, J Biomed Mater Res 32(4) (1996) 569-82.
[106] N.M. Coelho, M. Salmeron-Sanchez, G. Altankov, Fibroblasts remodeling of type IV collagen at a biomaterials interface, Biomater Sci-Uk 1(5) (2013) 494-502.
[107] K. Anselme, Osteoblast adhesion on biomaterials, Biomaterials 21(7) (2000) 667-681.
[108] S. Ricard-Blum, The Collagen Family, Csh Perspect Biol 3(1) (2011).
[109] A. Bhattacharjee, M. Bansal, Collagen structure: The Madras triple helix and the current scenario, Iubmb Life 57(3) (2005) 161-172.
[110] X. Garric, J.P. Moles, H. Garreau, J.J. Guilhou, M. Vert, Human skin cell cultures onto PLA(50) (PDLLA) bioresorbable polymers: Influence of chemical and morphological surface modifications, J Biomed Mater Res A 72a(2) (2005) 180-189.
[111] W. He, Z. Ma, T. Yong, W.E. Teo, S. Ramakrishna, Fabrication of collagen-coated biodegradable polymer nanofiber mesh and its potential for endothelial cells growth, Biomaterials 26(36) (2005) 7606-15.
[112] S. Yamada, [Vitronectin (VN)], Nihon Rinsho 62 Suppl 11 (2004) 303-6.
[113] G.W. Lynn, W.T. Heller, A. Mayasundari, K.H. Minor, C.B. Peterson, A model for the three-dimensional structure of human plasma vitronectin from small-angle scattering measurements, Biochemistry-Us 44(2) (2005) 565-574.

[114] B.C. Heng, J. Li, A.K.L. Chen, S. Reuveny, S.M. Cool, W.R. Birch, S.K.W. Oh, Translating Human Embryonic Stem Cells from 2-Dimensional to 3-Dimensional Cultures in a Defined Medium on Laminin- and Vitronectin-Coated Surfaces, Stem Cells Dev 21(10) (2012) 1701-1715.
[115] T. Yoshioka, T. Sato, A. Okuwaki, Hydrolysis of Waste Pet by Sulfuric-Acid at 150-Degrees-C for a Chemical Recycling, J Appl Polym Sci 52(9) (1994) 1353-1355.
[116] A. Palme, A. Peterson, H. de la Motte, H. Theliander, H. Brelid, Development of an efficient route for combined recycling of PET and cotton from mixed fabrics, Textiles and Clothing Sustainability 3(1) (2017) 4.
[117] D.V. Bax, N. Davidenko, D. Gullberg, S.W. Hamaia, R.W. Farndale, S.M. Best, R.E. Cameron, Fundamental insight into the effect of carbodiimide crosslinking on cellular recognition of collagen-based scaffolds, Acta Biomaterialia 49 (2017) 218-234.
[118] M.C. KARAASLAN, INVESTIGATION OF MESENCHYMAL STEM CELL EXPANSION IN PACKED BED BIOREACTOR, (Hacettepe University) (2020) 117.
[119] C.A. Edwards, W.D. O'Brien, Jr., Modified assay for determination of hydroxyproline in a tissue hydrolyzate, Clin Chim Acta 104(2) (1980) 161-7.
[120] G.K. Reddy, C.S. Enwemeka, A simplified method for the analysis of hydroxyproline in biological tissues, Clin Biochem 29(3) (1996) 225-9.
[121] C. Chollet, S. Lazare, C. Labrugère, F. Guillemot, R. Bareille, M.C. Durrieu, RGD peptides micro-patterning on poly(ethylene terephthalate) surfaces, IRBM 28(1) (2007) 2-12.
[122] K. Belbachir, R. Noreen, G. Gouspillou, C. Petibois, Collagen types analysis and differentiation by FTIR spectroscopy, Anal Bioanal Chem 395(3) (2009) 829-837.
[123] F. Sima, P. Davidson, E. Pauthe, O. Gallet, K. Anselme, I.N. Mihailescu, Thin films of vitronectin transferred by MAPLE, Appl Phys a-Mater 105(3) (2011) 611-617.
[124] S.B. Park, K.W. Seo, A.Y. So, M.S. Seo, K.R. Yu, S.K. Kang, K.S. Kang, SOX2 has a crucial role in the lineage determination and proliferation of mesenchymal stem cells through Dickkopf-1 and c-MYC, Cell Death Differ 19(3) (2012) 534-545.